THEORETICAL STUDY OF CYCLONE DESIGN

A Dissertation

by

LINGJUAN WANG

Submitted to the Office of Graduate Studies of
Texas A&M University
in partial fulfillment of the requirements for the degree of

DOCTOR OF PHILOSOPHY

May 2004

Major Subject: Biological & Agricultural Engineering

THEORETICAL STUDY OF CYCLONE DESIGN

A Dissertation

by

LINGJUAN WANG

Submitted to Texas A&M University
in partial fulfillment of the requirements
for the degree of

DOCTOR OF PHILOSOPHY

Approved as to style and content by:

Calvin Parnell, Jr. (Chair of Committee)	Bryan W. Shaw (Member)
Ronald E. Lacey (Member)	Dennis L. O'Neal (Member)
Gerald Riskowski (Head of Department)	

May 2004

Major Subject: Biological & Agricultural Engineering

ABSTRACT

Theoretical Study of Cyclone Design. (May 2004)

Lingjuan Wang,

B. Eng., Anhui Institute of Finance and Trade, China;

M.S., Texas A&M University

Chair of Advisory Committee: Dr. Calvin B. Parnell, Jr.

To design a cyclone abatement system for particulate control, it is necessary to accurately estimate cyclone performance. In this cyclone study, new theoretical methods for computing travel distance, numbers of turns and cyclone pressure drop have been developed. The flow pattern and cyclone dimensions determine the travel distance in a cyclone. The number of turns was calculated based on this travel distance. The new theoretical analysis of cyclone pressure drop was tested against measured data at different inlet velocities and gave excellent agreement. The results show that cyclone pressure drop varies with the inlet velocity, but not with cyclone diameter.

Particle motion in the cyclone outer vortex was analyzed to establish a force balance differential equation. Barth's "static particle" theory, particle (with diameter of d_{50}) collection probability is 50% when the forces acting on it are balanced, combined with the force balance equation was applied in the theoretical analyses for the models of cyclone cut-point and collection probability distribution in the cyclone outer vortex. Cyclone cut-points for different dusts were traced from measured cyclone overall collection efficiencies and the theoretical model for calculating cyclone overall efficiency. The cut-point correction models (K) for 1D3D and 2D2D cyclones were developed through regression fit from traced and theoretical cut-points. The regression results indicate that cut-points are more sensitive to mass median diameter (MMD) than to geometric standard deviation (GSD) of PSD. The theoretical overall efficiency model developed in this research can be used for cyclone total efficiency calculation with the corrected d_{50} and PSD.

1D3D and 2D2D cyclones were tested at Amarillo, Texas (an altitude of 1128 m / 3700 ft), to evaluate the effect of air density on cyclone performance. Two sets of inlet design velocities determined by the different air densities were used for the tests. Experimental results indicate that optimal cyclone design velocities, which are 16 m/s (3200 ft/min) for 1D3D cyclones and 15 m/s (3000 ft/min) for 2D2D cyclones, should be determined based on standard air density. It is important to consider the air density effect on cyclone performance in the design of cyclone abatement systems.

This dissertation is dedicated to my FAMILY, my ADVISORS, and all my FRIENDS.

Thank you all for your constant support and love in the past, present and future.

Words cannot express my grateful feelings to all of you.

This dissertation is also dedicated to the Center for Agricultural Air Quality Engineering and Science (CAAQES) at Texas A&M University. It has been a great pleasure for me to be part of the CREW.

ACKNOWLEDGMENTS

First of all, my greatest appreciation goes to Dr. Calvin B. Parnell, Jr. for directing me throughout my research and helping me through difficulties. In my heart, you are much more than an advisor - you are a special friend and an example for me to follow. Without your guidance, support and encouragement, none of this would be possible.

My grateful appreciation also goes to Dr. Bryan W. Shaw, Dr. Ronald E. Lacey and Dr. Dennis L. O’Neal for serving on my committee. Thank you all for helping me throughout my research and completion of this dissertation.

To my best friend, Bill A. Stout, thank you for believing in me and for being there whenever I needed a hand. Your positive attitude has been a true inspiration to me. Your friendship has made the world more meaningful and colorful to me.

To Mike Buser, Barry Goodrich, John Wanjura, Sergio Capareda, Shay Simpson, Jackie Price, Lee Hamm and Cale Boriack, “The Crew” in the Center for Agricultural Air Quality Engineering and Science (CAAQES), thank you all for helping me through all the difficult times in my studies and research. Your brainstorms have brought me light when I was in the dark. I will miss those days of our sampling trips together and will always remember “The Night Crew Is Da Best!”

To the student workers in the CAAQES, Amy Kettle, Clint Pargmann, Charles Bates, Ryan Batla, thank you for all your hours and hard work on my project. Without your help, I could not have finished this research.

My very special thanks also go to my family - my husband, my parents, parents-in-law, my brother and sisters for your silent support through all my "ups and downs". Without your support and encouragement, I could not spread my wings to soar.

To my dear daughter, Jing Li, thank you for being my angel and the source of my strength. You are the greatest blessing in my life forever.

Most of all, I thank GOD for carrying me through hard times.

"Trust in the LORD with all your heart and lean not on your own understanding; in all your ways acknowledge him, and he will make your paths straight. "

Proverbs 3:5, 6

TABLE OF CONTENTS

Page

LIST OF FIGURES

Page

LIST OF TABLES

CHAPTER I

INTRODUCTION

CYCLONE DESIGNS

Cyclone separators provide a method of removing particulate matter from air streams at low cost and low maintenance. In general, a cyclone consists of an upper cylindrical part referred to as the barrel and a lower conical part referred to as cone (see figure 1). The air stream enters tangentially at the top of the barrel and travels downward into the cone forming an outer vortex. The increasing air velocity in the outer vortex results in a centrifugal force on the particles separating them from the air stream. When the air reaches the bottom of the cone, an inner vortex is created reversing direction and exiting out the top as clean air while the particulates fall into the dust collection chamber attached to the bottom of the cyclone.

In the agricultural processing industry, 2D2D (Shepherd and Lapple, 1939) and 1D3D (Parnell and Davis, 1979) cyclone designs are the most commonly used abatement devices for particulate matter control. The D's in the 2D2D designation refer to the barrel diameter of the cyclone. The numbers preceding the D's relate to the length of the barrel and cone sections, respectively. A 2D2D cyclone has barrel and cone lengths of two times the barrel diameter, whereas the 1D3D cyclone has a barrel length equal to the barrel diameter and a cone length of three times the barrel diameter. The configurations

---

This dissertation follows the style and format of the journal *Transactions of the American Society of Agricultural Engineers.*

of these two cyclone designs are shown in figure 2. Previous research (Wang, 2000) indicated that, compared to other cyclone designs, 1D3D and 2D2D are the most efficient cyclone collectors for fine dust (particle diameters less than 100 μm).

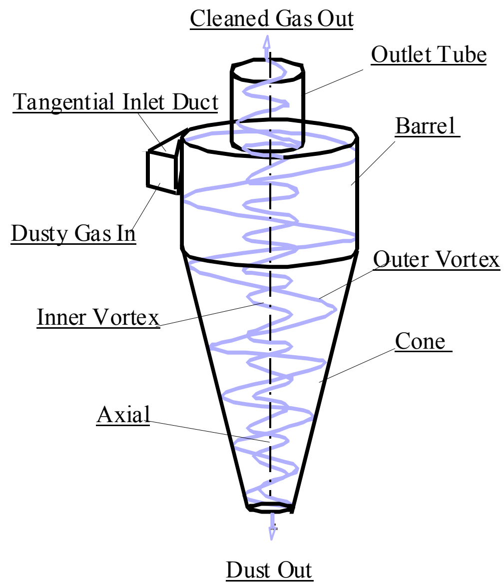

Figure 1.Schematic flow diagram of a cyclone.

Mihalski et al (1993) reported "cycling lint" near the trash exit for the 1D3D and 2D2D cyclone designs when the PM in the inlet air stream contained lint fiber. Mihalski reported a significant increase in the exit PM concentration for these high efficiency cyclone designs and attributed this to small balls of lint fiber "cycling" near the trash exit causing the fine PM that would normally be collected to be diverted to the clean air exit stream. Simpson and Parnell (1995) introduced a new low-pressure cyclone, called the 1D2D cyclone, for the cotton ginning industry to solve the cycling-lint problem. The 1D2D cyclone is a better design for high-lint content trash compared with 1D3D and

2D2D cyclones (Wang et al., 1999). Figure 3 illustrates the configuration of 1D2D cyclone design.

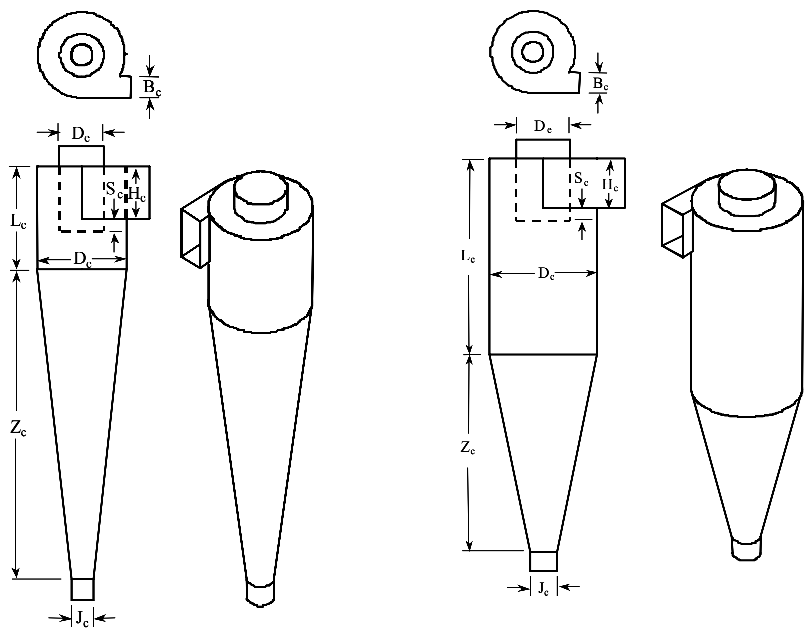

1D3D

$B_c = D_c/4$ $J_c = D_c/4$

$D_e = D_c/2$ $S_c = D_c/8$

$H_c = D_c/2$ $L_c = 1 \times D_c$

$Z_c = 3 \times D_c$

2D2D

$B_c = D_c/4$ $J_c = D_c/4$

$D_e = D_c/2$ $S_c = D_c/8$

$H_c = D_c/2$ $L_c = 2 \times D_c$

$Z_c = 2 \times D_c$

Figure 2. 1D3D and 2D2D cyclone configurations.

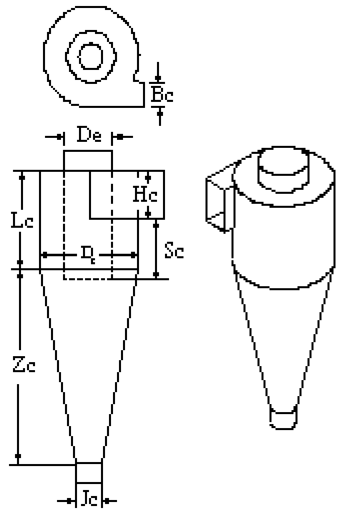

1D2D

$B_c = D_c/4$ $J_c = D_c/2$

$D_e = D_c/1.6$ $S_c = 5D_c/8$

$H_c = D_c/2$ $L_c = 1 \times D_c$

$Z_c = 2 \times D_c$

Figure 3. 1D2D cyclone configuration.

CLASSICAL CYCLONE DESIGN (CCD)

The cyclone design procedure outlined in Cooper and Alley (1994), hereafter referred to as the classical cyclone design (CCD) process, was developed by Lapple in the early 1950s. The CCD process (the Lapple model) is perceived as a standard method and has been considered by some engineers to be acceptable. However, there are several problems associated with this design procedure. First of all, the CCD process does not consider the cyclone inlet velocity in developing cyclone dimensions. It was reported (Parnell, 1996) that there is an "ideal" inlet velocity for the different cyclone designs for optimum cyclone performance. Secondly, the CCD does not predict the correct number of turns for different type cyclones. The overall efficiency predicted by the CCD process is incorrect because of the inaccurate fractional efficiency curve generated by the CCD process (Kaspar et al. 1993).

In order to use the CCD process, it is assumed that the design engineer will have knowledge of (1) flow conditions, (2) particulate matter (PM) concentrations and particle size distribution (PSD) and (3) the type of cyclone to be designed (high efficiency, conventional, or high throughput). The PSD must be in the form of mass fraction versus aerodynamic equivalent diameter of the PM. The cyclone type will provide all principle dimensions as a function of the cyclone barrel diameter (D). With these given data, the CCD process is as follows:

The Number of Effective Turns (N_e)

The first step of CCD process is to calculate the number of effective turns. The number of effective turns in a cyclone is the number of revolutions the gas spins while passing through the cyclone outer vortex. A higher number of turns of the air stream result in a higher collection efficiency. The Lapple model for N_e calculation is as follows:

$$N_e = \frac{1}{H_c}\left[L_c + \frac{Z_c}{2}\right] \tag{1}$$

Based on equation 1, the predicted numbers of turns for 4 cyclone designs were calculated and listed in the table 1. In table 1, 1D2D, 2D2D, and 1D3D cyclones are the cyclone designs shown in figures 2 and 3. These three cyclone designs have the same inlet dimensions (H_c and B_c), referred to as the 2D2D inlet. The 1D3Dt cyclone is a traditional 1D3D cyclone design, which has the same design dimensions as 1D3D cyclones in figure 2 except the inlet dimensions. The 1D3Dt cyclone has an inlet height equal to the barrel diameter ($H_c = D_c$) and an inlet width of one eighth of the barrel diameter ($B_c = D_c/8$). Table 1 gives the comparison of the predicted N_e vs. the observed N_e. It has been observed that the Lapple model for N_e produces an excellent estimation of the number of turns for the 2D2D cyclone designs. However, this model (equation 1) fails to give an accurate estimation of N_e for the cyclone design other than 2D2D design. This observation indicates a limitation for the Lapple model to accurately predict the number of effective turns. The N_e model is valid only for 2D2D cyclone designs, which was originally developed by Shepherd and Lapple (1939).

Table 1. Number of effective turns (N_e)

Cyclone	Lapple	Observed
1D2D	4	N/A
2D2D	6	6
1D3D	5	6
1D3Dt	2.5	6

Cut-Point (d_{50})

The second step of the CCD process is the calculation of the cut-point diameter. The cut-point of a cyclone is the aerodynamic equivalent diameter (AED) of the particle collected with 50% efficiency. As the cut-point diameter increases, the collection efficiency decreases.

The Lapple cut-point model was developed based upon force balance theory. The Lapple model for cut-point (d_{50}) is as follows:

$$d_{pc} = \left[\frac{9\mu W}{2\pi N_e V_i (\rho_p - \rho_g)} \right]^{1/2} \tag{2}$$

In the process to develop this cut-point model, it was assumed that the particle terminal velocity was achieved when the opposing drag force equaled the centrifugal force, and the drag force on every single particle was determined by Stokes law. As a result, the cut-point (d_{pc}, or d_{50}) determined by the Lapple model (equation 2) is an equivalent spherical diameter (ESD), or in other words, it is a Stokes diameter. The following equation can be used to convert ESD to AED for the spherical particles:

$$AED = \sqrt{\rho_p} * ESD \tag{3}$$

Since $\rho_p >> \rho_g$, it could be considered that $(\rho_p\text{-}\rho_g) \approx \rho_p$. Combining equations 2&3, the Lapple model for cut-point could be modified as follows:

$$d_{pc} = \left[\frac{9\mu W}{2\pi N_e V_i} \right]^{1/2} \text{ (in AED)} \tag{4}$$

Equation 4 is the Lapple model for cut-point in AED. This model indicates that the cut-point is totally independent of characteristics of the inlet PM. However, It has been reported (Wang et al. 2000) that the cyclone fractional efficiency curves are significantly affected by the particle size distribution of particulate matter entering. The cut-point shifted with the change of inlet PSD. The Lapple model for cut-point needs to be corrected for particle characteristics of inlet PM.

Fractional Efficiency Curve (FEC - η_j)

The third step of CCD process is to determine the fractional efficiency. Based upon the cut-point, Lapple then developed an empirical model (equation 5) for the prediction of the collection efficiency for any particle size, which is also known as fractional efficiency curve:

$$\eta_j = \frac{1}{1 + \left(d_{pc} / \bar{d}_{pj}\right)^2} \tag{5}$$

Overall Efficiency (η_o)

If a size distribution of the inlet particles is known, the overall collection efficiency of a cyclone can be calculated based on the cyclone fractional efficiency. The overall collection efficiency of a cyclone is the weighted average of the collection efficiencies for the various size ranges. It is given by:

$$\eta_o = \Sigma \eta_j m_j \tag{6}$$

Table 2 lists cyclone overall efficiencies predicted by the Lapple model and experimentally measured by Wang et al. (2000). The comparison in table 2 indicates that the Lapple model greatly underestimated the actual cyclone collection efficiency. As a result, the Lapple model for fractional efficiency curve (equation 5) needs to be corrected for accuracy.

Table 2. Overall efficiency

Cyclone	Lapple Model	Measured (Wang et. al, 2000)
1D2D	78.9 %	95 %
2D2D	86.6 %	96 %
1D3D	85.2 %	97 %

Pressure Drop (ΔP)

Cyclone pressure drop is another major parameter to be considered in the process of designing a cyclone system. Two steps are involved in the Lapple approach to estimation of cyclone pressure drop. The first step in this approach is to calculate the pressure drop in the number of inlet velocity heads (H_v) by equation 7. The second step in this approach is to convert the number of inlet velocity heads to a static pressure drop (ΔP) by equation 8:

$$H_v = K\frac{HW}{D_e^2} \tag{7}$$

$$\Delta P = \frac{1}{2}\rho_g V_i^2 H_v \tag{8}$$

There is one problem associated with this approach. "The Lapple pressure drop equation does not consider any vertical dimensions as contributing to pressure drop" (Leith and Mehta, 1973). This is a misleading in that a tall cyclone would have the same pressure drop as a short one as long as cyclone inlets and outlets dimensions and inlet velocities are the same. It has been considered that cyclone efficiency increases with an increase of the vertical dimensions. With the misleading by Lapple pressure drop model, one could conclude that the cyclone should be as long as possible since it would increase cyclone efficiency at no cost in pressure drop (Leith and Mehta, 1973). A new scientific approach is needed to predict cyclone pressure drop associated with the dimensions of a cyclone.

TEXAS A&M CYCLONE DESIGN (TCD)

Sizing Cyclone

Parnell (1996) addressed problems associated with the design of cyclones using the classical cyclone design (CCD) process and presented the Texas A&M cyclone design process (TCD) as an alternative. The TCD approach to design cyclones was to initially determine optimum inlet velocities (design velocities) for different cyclone designs. The design inlet velocities for 1D3D, 2D2D, and 1D2D cyclones are 16 m/s ±2 m/s (3200 ft/min ±400 ft/min), 15 m/s ±2 m/s (3000 ft/min ±400 ft/min), and 12 m/s ±2 m/s (2400 ft/min ±400 ft/min), respectively. This design process allows an engineer to design the cyclone using a cyclone inlet velocity specific to the type of cyclone desired. Knowing the design inlet velocities, a cyclone's dimensions could easily be determined by:

$$D_c = \sqrt{\frac{8Q}{V_i}} \qquad (9)$$

Pressure Drop (ΔP)

TCD process also provides an empirical model (equation 10) for cyclone pressure drop calculation. In this model, K is a dimensionless empirical constant and equals to 5.1, 4.7 and 3.4 for the 1D3D, 2D2D and 1D2D cyclones, respectively:

$$\Delta P = K * (VP_i + VP_o) \tag{10}$$

The TCD process is simpler by comparison with the CCD procedure and provides more accurate results for estimating pressure drop. But, the TCD process doesn't incorporate means for calculating the cyclone cut-point and fractional efficiency curve, so it cannot be used to estimate cyclone efficiency and emission concentration.

FRACTIONAL EFFICIENCY CURVE

The cyclone fractional efficiency curve (FEC) relates percent efficiency to the particle diameter and can be obtained from test data that include inlet and outlet concentrations and particle size distribution (PSD's). It is commonly assumed that the FEC can be defined by a cumulative lognormal distribution. As a lognormal distribution curve, the cyclone FEC can be characterized by the cut-point (d_{50}) and sharpness-of-cut (the slope of the FEC) of the cyclone (see figure 4). As mentioned above, the cut-point of a cyclone is the AED of the particle collected with 50% efficiency. The sharpness-of-cut (the slope of FEC) is defined as follows:

$$\text{Slope} = \frac{d_{84.1}}{d_{50}} = \frac{d_{50}}{d_{15.9}} \tag{11}$$

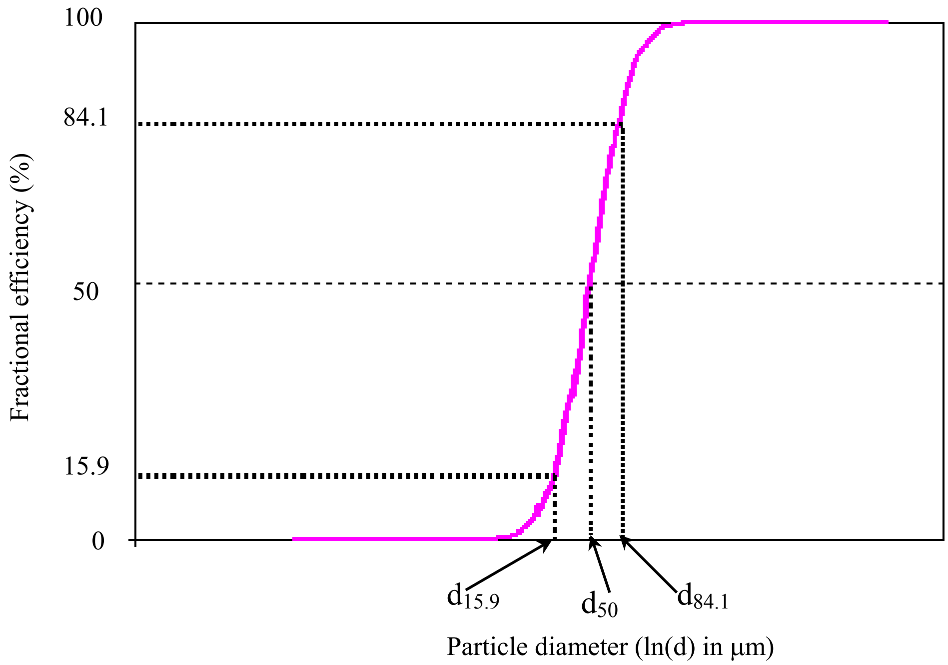

Figure 4. Fractional efficiency curve characteristics

CHAPTER II

RESEARCH OBJECTIVES

The goal of this research was to develop a sound scientific description of the operation of a cyclone that can be used to facilitate engineering design with a minimum of empirical data. The goal was achieved by developing the following models:

- Mathematical model for the number of effective turns.
- Theoretical model for predicting cyclone collection efficiency.
- Theoretical model for predicting cyclone pressure drop.

CHAPTER III

THE NUMBER OF EFFECTIVE TURNS

INTRODUCTION

A theoretical study of cyclone performance requires knowledge of the characteristics of the internal flow. This knowledge of the flow pattern in a cyclone fluid field is the basis for theoretical considerations for the prediction of the number of effective turns, pressure drop and dust collection efficiency. Many investigations have been made to determine the flow pattern (velocity profile) in a cyclone rotational field. Shepherd and Lapple (1939) reported that the primary flow pattern consisted of an outer spiral moving downward from the cyclone inlet and an inner spiral of smaller radius moving upward into the exit pipe (known as outer vortex and inner vortex). The transfer of fluid from the outer vortex to the inner vortex apparently began below the bottom of the exit tube and continued down into the cone to a point near the dust outlet at the bottom of the cyclone. They concluded from streamer and pitot tube observations that the radius marking the outer limit of the inner vortex and the inner limit of the outer vortex was roughly equal to the exit duct radius. Ter Linden (1949) measured the details of the flow field in a 36 cm (14 inch) cyclone. He reported that the interface of the inner vortex and outer vortex occurred at a radius somewhat less than that of the exit duct in the cylindrical section of the cyclone and approached the centerline in the conical section. In this research, the interface diameter was assumed to be the cyclone exit tube diameter ($D_o = D_e$).

The velocity profile in a cyclone can be characterized by three velocity components (tangential, axial and radial). The tangential velocity is the dominant velocity component. It also determines the centrifugal force applied to the air stream and to the particles. Research results (shown in figure 5) of Shepherd and Lapple (1939), Ter Linden (1949) and First (1950) indicated that tangential velocity in the annular section (at the same cross-sectional area) of the cyclone could be determined by:

$$V_t * r^n = C_1 \tag{12}$$

In equation 12, n is flow pattern factor and n is 0.5~0.8 in outer vortex; n is 0 at the boundary of inner vortex and outer vortex. The tangential velocity increases with a decrease of the rotational radius (r) in the outer vortex. It increases to the maximum at the boundary ($r = D_o/2$) of the outer vortex and inner vortex. In the inner vortex the tangential velocity decreases as the rotational radius decreases. In the inner vortex, the relationship of the tangential velocity and the rotational radius can be modeled by:

$$V_t / r = \omega = C_2 \tag{13}$$

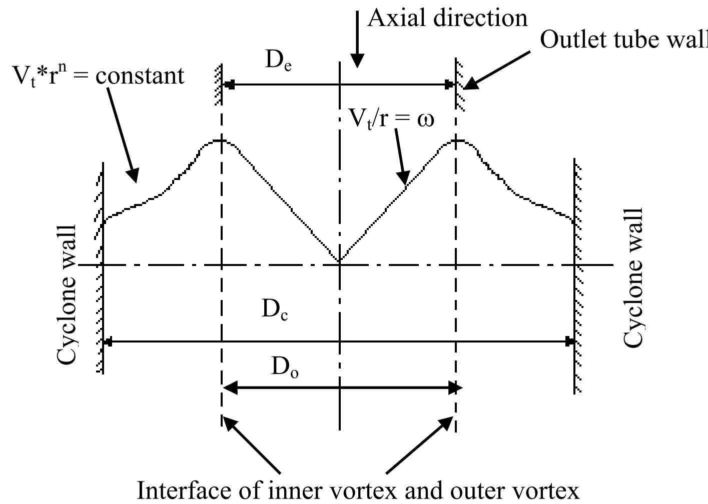

Figure 5. Tangential velocity distribution in a cyclone fluid field

FLOW PATTERN IN THE OUTER VORTEX

The following assumptions were made for the study of flow pattern:

- In the barrel part, there are two velocity components: tangential velocity (V_t) and axial velocity (V_z). Airflow rate in this zone is constant.
- In the cone, the air stream is squeezed because of change of the body shape. As a result, air leaks from outer vortex to inner vortex through their interface (D_o). The air leak (airflow rate) follows a linear model from the top of the cone part to the intersection of the vortexes interface and the cone walls. This assumption yields an effective length for the dust collection (Z_o, see figure 6). This cyclone effective length (also the length of inner vortex core) is determined by the diameter (D_o in figure 6) of the interface of the inner vortex and the outer vortex. Cyclone effective length does not necessarily reach the bottom of the cyclone

(Leith and Mehta, 1973). When the cyclone effective length is shorter than the cyclone physical length, the space between the bottom of the vortex and the bottom of the cyclone will not be used for particle collection. On the other hand, if the effective length is longer than the cyclone physical length, the vortex will extend beyond the bottom of the cyclone, and a dust re-entrance problem will occur. There are three velocity components in the cone part: tangential velocity (V_t), axial velocity (V_z) and radial velocity (V_r). (3) There is no radial acceleration for the air stream. In other words, the radial velocity of air stream is constant.

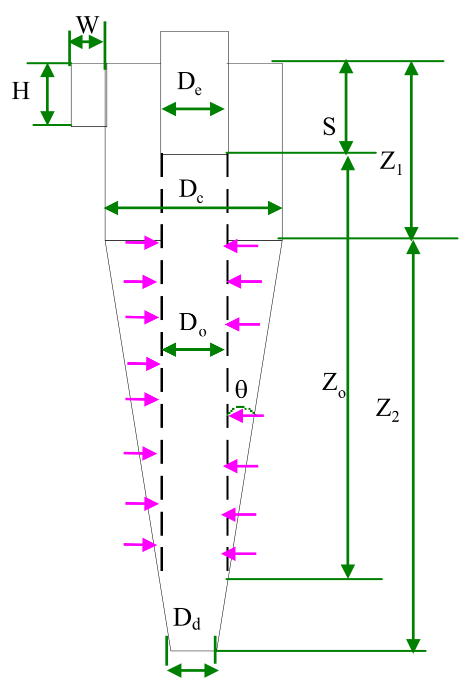

Figure 6. Interface (D_o) and effective length (Z_o) dimensions

Tangential Velocity (V_t)

Since the tangential velocity is the dominant velocity component that determines the centrifugal force applied to the air stream, it is essential to develop a theoretical model to determine the tangential velocity. The theoretical analysis for the tangential velocity starts with the analysis of the force on a unit control volume (I) of air stream. Figure 7 shows the forces acting on the control volume (I).

The size of the control volume (I) is (h*r*dr*dϕ). The centrifugal force acting on the control volume (I) is determined by:

$$F_c = \rho * h * r * d\phi * dr * \frac{V_t^2}{r} \tag{14}$$

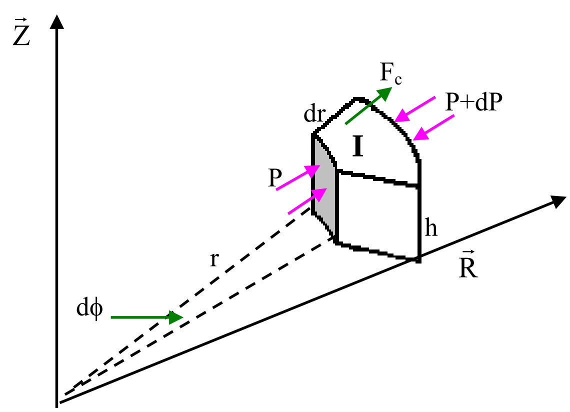

Figure 7. Force balance diagram on a unit control volume (I) of air stream

The pressure forces acting on the surfaces of the control volume are as follows

$$F_p = P * A_p = P * h * r * d\phi \tag{15}$$

$$F_{p+dp} = (P + dP) * A_{p+dp} = (P + dP) * h * (r + dr) * d\phi$$
$$\approx (P + dP) * h * r * d\phi \tag{16}$$

Based upon the assumption that there is no radial acceleration for the air stream, momentum conservation yields the force balance equation for the fluid as:

$F_c + F_p - F_{p+dp} = 0$, then

$$\rho * h * r * d\phi * dr * \frac{V_t^2}{r} + P * h * r * d\phi - (P + dP) * h * r * d\phi = 0 \tag{17}$$

It has been reported that in a cyclone outer vortex, fluid is irrotational flow. In other words, the fluid motion follows its streamline. Bernoulli's equation can be used to determine the pressure drop along the streamline, then

$$P + \rho * \frac{V_t^2}{2} = C_3 \tag{18}$$

Take the derivative of the equation 18 with respect to r, then

$$\frac{dP}{dr} + \rho * V_t * \frac{dV_t}{dr} = 0 \tag{19}$$

Combine equations 17 &19, the following relationship is obtained

$$\frac{dV_t}{V_t} + \frac{dr}{r} = 0 \tag{20}$$

The solution of equation 20 is

$$V_t * r = C_4 \tag{21}$$

This is the theoretical model for the tangential velocity distribution in the radial direction. It is assumed that in the barrel part of a cyclone, the tangential velocity (V_{t1}) is the same as inlet velocity along the cyclone wall, that is

$$V_{t1} = V_{in} \tag{22}$$

However, in the cone part, the tangential velocity along the cyclone wall (V_{t2}) follows the model in equation 21 such as $V_{t2} * r = V_{in} * R$ = constant, so

$$V_{t2} = \frac{R}{r} * V_{in} = \frac{R * V_{in}}{r_o + Z * \tan\theta} \tag{23}$$

Since tan θ = 1/8 for 1D3D, tan θ = 3/16 for 2D2D and tan θ = 1/8 for 1D2D (see figure 6 for the definition of θ), then

$$V_{t2} = \frac{4D_c * V_{in}}{Z + 2D_c} \qquad \text{(For 1D3D)}$$

$$V_{t2} = \frac{8D_c * V_{in}}{3Z + 4D_c} \qquad \text{(For 2D2D)}$$

$$V_{t2} = \frac{8D_c * V_{in}}{2Z + 5D_c} \qquad \text{(For (1D2D)} \tag{24}$$

Axial Velocity (V_z)

<u>In the barrel part (V_{z1})</u>

It is assumed that in the barrel part, the airflow rate is constant in the outer vortex; as a result, the axial velocity (V_z) can be determined by the following analysis:

Let $V_{z1} * \left(\frac{\pi * D_c^2}{4} - \frac{\pi * D_e^2}{4} \right) = V_{in} * \frac{D_c^2}{8}$ for the constant flow rate. Plug in D_e dimension for 1D3D, 2D2D and 1D2D cyclone designs (see figures 2&3), then

$$V_{z1} = \frac{2V_{in}}{3\pi} \qquad \text{(For 1D3D and 2D2D)}$$

$$V_{z1} = \frac{8V_{in}}{13\pi} \qquad \text{(For 1D2D)} \tag{25}$$

<u>In the cone part (V_{z2})</u>

As assumed above, in the cone part of a cyclone, the airflow leaks from outer vortex to inner vortex flowing a linear model as:

$$Q_z = Q_{in} * \frac{Z}{Z_{o2}} \tag{26}$$

So, the axial velocity in the cone part can be determined by

$$V_{z2} = -\frac{Q_z}{A_z} = \frac{-Q_{in}}{\pi * (R - r_o)} * \frac{1}{\frac{R - r_o}{Z_{o2}} * Z + 2r_o} \tag{27}$$

Figure 8 shows the dimensions for the axial velocity calculation in the cone part. Z_{o2} is the effective length in the cone part. It is determined by the interface diameter and cyclone design. For 1D3D, 2D2D and 1D2D cyclone designs, Z_{o2} dimensions are Z_{o2} = $2D_c$ (for 1D3D), $Z_{o2} = 4D_c/3$ (for 2D2D) and $Z_{o2} = 3D_c/2$ (for 1D2D).

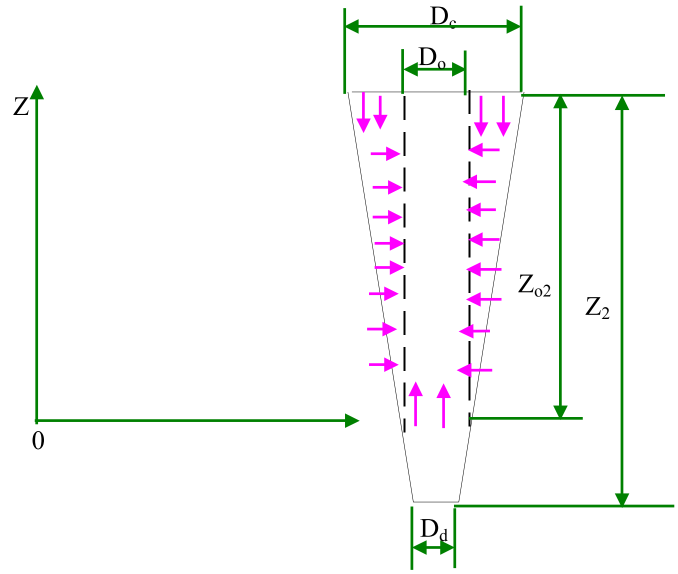

Figure 8. Cyclone cone dimensions

Based upon Z_{o2} dimension and equation 27, the axial velocities for 1D3D, 2D2D and 1D2D designs are as follows:

$$V_{z2} = -\frac{4D_c * V_{in}}{(Z + 4D_c) * \pi} \qquad \text{(For 1D3D)}$$

$$V_{z2} = -\frac{8D_c * V_{in}}{(3Z + 8D_c) * \pi} \qquad \text{(For 2D2D)} \qquad (28)$$

For the 1D2D cyclone design, the outlet tube is extended into cyclone cone part for the length of $D_c/8$ (see figure 3 for 1D2D design). This divides the cone part into two zones. In zone 1, which is from the top of the cone to the bottom of outlet tube, there is no air leak from outer vortex to inner vortex. As a result, the axial velocity in this zone (V_{z21}) is the same as in the barrel part, which is

$$V_{z21} = -\frac{8V_{in}}{13\pi} \qquad \text{(For 1D2D in the zone 1 of cone part)} \qquad (29)$$

In the zone 2 of the cone part, which is from the bottom of outlet tube to the bottom of interface cone, the air leaks from outer vortex to inner vortex following a linear pattern as defined in equations 26 and 27. In this zone, the axial velocity (V_{z22}) is as follows:

$$V_{z22} = -\frac{16D_c * V_{in}}{(3Z + 15D_c) * \pi} \qquad \text{(For 1D2D in the zone 2 of cone part)} \qquad (30)$$

Radial Velocity (V_r)

It was assumed that the radial velocity is zero in the barrel part. In the cone part of a cyclone the radial velocity can be determined by $V_{r2} = V_{z2} * \tan\theta$, so

$$V_{r2} = \frac{D_c * V_{in}}{(2Z + 8D_c) * \pi} \qquad \text{(For 1D3D)}$$

$$V_{r2} = \frac{3D_c * V_{in}}{(6Z + 16D_c) * \pi} \qquad \text{(For 2D2D)}$$

$$V_{r21} = \frac{V_{in}}{13\pi} \qquad \text{(For 1D2D in the zone 1)}$$

$$V_{r22} = \frac{2D_c * V_{in}}{(3Z + 15D_c) * \pi} \qquad \text{(For 1D2D in the zone 2)} \qquad (31)$$

AIR STREAM TRAVEL DISTANCE

Travel Distance in the Barrel Part (L_1)

To calculate air stream travel distance in the barrel part, it is first necessary to determine the total average velocity (V_1) of air stream. Since there are only two velocity components in the barrel part, the total average velocity can be obtained by

$$V_1 = \sqrt{V_{t1}^2 + V_{z1}^2} \qquad (32)$$

V_{t1} and V_{z1} are determined by equations 22 and 25. Then, the travel distance can be calculated by the velocity and traveling time such as

$$L_1 = \int_0^{t_1} V_1 dt = \int_0^{Z_1} \sqrt{V_{t1}^2 + V_{z1}^2} \frac{dz}{V_{z1}} \qquad (33)$$

The solutions for equation 33 are as follows

$L_1 = 1.53\ \pi D_c = 4.8\ D_c$ (For 1D3D)

$L_1 = 3.06\ \pi D_c = 9.6\ D_c$ (For 2D2D)

$L_1 = 1.66\ \pi D_c = 5.2\ D_c$ (For 1D2D) (34)

Travel Distance in the Cone Part (L_2)

In the cone part of a cyclone, the total average velocity is determined by three velocity components as follows:

$$V_2 = \sqrt{V_{t2}^2 + V_{z2}^2 + V_{r2}^2} \qquad (35)$$

In this equation, V_{t2}, V_{z2} and V_{r2} are modeled by equations 24, 28, 29, 30 and 31. The travel distance in the cone part can be obtained through the following calculations:

$$L_2 = \int_0^{t_2} V_2 dt = \int_0^{Z_{o2}} \sqrt{V_{t2}^2 + V_{z2}^2 + V_{r2}^2} \frac{dz}{V_{z2}} \quad (36)$$

- For the 1D3D cyclone:

$$L_2 = \int_0^{2D_c} \sqrt{\left(\frac{1}{Z + 2D_c}\right)^2 + \left(\frac{1}{Z\pi + 4\pi D_c}\right)^2 + \left(\frac{1}{8\pi Z + 32\pi D_c}\right)} * (Z + 4D_c)\pi * dz$$

- For the 2D2D cyclone:

$$L_2 = \int_0^{4D_c/3} \sqrt{\left(\frac{1}{3Z + 4D_c}\right)^2 + \left(\frac{1}{3Z\pi + 8\pi D_c}\right)^2 + \left(\frac{1}{48\pi Z + 128\pi D_c}\right)} * (3Z + 8D_c)\pi * dz$$

- For 1D2D cyclone:

$$L_2 = \int_{11D_c/8}^{3D_c/2} \sqrt{\left(\frac{D_c}{2Z + 5D_c}\right)^2 + \left(\frac{1}{13\pi}\right)^2 + \left(\frac{1}{104\pi}\right)^2} * 13\pi * dz$$

$$+ \int_0^{11D_c/8} \sqrt{\left(\frac{1}{4Z + 10D_c}\right)^2 + \left(\frac{1}{3Z\pi + 15D_c\pi}\right)^2 + \left(\frac{1}{24Z\pi + 120D_c\pi}\right)^2} * (3Z + 15D_c) * dz$$

Software Mathcad (2002) was used to solve L_2's for different cyclone diameters i.e. D_c = 0.1 m (4 inch), 0.15 m (6 inch), 0.3 m (12 inch), 0.6 m (24 inch) and 0.9 m (36 inch). The detailed Mathcad calculations are included in appendix D. The general solutions for the L_2's with different cyclone diameters are:

$L_2 = 10.83\ D_c$ (For 1D3D)

$L_2 = 7.22\ D_c$ (For 2D2D)

$L_2 = 2.57\ D_c$ (For 1D2D) (37)

NUMBER OF EFFECTIVE TURNS

In theory, the air stream travel distance in the outer vortex and the cyclone dimensions determine the number of effective turns (Wang et al, 2001). In a cyclone barrel part the number of turns is defined by

$$N_{e1} = \frac{L_1}{\pi * D_c} \tag{38}$$

In the cone part of a cyclone the number of turns is determined by

$$N_{e2} = \frac{L_2}{\pi * \left(\frac{D_c + D_o}{2}\right)} \tag{39}$$

Table 3 summarizes the calculation of air stream travel distance and number of effective turns for 1D3D, 2D2D and 1D2D cyclones with different sizes.

Table 3. Air stream travel distance and number of effective turns

Cyclone	Barrel Part		Cone Part		Total	
Design	L_1	N_{e1}	L_2	N_{e2}	L	N_e
1D3D	4.8 D_c	1.53	10.83 D_c	4.60	15.63 D_c	6.13
2D2D	9.6 D_c	3.06	7.22 D_c	3.07	16.82 D_c	6.13
1D2D	5.2 D_c	1.66	2.57 D_c	1.01	7.77 D_c	2.67

SUMMARY

A new theoretical method for computing air stream travel distance and number of turns has been developed in this chapter. The flow pattern and cyclone dimensions determine the air stream travel distance in the outer vortex of a cyclone. The number of effective turns for different cyclone sizes was calculated based upon the air stream travel distance and cyclone dimensions. The calculations indicate that the number of effective turns is determined by the cyclone design, and is independent of cyclone diameter (size) and inlet velocity. There are 6.13 turns in both 1D3D and 2D2D cyclones and 2.67 turns in the 1D2D cyclones.

CHAPTER IV

CYCLONE PRESSURE DROP

INTRODUCTION

In the evaluation of a cyclone design, pressure drop is a primary consideration. Because it is directly proportional to the energy requirement, under any circumstance, knowledge of pressure drop through a cyclone is essential in designing a fan system.

Many models have been developed to determine the cyclone pressure drop such as Shepherd and Lapple (1939), Stairmand (1949, 1951), First (1950) and Barth (1956). However, the equations are either empirical models or involve variables and dimensionless parameters not easily evaluated for in practical applications. It is known that cyclone pressure drop is dependent on the cyclone design and its operating parameters such as inlet velocity. The empirical models cannot be used for all the cyclone designs as new cyclone technology and new cyclone designs are developed. Further theoretical research is needed to scientifically evaluate the cyclone performance including predicting cyclone pressure drop.

Shepherd and Lapple (1939) reported that a cyclone pressure drop was composed of the following components:

1. Loss due to expansion of gas when it enters the cyclone chamber.
2. Loss as kinetic energy of rotation in the cyclone chamber.
3. Loss due to wall friction in the cyclone chamber.

4. Any additional friction losses in the exit duct, resulting from the swirling flow above and beyond those incurred by straight flow.
5. Any regain of the rotational kinetic energy as pressure energy.

THEORETICAL ANALYSIS OF PRESSURE DROP

In general, cyclone pressure loss can be obtained by summing all individual pressure loss components. The following pressure loss components are involved in the analysis of cyclone pressure loss for this research:

1. Cyclone entry loss (ΔP_e).
2. Kinetic energy loss (ΔP_k).
3. Frictional loss in the outer vortex (ΔP_f).
4. Kinetic energy loss caused by the rotational field (ΔP_r).
5. Pressure loss in the inner vortex and exit tube (ΔP_o).

Cyclone Entry Loss (ΔP_e)

A cyclone entry loss is the dynamic pressure loss in the inlet duct and can be determined by:

$$\Delta P_e = C_5 * VP_{in} \tag{40}$$

In this equation, C_5 is the dynamic loss constant and VP_{in} is the inlet velocity pressure.

Kinetic Energy Loss (ΔP_k)

This part of energy loss is caused by the area change (velocity change) from the inlet tube to outlet tube. It can be calculated by:

$$\Delta P_k = VP_{in} - VP_{out} \qquad (41)$$

Frictional Loss in the Outer Vortex (ΔP_f)

The frictional pressure loss is the pressure loss in the cyclone outer vortex caused by the friction of air/surface wall. In the outer vortex, air stream flows in a downward spiral through the cyclone. It may be considered that the air stream travels in an imaginary spiral tube (figure 9) with diameter D_s and length L (travel distance in the outer vortex). The frictional pressure loss can be determined by Darcy's equation:

$$d\Delta P_f = f * \frac{VP_s}{D_s} * dL \qquad (42)$$

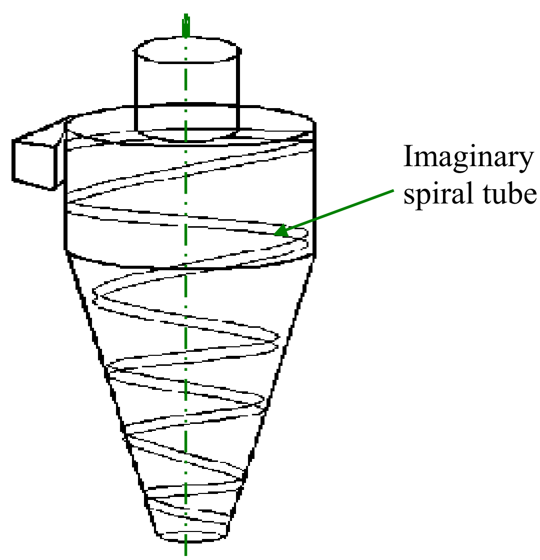

Figure 9. Imaginary spiral tube of air stream in the outer vortex

In the barrel part (ΔP_{f1})

The equivalent stream diameter (D_{s1}) was used to quantify the size of oval-shape stream (stream in the imaginary spiral tube). The flow rate and total velocity of the stream determine this equivalent diameter as shown in the equation 43:

$$V_{s1} * \frac{\pi * D_{s1}^2}{4} = V_{in} * \frac{D_c^2}{8} \tag{43}$$

In this equation, V_{s1} is the total velocity of air stream in the outer vortex of barrel part. So, $V_{s1} = V_1$ determined by equation 32, then

$D_{s1} = 0.395\ D_c$ (for 1D3D, 2D2D and 1D2D)

The friction pressure loss in the barrel part can be determined as follows:

$$\Delta P_{f1} = \int_0^{L_1} f * \frac{VP_{s1}}{D_{s1}} dL = \int_0^{Z_1} f * \frac{VP_{s1}}{D_{s1}} * V_1 * \frac{dZ}{V_{z1}} \tag{44}$$

In this equation, VP_{s1} is the stream velocity pressure determined by stream velocity V_{s1}. f is the friction factor and is a function of Reynolds number (R_e, equation 45) and the degree of roughness of imaginary spiral tube surface.

$$R_e = \frac{D * V * \rho}{\mu} \tag{45}$$

The friction factor (f) can be obtained from the Moody chart (the friction chart) based upon the relative roughness factor (e/D) of tube surface and fluid Reynolds number. In this case, since the imaginary tube consists of the cyclone inside surface on the one side and air stream on the other side. one-half of the friction factors obtained from chart were used for pressure drop calculation in equation 44. Table 4 lists the friction factors for 1D3D, 2D2D and 1D2D cyclones at their respective design inlet velocities.

Table 4. Friction factors (f) for frictional pressure loss calculation

Cyclone	Size (D_c)	e/D_c	Re	f (moody chart)	f (for ΔP_f models)
1D3D	0.2 m (6 inch)	0.0010	$1.64 *10^5$	0.022	0.011
	0.9 m (36 inch)	0.0002	$9.85*10^5$	0.016	0.008
2D2D	0.2 m (6 inch)	0.0010	$1.54 *10^5$	0.022	0.011
	0.9 m (36 inch)	0.0002	$9.20*10^5$	0.015	0.008
1D2D	0.2 m (6 inch)	0.0010	$1.23 *10^5$	0.023	0.012
	0.9 m (36 inch)	0.0002	$7.40*10^5$	0.015	0.008

Equation 44 is the friction loss model in the barrel part of a cyclone. This model indicates that the friction pressure loss is a function of the air stream travel distance in the outer vortex of the barrel part. In other words, the friction loss is a function of the cyclone height. The higher a cyclone body, the higher the friction loss. The following results were obtained from equation 44 for predicting friction loss in the barrel part of a cyclone:

$$\Delta P_{f1} = 0.13 * VP_{s1} = 0.14 * VP_{in} \quad \text{(For 1D3D)}$$

$$\Delta P_{f1} = 0.27 * VP_{s1} = 0.28 * VP_{in} \quad \text{(For 2D2D)}$$

$$\Delta P_{f1} = 0.14 * VP_{s1} = 0.15 * VP_{in} \quad \text{(For 1D2D)} \qquad (46)$$

<u>In the cone part (ΔP_{f2})</u>

In the cone part, the equivalent stream diameter (D_{s2}) is determined by

$$V_{s2} * \frac{\pi * D_{s2}^2}{4} = V_{in} * \frac{D_c^2}{8} * \frac{Z}{Z_{o2}} \tag{47}$$

The friction pressure loss in the cone part can be determined as follows:

$$\Delta P_{f2} = \int_0^{L_2} f * \frac{VP_{s2}}{D_{s2}} dL = \int_{Z_{o2}}^{0} f * \frac{VP_{s2}}{D_{s2}} * V_2 * \frac{dZ}{V_{z2}} \tag{48}$$

The solutions of equation 48 for 1D3D, 2D2D and 1D2D are as follows:

- For the 1D3D cyclone:

$$\Delta P_{f2} = \int_0^{2D_c} \frac{f}{2} * VP_{in} * \left(\frac{\pi}{D_c}\right)^{\frac{3}{2}} * \left(\frac{Z + 4D_c}{\sqrt{Z}}\right) * \left[\left(\frac{4D_c}{Z + 2D_c}\right)^2 + \left(\frac{4D_c}{Z\pi + 4D_c\pi}\right)^2 + \left(\frac{D_c}{2Z\pi + 8D_c\pi}\right)^2\right]^{\frac{7}{4}} dZ$$

- For the 2D2D cyclone:

$$\Delta P_{f2} = \int_0^{4D_c/3} \frac{f}{\sqrt{24}} * VP_{in} * \left(\frac{\pi}{D_c}\right)^{\frac{3}{2}} * \left(\frac{3Z + 8D_c}{\sqrt{Z}}\right) * \left[\left(\frac{8D_c}{3Z + 4D_c}\right)^2 + \left(\frac{8D_c}{3Z\pi + 8D_c\pi}\right)^2 + \left(\frac{3D_c}{6Z\pi + 16D_c\pi}\right)^2\right]^{\frac{7}{4}} dZ$$

- For 1D2D cyclone:

$$\Delta P_{f2} = \int_0^{3D_c/2} \frac{f\sqrt{3}}{16} * VP_{in} * \left(\frac{\pi}{D_c}\right)^{\frac{3}{2}} * \left(\frac{3Z + 15D_c}{\sqrt{Z}}\right) * \left[\left(\frac{8D_c}{2Z + 5D_c}\right)^2 + \left(\frac{16D_c}{3Z\pi + 15D_c\pi}\right)^2 + \left(\frac{2D_c}{3Z\pi + 15D_c\pi}\right)^2\right]^{\frac{7}{4}} dZ$$

These solutions of equation 48 are the models to predict friction loss in the cone part of a cyclone. The friction factor, f, is determined in table 4. Again, the above models indicate that the friction loss in the cone part is a function of air stream travel distance in the outer vortex of the cone. Therefore, the friction loss in the cone is a function of the height of the cone. Appendix E demonstrates the calculations of friction loss in the cone part of a cyclone with different inlet velocities and cyclone diameters.

Kinetic Energy Loss Caused by the Rotational Field (ΔP_r)

In the cyclone cone, the rotation of the airflow establishes a pressure field because of radial acceleration. The rotational energy loss is the energy that is used to overcome centrifugal force and allow the stream to move from outer vortex to inner vortex. To develop an equation for the rotational kinetic energy loss, it is assumed that the direction of rotation in both inner vortex and outer vortex is the same so that little friction is to be expected at their interface (the junction point).

The rotational loss can be quantified as the pressure change in the pressure field from cyclone cone wall to the vortex interface. This pressure change has been determined in the theoretical analysis of tangential velocity (equation 17). In fact equation 17 indicates the following

$$dP = \rho * \frac{V_t^2}{r} * dr \tag{49}$$

Solving equation 49, the rotational loss can be obtained as the follows:

$$\Delta P_r = \rho * V_{in}^2 * \left(\frac{R}{r_o} - 1\right) \tag{50}$$

Then, $\Delta P_r = 2\ VP_{in}$ (For 1D3D and 2D2D)

$\Delta P_r = 1.22\ VP_{in}$ (For 1D2D)

Pressure Loss in the Inner Vortex and Exit Tube (ΔP_o)

The inner vortex is assumed to have a constant height of spiral and constant angle of inclination to the horizontal, and to have the same rotational velocity at the same radius at any vertical position. The method of calculation on this part of the pressure component will be to determine the average pressure loss in the inner vortex and the exit tube. It can be determined as follows:

$$\Delta P_o = C_6 * VP_{out} \tag{51}$$

In this equation, C_6 is the dynamic loss constant and VP_{out} is the outlet velocity pressure.

Cyclone Total Pressure Loss (ΔP_{total})

Cyclone total pressure is obtained by simply summing up the five pressure drop components as follows:

$$\Delta P_{total} = \Delta P_e + \Delta P_k + \Delta P_f + \Delta P_r + \Delta P_o \tag{52}$$

Cyclone Pressure Drop Predictions

Equations 40, 41, 46, 48, 50 and 51 are the models to predict five pressure loss components. Based on these models pressure drops for different sizes of cyclones with different inlet velocities were calculated. Details of the calculations for friction losses in the cone part are included in appendix E. Predicted pressure drops listed in tables 5 – 13. The predictions of pressure drop indicate: (1) Cyclone pressure drop is independent of cyclone size. (2) Frictional loss in the outer vortex and the rotational energy loss in a cyclone are the major pressure loss components. (3) Frictional loss is a function of cyclone height. The higher a cyclone height, the higher the friction loss.

Table 5. Predicted pressure drop for 1D3D at V_{in} = 16 m/s (3200 ft/min)

Cyclone Size	ΔP_e	ΔP_k	ΔP_f		ΔP_r	ΔP_o	Total ΔP
			ΔP_{f1}	ΔP_{f2}			
0.1 (4)	159 (0.64)	95 (0.38)	22 (0.09)	359 (1.44)	319 (1.28)	117 (0.47)	1071 (4.3)
0.2 (6)	159 (0.64)	95 (0.38)	22 (0.09)	359 (1.44)	319 (1.28)	117 (0.47)	1071 (4.3)
0.3 (12)	159 (0.64)	95 (0.38)	22 (0.09)	359 (1.44)	319 (1.28)	117 (0.47)	1071 (4.3)
0.6 (24)	159 (0.64)	95 (0.38)	22 (0.09)	359 (1.44)	319 (1.28)	117 (0.47)	1071 (4.3)
0.9 (36)	159 (0.64)	95 (0.38)	22 (0.09)	359 (1.44)	319 (1.28)	117 (0.47)	1071 (4.3)

- Cyclone size: meter (inch) and pressure drop: Pa (inch H_2O)

Table 6. Predicted pressure drop for 1D3D with D_c = 0.2 m (6 inch)

Velocity	ΔP_e	ΔP_k	ΔP_f	ΔP_r	ΔP_o	Total
5 (1000)	16 (0.06)	9 (0.04)	37 (0.15)	31 (0.12)	11 (0.05)	104 (0.42)
8 (1500)	35 (0.14)	21 (0.08)	84 (0.34)	70 (0.28)	26 (0.10)	235 (0.94)
10 (2000)	62 (0.25)	37 (0.15)	149 (0.60)	124 (0.50)	45 (0.18)	417 (1.68)
13 (2500)	97 (0.39)	58 (0.23)	232 (0.93)	194 (0.78)	71 (0.28)	652 (2.62)
15 (3000)	140 (0.56)	83 (0.33)	335 (1.35)	279 (1.12)	102 (0.41)	939 (3.77)
16 (3200)	159 (0.64)	95 (0.38)	381 (1.53)	319 (1.28)	117 (0.47)	1071 (4.29)
18 (3500)	190 (0.76)	113 (0.45)	456 (1.83)	380 (1.53)	139 (0.56)	1279 (5.13)
20 (4000)	248 (1.00)	148 (0.59)	596 (2.39)	497 (2.00)	181 (0.73)	1670 (6.71)

- Velocity: m/s (ft/min) and pressure drop: Pa (inch H_2O)

Table 7. Predicted pressure drop for 1D3D with D_c = 0.9 m (36 inch)

Velocity	ΔP_e	ΔP_k	ΔP_f	ΔP_r	ΔP_o	Total
5 (1000)	16 (0.06)	9 (0.04)	37 (0.15)	31 (0.12)	11 (0.05)	104 (0.42)
8 (1500)	35 (0.14)	21 (0.08)	84 (0.34)	70 (0.28)	26 (0.10)	235 (0.94)
10 (2000)	62 (0.25)	37 (0.15)	149 (0.60)	124 (0.50)	45 (0.18)	417 (1.68)
13 (2500)	97 (0.39)	58 (0.23)	232 (0.93)	194 (0.78)	71 (0.28)	652 (2.62)
15 (3000)	140 (0.56)	83 (0.33)	335 (1.35)	279 (1.12)	102 (0.41)	939 (3.77)
16 (3200)	159 (0.64)	95 (0.38)	381 (1.53)	319 (1.28)	117 (0.47)	1071 (4.29)
18 (3500)	190 (0.76)	113 (0.45)	456 (1.83)	380 (1.53)	139 (0.56)	1279 (5.13)
20 (4000)	248 (1.00)	148 (0.59)	596 (2.39)	497 (2.00)	181 (0.73)	1670 (6.71)

- Velocity: m/s (ft/min) and pressure drop: Pa (inch H_2O)

Table 8. Predicted pressure drop for 2D2D at V_{in} = 15 m/s (3000 ft/min)

Cyclone	ΔP_e	ΔP_k	ΔP_f		ΔP_r	ΔP_o	Total
Size			ΔP_{f1}	ΔP_{f2}			ΔP
0.1 (4)	140 (0.56)	82 (0.33)	40 (0.16)	212 (0.85)	279 (1.12)	103 (0.41)	854 (3.43)
0.2 (6)	140 (0.56)	82 (0.33)	40 (0.16)	212 (0.85)	279 (1.12)	103 (0.41)	854 (3.43)
0.3 (12)	140 (0.56)	82 (0.33)	40 (0.16)	212 (0.85)	279 (1.12)	103 (0.41)	854 (3.43)
0.6 (24)	140 (0.56)	82 (0.33)	40 (0.16)	212 (0.85)	279 (1.12)	103 (0.41)	854 (3.43)
0.9 (36)	140 (0.56)	82 (0.33)	40 (0.16)	212 (0.85)	279 (1.12)	103 (0.41)	854 (3.43)

- Cyclone size: meter (inch) and pressure drop: Pa (inch H_2O)

Table 9. Predicted pressure drop for 2D2D with D_c = 0.2 m (6 inch)

Velocity	ΔP_e	ΔP_k	ΔP_f	ΔP_r	ΔP_o	Total
5 (1000)	16 (0.06)	9 (0.04)	27 (0.11)	31 (0.12)	11 (0.05)	94 (0.38)
8 (1500)	35 (0.14)	21 (0.08)	62 (0.25)	70 (0.28)	26 (0.10)	213 (0.86)
10 (2000)	62 (0.25)	37 (0.15)	111 (0.45)	124 (0.50)	45 (0.18)	379 (1.53)
13 (2500)	97 (0.39)	58 (0.23)	174 (0.70)	194 (0.78)	71 (0.28)	593 (2.38)
15 (3000)	140 (0.56)	83 (0.33)	250 (1.00)	279 (1.12)	102 (0.41)	854 (3.43)
16 (3200)	159 (0.64)	95 (0.38)	285 (1.14)	319 (1.28)	117 (0.47)	972 (3.91)
18 (3500)	190 (0.76)	113 (0.45)	339 (1.36)	380 (1.53)	139 (0.56)	1161 (4.66)
20 (4000)	248 (1.00)	148 (0.59)	445 (1.79)	497 (2.00)	181 (0.73)	1519 (6.10)

- Velocity: m/s (ft/min) and pressure drop: Pa (inch H_2O)

Table 10. Predicted pressure drop for 2D2D with D_c = 0.9 m (36 inch)

Velocity	ΔP_e	ΔP_k	ΔP_f	ΔP_r	ΔP_o	Total
5 (1000)	16 (0.06)	9 (0.04)	27 (0.11)	31 (0.12)	11 (0.05)	94 (0.38)
8 (1500)	35 (0.14)	21 (0.08)	62 (0.25)	70 (0.28)	26 (0.10)	213 (0.86)
10 (2000)	62 (0.25)	37 (0.15)	111 (0.45)	124 (0.50)	45 (0.18)	379 (1.53)
13 (2500)	97 (0.39)	58 (0.23)	174 (0.70)	194 (0.78)	71 (0.28)	593 (2.38)
15 (3000)	140 (0.56)	83 (0.33)	250 (1.00)	279 (1.12)	102 (0.41)	854 (3.43)
16 (3200)	159 (0.64)	95 (0.38)	285 (1.14)	319 (1.28)	117 (0.47)	972 (3.91)
18 (3500)	190 (0.76)	113 (0.45)	339 (1.36)	380 (1.53)	139 (0.56)	1161 (4.66)
20 (4000)	248 (1.00)	148 (0.59)	445 (1.79)	497 (2.00)	181 (0.73)	1519 (6.10)

- Velocity: m/s (ft/min) and pressure drop: Pa (inch H_2O)

Table 11. Predicted pressure drop for 1D2D at V_{in} = 12 m/s (2400 ft/min)

Cyclone Size	ΔP_e	ΔP_k	ΔP_f		ΔP_r	ΔP_o	Total ΔP
			ΔP_{f1}	ΔP_{f2}			
0.1 (4)	89 (0.36)	75 (0.30)	12 (0.05)	80 (0.32)	107 (0.43)	27 (0.11)	392 (1.57)
0.2 (6)	89 (0.36)	75 (0.30)	12 (0.05)	80 (0.32)	107 (0.43)	27 (0.11)	392 (1.57)
0.3 (12)	89 (0.36)	75 (0.30)	12 (0.05)	80 (0.32)	107 (0.43)	27 (0.11)	392 (1.57)
0.6 (24)	89 (0.36)	75 (0.30)	12 (0.05)	80 (0.32)	107 (0.43)	27 (0.11)	392 (1.57)
0.9 (36)	89 (0.36)	75 (0.30)	12 (0.05)	80 (0.32)	107 (0.43)	27 (0.11)	392 (1.57)

- Cyclone size: meter (inch) and pressure drop: Pa (inch H_2O)

Table 12. Predicted pressure drop for 1D2D with D_c = 0.2 m (6 inch)

Velocity	ΔP_e	ΔP_k	ΔP_f	ΔP_r	ΔP_o	Total
5 (1000)	16 (0.06)	13 (0.05)	17 (0.07)	19 (0.07)	5 (0.02)	69 (0.28)
8 (1500)	35 (0.14)	29 (0.12)	37 (0.15)	42 (0.17)	11 (0.04)	153 (0.62)
10 (2000)	62 (0.25)	52 (0.21)	64 (0.26)	75 (0.30)	19 (0.07)	271 (1.09)
12 (2400)	89 (0.36)	75 (0.30)	94 (0.38)	107 (0.43)	27 (0.11)	392 (1.57)
15 (3000)	140 (0.56)	117 (0.47)	146 (0.59)	168 (0.67)	42 (0.17)	611 (2.46)
16 (3200)	159 (0.64)	133 (0.53)	168 (0.67)	191 (0.77)	47 (0.19)	697 (2.80)
18 (3500)	190 (0.76)	159 (0.64)	200 (0.80)	228 (0.92)	57 (0.23)	834 (3.35)
20 (4000)	248 (1.00)	207 (0.83)	261 (1.05)	298 (1.20)	74 (0.30)	1089 (4.37)

- Velocity: m/s (ft/min) and pressure drop: Pa (inch H_2O)

Table 13. Predicted pressure drop for 1D2D with D_c = 0.9 m (36 inch)

Velocity	ΔP_e	ΔP_k	ΔP_f	ΔP_r	ΔP_o	Total
5 (1000)	16 (0.06)	13 (0.05)	17 (0.07)	19 (0.07)	5 (0.02)	69 (0.28)
8 (1500)	35 (0.14)	29 (0.12)	37 (0.15)	42 (0.17)	11 (0.04)	153 (0.62)
10 (2000)	62 (0.25)	52 (0.21)	64 (0.26)	75 (0.30)	19 (0.07)	271 (1.09)
12 (2400)	89 (0.36)	75 (0.30)	94 (0.38)	107 (0.43)	27 (0.11)	392 (1.57)
15 (3000)	140 (0.56)	117 (0.47)	146 (0.59)	168 (0.67)	42 (0.17)	611 (2.46)
16 (3200)	159 (0.64)	133 (0.53)	168 (0.67)	191 (0.77)	47 (0.19)	697 (2.80)
18 (3500)	190 (0.76)	159 (0.64)	200 (0.80)	228 (0.92)	57 (0.23)	834 (3.35)
20 (4000)	248 (1.00)	207 (0.83)	261 (1.05)	298 (1.20)	74 (0.30)	1089 (4.37)

- Velocity: m/s (ft/min) and pressure drop: Pa (inch H_2O)

TESTING OF THE NEW MODELS

System Setup

An experiment was conducted to measure cyclone pressure drops at different inlet velocities for the comparison of measured pressure drop versus predicted pressure drop by the new theory developed in this research. The experimental setup is shown in figure 10. The tested cyclones were 0.2 meter (6 inch) in diameter. Pressure transducers and data loggers (HOBO) were used to obtain the differential pressure from cyclone inlet and outlet and the pressure drop across orifice meter.

The orifice pressure drop was used to monitor the system airflow rate by the following relationship:

$$Q = 3.478 * K * D_o^2 * \sqrt{\frac{\Delta P}{\rho_a}} \qquad (53)$$

In this equation, K is a dimensionless orifice meter coefficient determined by experimental calibration of the orifice meter with a Laminar Flow Element. A problem was observed during the tests. In order to measure the static pressure drop through cyclones, the static pressure taps (figure 11) were inserted into air stream such that the static pressure sensing position was in the direction of airflow. In the outlet tube, the air stream is spiraling upward. This spiral path caused some difficulties in measuring static pressure in the outlet tube if the static pressure taps were not placed properly in the exit tube.

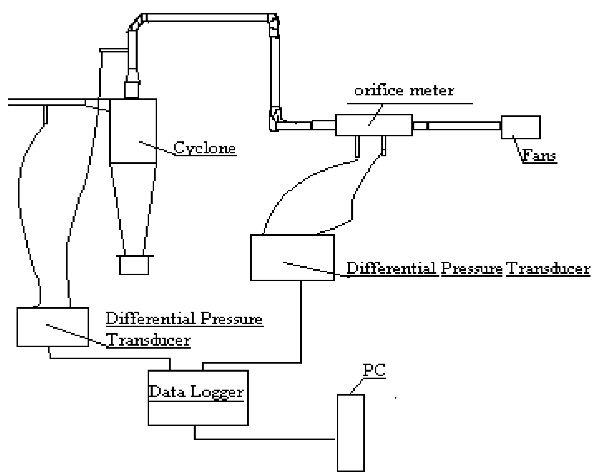

Figure 10. Pressure drop measurement system setup

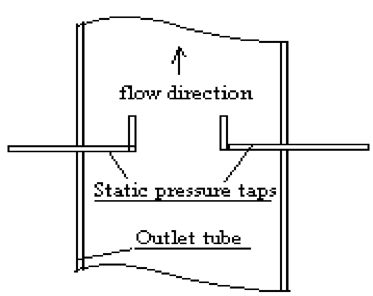

Figure 11. Static pressure taps in a cyclone outlet tube for pressure drop measurement

Three measurements were made on 2D2D and 1D2D cyclone designs and four measurements on 1D3D cyclone design at different inlet velocities. For the 1D3D cyclone, measurements #1, 2, and 3 were conducted on 0.2 m (6 inch) cyclone and #4 was on 0.1 m (4 inch) cyclone. Testing results are listed in table 14.

Table 14. Average measured pressure drop

1D3D		2D2D		1D2D	
V_{in}	ΔP_{1D3D}	V_{in}	ΔP_{2D2D}	V_{in}	ΔP_{1D2D}
4.5 (900)	75 (0.3)	4.1 (805)	56 (0.2)	4.5 (891)	25 (0.1)
6.5 (1273)	174 (0.7)	5.0 (986)	100 (0.4)	5.0 (986)	47 (0.2)
8.7 (1707)	299 (1.2)	7.9 (1559)	199 (0.8)	6.1 (1207)	80 (0.3)
11.4 (2241)	535 (2.2)	9.4 (1844)	249 (1.0)	7.9 (1559)	149 (0.6)
12.9 (2545)	697 (2.8)	9.8 (1930)	299 (1.2)	9.1 (1800)	212 (0.9)
14.7 (2902)	847 (3.4)	10.6 (2091)	405 (1.6)	10.4 (2052)	286 (1.2)
15.8 (3117)	971 (3.9)	11.4 (2241)	498 (2.0)	11.4 (2241)	349 (1.4)
16.5 (3245)	1121 (4.5)	12.8 (2513)	623 (2.5)	12.5 (2464)	436 (1.8)
17.4 (3415)	1220 (4.9)	13.6 (2670)	697 (2.8)	13.1 (2577)	473 (1.9)
18.2 (3577)	1370 (5.5)	14.7 (2902)	784 (3.2)	14.3 (2817)	585 (2.4)
18.3 (3600)	1469 (5.9)	15.2 (2984)	909 (3.7)	15.6 (3065)	685 (2.8)
		16.0 (3146)	1046 (4.2)	16.5 (3245)	784 (3.2)
		17.1 (3367)	1220 (4.9)	17.1 (3367)	859 (3.5)
		17.7 (3485)	1320 (5.3)	17.7 (3485)	934 (3.8)
		18.5 (3644)	1444 (5.8)	18.3 (3600)	1021 (4.1)

- Velocity: m/s (ft/min) and pressure drop: Pa (inch H_2O)

Comparison of Theoretical Prediction with Testing Results

As shown in tables 5 – 13, cyclone pressure drop is a function of inlet velocity and is independent of cyclone size. Figures 12 – 14 show the comparison of the predicted and measured cyclone pressure drop curves (pressure drop vs. inlet velocity). For the 1D3D cyclone, there are no significant pressure drop differences among tests #1, 2, 3, and 4 (see figure 12). As mentioned before, tests #1, 2, 3 were conducted on 0.2 m (6 inch) cyclone and test #4 was on 0.1 m (4 inch) cyclone. Therefore, the measured results also indicate that pressure drop is independent of cyclone size. Comparisons of pressure drop curves for 1D3D, 2D2D and 1D2D cyclones also verify that the theoretical predictions of pressure drops are in excellent agreement with experimental measurements. Thus, the new theoretical methods developed in this research for predicting cyclone pressure drop are reliable.

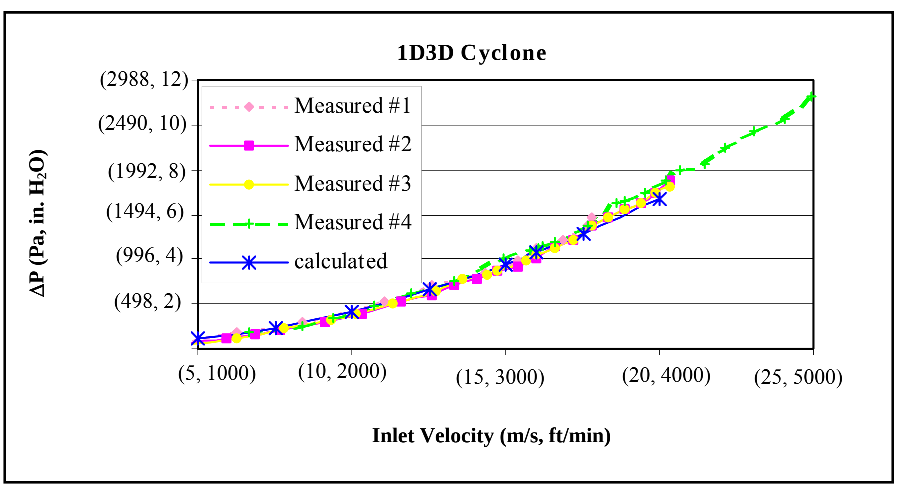

Figure 12. Measured and calculated pressure drop vs. inlet velocities for 1D3D cyclone

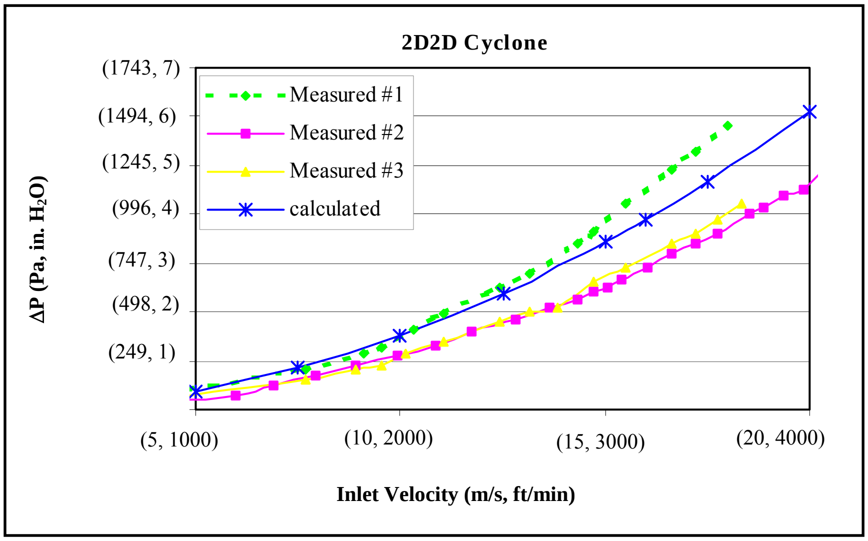

Figure 13. Measured and calculated pressure drop vs. inlet velocities for 2D2D cyclone

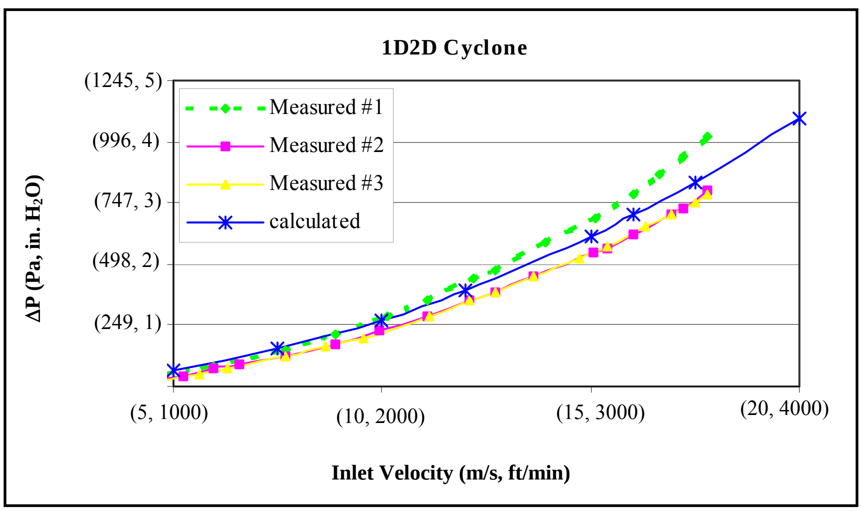

Figure 14. Measured and calculated pressure drop vs. inlet velocities for 1D2D cyclone

SUMMARY

Cyclone pressure drop consists of five individual pressure drop components. The frictional loss in the outer vortex and the rotational energy loss in the cyclone are the major pressure loss components. The theoretical analyses of the pressure drop for five different size cyclones (0.1 m (4 inch), 0.2 m (6 inch), 0.3 m (12 inch), 0.6 m (24 inch) and 0.9 m (36 inch)) show that cyclone pressure is independent of its diameter. However, cyclone pressure drop is a function of cyclone body height. Experiments were conducted to verify the theoretical analysis results and gave excellent agreement. Thus, the new theoretical method can be used to predict the air stream travel distance, number of turns and cyclone pressure drop. For the 1D3D, 2D2D and 1D2D cyclone designs, the predictions of pressure drop are 1071 Pa (4.3 inch H_2O), 854 Pa (3.43 inch H_2O) and 390 Pa (1.57 inch H_2O) respectively at their own design inlet velocity (16 m/s (3200 fpm), 15 m/s (3000 fpm) and 12 m/s (2400 fpm), respectively).

CHAPTER V

CYCLONE COLLECTION EFFICIENCY

INTRODUCTION

Cyclones, as the most cost-effective air pollution device for particulate matter removal, have been studied for decades. Although many procedures for calculating collection efficiency have been developed, current design practice either emphasizes past experience rather than an analytical design procedure, or cannot accurately predict cyclone collection efficiency.

In the literature, theories to predict cyclone efficiency have been reported for many years. As it is mentioned before, Lapple (1951) developed a theory (also known as CCD) for cut-point (d_{50}) based upon a force balance and representation of residence time with the air stream number of turns within a cyclone. The Lapple model is easy to use, but it cannot accurately predict cyclone collection efficiency. In 1972, Leith and Licht presented another theory (back-mixing) for the study of cyclone collection efficiency. Their back-mixing theory suggests that the turbulent mixing of uncollected particles in any plane perpendicular to the cyclone axis produces a uniform uncollected dust concentration through any horizontal cross section of a cyclone. Based upon this theory, they developed a model to predict efficiency for any size particles. It has been reported that the Leith and Licht model for efficiency appears to work best compared with other theories in the literature (Leith and Mehta, 1973). However, this model has not been tested with experimental data and it involves variables and dimensionless parameters not easily accounted for in practical applications.

Stairmand (1951) and Barth (1956) first developed the "static particle theory" for the analysis of cyclone collection efficiency in the 50's. Since then, this static particle theory based upon a force balance analysis has been adopted by many other researchers in their theoretical analyses for characterizing cyclone performance. Basically the "static particle theory" suggested that force balance on a particle yields a critical particle, which has 50% chance to be collected and 50% chance to penetrate the cyclone. The diameter of the critical particle is d_{50}. The critically sized particle (d_{50}) is smaller than the smallest particle, which is collected, and larger than the largest particle that penetrates the cyclone. The critical particle with diameter of d_{50} is theoretically suspended in the outer vortex forever due to the force balance.

COLLECTION MECHANISM IN THE OUTER VORTEX

Particle Motion in the Outer Vortex

Study of the particle collection mechanism in the outer vortex is a way to understand the relationship between the cyclone performance characteristics and the design and operating parameters. The first step in this study is to characterize the particle motion in the outer vortex. In the study of particle motion and trajectory in the outer vortex, the following assumptions were made:

- Particle is spherical. For irregular non-spherical particles, their Stokes' diameters (also known as ESD) are used for analysis.

- The relative velocity between the air stream and particle does not change the fluid pattern, i.e. the air stream velocity profile in the outer vortex.
- Particle motion is not influenced by the neighboring particles.
- The particle tangential velocity is the same as the air stream tangential velocity. In other words, the particle does not "slip" tangentially.
- Particle $R_e < 1$, the drag force on a particle is given by Stokes Law.
- Force balance on a particle yields 50% collection probability on this particle.
- Particle moves from the interface of inner vortex and outer vortex towards the cyclone wall, once the particle hits the wall, it will be collected.

Particle velocity and acceleration vectors

The analysis of particle motion in the outer vortex is conducted in a cylindrical coordinate system. When the air stream brings a particle with diameter d_p and density ρ_p into the cyclone outer vortex, centrifugal force acting on the particle generates a radial acceleration. The relative velocity between the particle and air stream generates a different path for the particle and air stream. Figure 15 shows the trend of a particle path and air stream path when the particle is moving in the outer vortex.

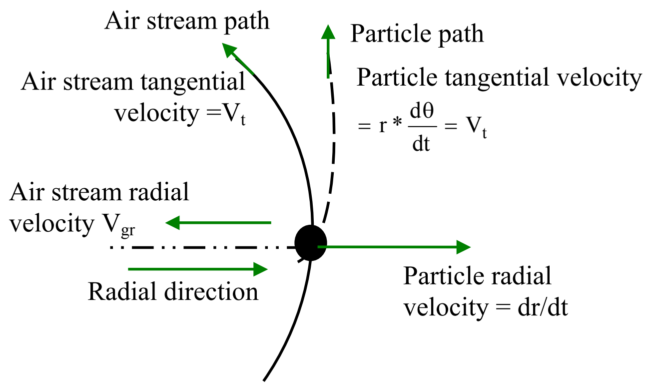

Figure 15. Paths of a particle and air stream in the outer vortex

In the rθ coordinates, the particle velocity can be described as

$$\vec{V}_p = r * \frac{d\theta}{dt}\vec{T} + \frac{dr}{dt}\vec{R} \tag{54}$$

The particle acceleration can be obtained by the following analysis:

$$\vec{a} = \frac{d\vec{V}_p}{dt} = \frac{\partial V_p}{\partial \theta}\frac{\partial \theta}{\partial t} + \frac{\partial V_p}{\partial r}\frac{\partial r}{\partial t}$$

$$= \frac{dr}{dt}\frac{d\theta}{dt}\vec{T} + r\frac{d^2\theta}{dt^2}\frac{dr}{dt}\vec{T} + r\frac{d\theta}{dt}\frac{d\vec{T}}{dt} + \frac{d^2 r}{dt^2}\vec{R} + \frac{dr}{dt}\frac{d\vec{R}}{dt}$$

Since $\frac{d\vec{T}}{dt} = -\frac{d\theta}{dt}\vec{R}$, and $\frac{d\vec{R}}{dt} = -\frac{d\theta}{dt}\vec{T}$, then

$$\vec{a} = \vec{a}_t + \vec{a}_r = \left[2\frac{dr}{dt}\frac{d\theta}{dt} + r\frac{d^2\theta}{dt^2}\right]\vec{T} + \left[\frac{d^2 r}{dt^2} - r\left(\frac{d\theta}{dt}\right)^2\right]\vec{R} \tag{55}$$

It was assumed that particle tangential velocity is the same as air stream tangential velocity (V_t), which is constant with respect to time. Therefore, there is no tangential acceleration for the particle ($\vec{a}_t = 0$).

Forces acting on a particle

The particle motion in the cyclone outer vortex can be determined by Newton's law as follows:

$$m_p * \frac{d\vec{V}_p}{dt} = \sum \vec{F} \qquad (56)$$

Gravity Force (F_G)

The impact of gravity force on the particle motion is in the form of particle terminal settling velocity (V_{TS}). Based on the definition of particle terminal settling velocity (Hinds, 1999), the drag force of the air on a particle (F_{DG}) is exactly equal and opposite to the force of gravity when the particle is released in air and quickly reaches its terminal settling velocity, such as,

$$F_{DG} = F_G = mg \qquad (57)$$

In this equation, F_{DG} is the gas resistance force to the particle motion caused by gravity. It can be determined by the Stokes law as:

$$F_{DG} = 3\pi * \mu * V_{TS} * d_p \qquad (58)$$

Combining equations 57 and 58, a particle terminal settling velocity is obtained as follows:

$$V_{TS} = \frac{\rho_p * d_p^2 * g}{18\mu} \qquad (59)$$

In this equation, particle density (ρ_p) is in kg/m^3; g is the acceleration of gravity in m/s^2; μ is gas viscosity in Pa.S; d_p is the particle diameter in m and V_{TS} is the particle terminal gravity settling velocity in m/s. Since particles of interest in the air quality research are less than or equal to 100 μm; as a result, the particle settling velocity caused by gravity is negligible compared to the particle traveling velocity in the outer vortex ($V_{TS} << V_p$). Therefore the impact of gravity force on particle motion is negligible.

Centrifugal Force (F_C)

Centrifugal force is the force acting on the particle in the radial direction for the particle separation. It is determined by

$$F_C = m\vec{a}_r = \frac{\pi * d_p^3 * \rho_p}{6} * \left[\frac{d^2 r}{dt^2} - r\left(\frac{d\theta}{dt}\right)^2\right] \qquad (60)$$

Drag Force (F_D)

Along the radial direction, there is another force, which is the gas resistance force to the particle motion caused by centrifugal force. It was assumed that the particle Reynolds number is less than one (R_e<1), which means Stokes' law, applies. As a result, the drag force on a spherical particle is

$$F_D = 3\pi\mu d_p * (V_{pr} - V_{gr}) = 3\pi\mu d_p * \left(\frac{dr}{dt} - V_{gr}\right) \qquad (61)$$

Force Balance Differential Equation

As mentioned above, in the cyclone outer vortex fluid field, there are only two forces (centrifugal force F_C & drag force F_D) acting on the particle in the radial direction. When $F_C > F_D$, the particle moves towards the cyclone wall to be collected. Whereas, when $F_C < F_D$, the particle will move to the inner vortex and then to penetrate the cyclone. The force balance ($F_C = F_D$) gives a particle a 50% chance to penetrate and 50% chance to be collected. The force balance differential equation can be set up by letting equation 60 equal to equation 61, i.e. $F_C = - F_D$, it yields equation 62.

$$\left[\frac{d^2r}{dt^2} - r\left(\frac{d\theta}{dt}\right)^2\right] + \frac{18\mu}{\rho_p * d_p^2} * \left(\frac{dr}{dt} - V_{gr}\right) = 0 \qquad (62)$$

This is a general force balance differential equation, which describes particle motion in the outer vortex space. The solution of this particle force balance differential equation gives the particle radial critical trajectory in polar (rθ) coordinates. This trajectory is the critical path in the radial direction and is a function of particle diameter. As mentioned above, the force balance gives a 50% collection probability. In other words, the particle diameter is d_{50} when the forces on a particle are in equilibrium on the critical path. The force balance differential equation yields a d_{50} distribution in the cyclone outer vortex.

Particle Critical Trajectory in the Outer Vortex

The particle tangential velocity, $r\frac{d\theta}{dt}$, is the same as air stream tangential velocity V_t. If $\tau = \frac{\rho_p d_p^2}{18\mu}$, then the force balance differential equation 62 can be rewritten as:

$$\frac{d^2r}{dt^2} + \frac{1}{\tau}\frac{dr}{dt} - \left(\frac{V_t^2}{r} + \frac{V_{gr}}{\tau}\right) = 0 \qquad (63)$$

To solve this force balance differential equation, the following initial conditions are used:

1. $r = r_o$ at $t = 0$ and r_o = radius of the interface of the inner vortex and outer vortex = radius of the outlet tube

2. $\frac{dr}{dt} = V_{pr}$, and $V_{pr} = 0$ at $t = 0$

On the other hand, the particle trajectory in the axial direction (rz coordinates) is of more concern. So the differential equation 63 should also be solved for the axial direction. It is assumed that the particle motion in axial direction follows a linear path and gas radial velocity is zero. As a result, the acceleration term, d^2r/dt^2, can be neglected in the equation 63. The V_t term is determined by equation 12. So, the force balance differential equation can be further simplified as:

$$\frac{1}{\tau}\frac{dr}{dt} = \frac{R * V_{in}^2}{r^2} \quad (r_o < r < R) \tag{64}$$

In equation 64, $t = \frac{Z_p}{V_{pz}}$ = particle traveling time in the Z distance along the axial direction, then $dt = \frac{dZ_p}{V_{pz}}$ = particle traveling time in the dz distance along the axial direction. The solution of equation 64 gives the particle critical radial trajectory function in the rz plane in the outer vortex as

$$r_p(z) = \sqrt[3]{r_o^3 + \frac{\rho_p * \pi * R * V_{in} * d_p^2}{4\mu} * Z_p} \tag{65}$$

d_{50} Distribution in the Outer Vortex

As mentioned before, the force balance on the particle gives the particle a 50% chance to be collected and a 50% chance to penetrate. In other words, the collection efficiency on this particle will be 50% when the particle is under the force balance condition. It is notated that the particle diameter is d_{50} when the particle is at the force balance situation. In fact, d_{50} is the critical separating diameter. If a particle is larger than d_{50}, it will move towards the wall, whereas, if a particle is smaller than the d_{50}, it will move towards the inner vortex. The particle diameter (d_p) is the critical separating diameter (d_{50}) in equation 65. Studying this equation, it is observed that in the cyclone outer vortex space, there is a d_{50} distribution. This distribution is the function of the location (r, z), particle density, cyclone design and inlet velocity. The d_{50} distribution function in the outer vortex space can be obtained by rewriting equation 65 as the follows:

$$d_{50} = \sqrt{\frac{4\mu * \left(r_p^3 - r_o^3\right)}{\rho_p * \pi * R * V_{in} * Z_p}} \tag{66}$$

Particle Collection Probability Distribution in the Outer Vortex

Based on the above analyses, d_{50} distribution defines the critical separation diameter (d_{50}) at the any point P(r, z) in the outer vortex. At the point P(r, z), if the particle diameter $d > d_{50}$, the particle will move to the wall and be collected, whereas if the particle diameter $d < d_{50}$, the particle will move to the inner vortex and penetrate. For a given inlet particle size distribution, the ratio of all the particles larger than d_{50} to the total inlet particles is the particle collection probability at the point P(r, z). If it is assumed that the inlet particle size distribution is a lognormal distribution with mass median diameter (MMD) and geometric standard deviation (GSD) as shown in equation

67, then equation 68 can be used to determine the particle collection probability at any point P(r, z) in the outer vortex.

$$F(d) = \int_{-\infty}^{\infty} \frac{1}{\sqrt{2\pi} d_p \ln(GSD)} \exp\left[-\frac{(\ln(d_p) - \ln(MMD))^2}{2(\ln(GSD))^2}\right] dd_p \qquad (67)$$

$$P(d) = \int_{d_{50}}^{\infty} \frac{1}{\sqrt{2\pi} d_p \ln(GSD)} \exp\left[-\frac{(\ln(d_p) - \ln(MMD))^2}{2(\ln(GSD))^2}\right] dd_p \qquad (68)$$

The particle collection probability distribution (equation 68) is in fact the particle collection rate distribution in the outer vortex. It is also the collected concentration distribution in the outer vortex.

THEORETICAL MODEL FOR CYCLONE CUT-POINT (d_{50})

Force balance theory is a unique way to develop a mathematical model for the cut-point. However the general force balance differential equation 62 is not readily solvable. An approximate solution can be obtained based upon some assumptions. To solve the general force balance differential equation 62, Barth (1956) made several assumptions. First, the particle radial velocity was assumed to be zero because of static status. It was also assumed that air uniformly leaked from the outer vortex to the inner vortex. So, the air inwards radial velocity was determined by

$$V_{gr} = \frac{Q}{\pi * D_o * Z_o} \qquad (69)$$

The Barth solution for theoretical cut-point model was

$$d_{50} = \sqrt{\frac{9\mu Q}{\rho_p * \pi * V_{in}^2 * Z_o}} \tag{70}$$

THEORETICAL MODEL FOR CYCLONE OVERALL EFFICIENCY

Equation 68 is the particle collection probability distribution in the outer vortex in which d_{50} is the critical separation diameter in the space. When the critical diameter on the interface is used in equation 68, the integration yields the cyclone total collection efficiency. In other words, equation 68 with d_{50} = cut-point is the theoretical model for calculating cyclone overall efficiency.

TRACING CUT-POINT (d_{50})

There is an inherent problem associated with the force balance analyses. The mathematical model for cut-point (equation 70) was based only upon the analysis for an individual particle. It did not consider the particle size distribution of the inlet PM. However, the cyclone cut-point changes with the PSD of inlet PM (Wang et al, 2002). So, a correction factor, which is function of PSD, is needed.

To determine the relationship of cyclone cut-points and the PSD's, equation 68 was used to theoretically trace the d_{50} from measured cyclone total efficiency with five kinds of dust (Wang, 2000). The traced d_{50} for 1D3D and 2D2D cyclones are listed in table 15.

Table 15. Traced cut-points (d_{50}) from measured efficiency and PSD for 1D3D and 2D2D cyclones

		PSD	1D3D		2D2D	
Dust	ρ_p	MMD/GSD	measured η_{total}	Traced d_{50}	measured η_{total}	Traced d_{50}
A	1.77	20 / 2.0	99.7 %	3.00	99.6 %	3.20
B	1.82	21 / 1.9	99.3 %	4.30	98.9%	4.82
C	1.87	23 / 1.8	99.7 %	4.50	99.6 %	4.80
Cornstarch	1.52	19 / 1.4	99.3 %	8.25	99.2 %	8.50
Flyash	2.73	13 / 1.7	96.8%	4.85	95.5 %	5.25

- PSD: particle size distribution
- Dusts A, B, and C are fine cotton gin dusts from different ginning processing streams. The dusts had been passed through a screen with 100 μm openings.
- MMD: mass median diameter (μm) of PSD
- GSD: geometric standard deviation
- ρ_p: particle density (g/cm^3)
- Measured η_{total}: measured overall cyclone efficiency from previous research (Wang, 200).
- Traced d_{50}: d_{50} (μm) obtained from equation 67 by setting P (d) equal to the overall efficiency.

It is observed from table 15 that the cut-point of a cyclone changes with the PSD. This is the same observation reported by Wang (2000) from the previous experimental research. Table 16 shows the results of traced d_{50}'s and experimental d_{50}'s. The results listed in the table 16 suggest that a cyclone cut-point is a function of MMD and GSD of inlet dust PSD. When the GSD is larger than 1.5, the cut-points decrease with an increase of MMD (see gin dust vs. fly ash), whereas the cut-points increase with an increase of MMD when the dust GSD is less than 1.5.

Table 16. Comparison of the traced cut-points against experimental cut-points

	1D3D		2D2D	
Dust	Traced d_{50}	Experimental d_{50}	Traced d_{50}	Experimental d_{50}
A	3.00	2.50	3.20	2.74
B	4.30	3.55	4.82	3.75
C	4.50	3.34	4.80	3.60
Cornstarch	8.25	---	8.50	---
Flyash	4.85	4.25	5.25	4.40

- Traced d_{50}: d_{50} (μm) obtained from equation 67 by setting P (d) equal to the overall efficiency
- Dusts A, B, and C are fine cotton gin dusts from different ginning processing stream. The dusts had been passed through a screen with 100 μm openings
- Experimental d_{50} (μm) were determined from experimental fractional efficiency curves calculated from experimental measurements of inlet and outlet concentration and PSD's (Wang et al. 2002)
- No experimental d_{50} available for cornstarch.

CORRECTING d_{50} MODEL FOR PARTICLE SIZE DISTRIBUTION (PSD)

The comparisons of cut-points obtained by using the Barth model (equation 70) and the traced cut-points solved by using equation 68 and measured overall efficiencies for the different dusts are shown in the table 17. The cut-points from the Barth model do not change with PSD, which is not consistent with the experimental research.

Table 17. Comparison of the traced cut-points against cut-points obtained from theoretical model (Barth model: equation 70)

	1D3D		2D2D	
Dust	Traced d_{50}	Barth d_{50}	Traced d_{50}	Barth d_{50}
A	3.00	3.58	3.20	3.46
B	4.30	3.58	4.82	3.46
C	4.50	3.58	4.80	3.46
Cornstarch	8.25	3.58	8.50	3.46
Flyash	4.85	3.58	5.25	3.46

- Traced d_{50}: d_{50} (μm) obtained from equation 67 by setting P (d) equal to the overall efficiency
- Dusts A, B, and C are fine cotton gin dusts from different ginning processing stream. The dusts had been passed through a screen with 100 μm openings
- Barth d_{50}'s are determined by equation 70 in AED

It is necessary to introduce a cut-point correction factor (K) to modify the theoretical d_{50} model to quantify the effect of PSD on the cut-point calculation. Table 18 lists K values based on Barth's d_{50}'s and traced d_{50}'s. It is obvious that the K value is a function of MMD and GSD. A regression analysis was performed to determine the relationship of K and MMD and GSD. Equations 71 and 72 show the results of regression fit based upon the data in table 18. It is noticed from the regression that the GSD has greater effect on K than MMD. In other words, the cut-points are more sensitive to GSD than to MMD.

Table 18. Cut-point correction factor for 1D3D and 2D2D cyclones with different dusts

	PSD		Cut-Point correction factor (K)	
Dust	MMD	GSD	1D3D	2D2D
A	20	2.0	0.84	0.92
B	21	1.9	1.20	1.39
C	23	1.8	1.26	1.39
Cornstarch	19	1.4	2.31	2.46
Flyash	13	1.7	1.36	1.52

- PSD: particle size distribution
- Dusts A, B, and C are fine cotton gin dusts from different ginning processing streams. The dusts had been passed through a screen with 100 μm openings.
- MMD: mass median diameter (μm) of PSD
- GSD: geometric standard deviation

$$K_{1D3D} = 5.3 + 0.02 * \mathrm{MMD} - 2.4 * \mathrm{GSD} \tag{71}$$

$$K_{2D2D} = 5.5 + 0.02 * \mathrm{MMD} - 2.5 * \mathrm{GSD} \tag{72}$$

Putting the cut-point correction factor into the Barth d_{50} model, the cyclone cut-point can be determined by the equation 73 which is referred to as the corrected theoretical cut-point model.

$$d_{50} = K * \sqrt{\frac{9\mu Q}{\rho_p * \pi * V_{in}^2 * Z_o}} \tag{73}$$

The theory and the methodology used in this research for correcting the cut-point model indicate that it is not necessary to develop a fractional efficiency curve to calculate the cyclone overall efficiency. The process for calculating cyclone efficiency can be summarized as the following steps:

1. Obtain PSD (MMD and GSD) of the cyclone inlet dust
2. Calculate the cut-point correction factor for the different cyclone design and the given PSD (MMD and GSD) by equations 71 or 72.
3. Determine the cut-point using the corrected d_{50} model (equation 73).
4. Determine the overall efficiency by integrating equation 68 based upon the corrected cut-point and PSD (MMD and GSD).

SUMMARY

Particle motion in the cyclone outer vortex was analyzed in this chapter to establish the force balance differential equation. Barth's "static particle" theory combined with the force balance equation was applied in the theoretical analyses for the models of cyclone cut-point and collection probability distribution in the cyclone outer vortex. Cyclone cut-points for different dusts were traced from measured cyclone overall collection efficiencies and the theoretical model for the cyclone overall efficiency calculation. The theoretical predictions of cut-points for 1D3D and 2D2D cyclones with fly ash are 4.85 μm and 5.25 μm. Based upon the theoretical study in this chapter the following main observations are obtained:

1. The traced cut-points indicate that cyclone cut-point is the function of dust PSD (MMD and GSD).
2. Theoretical d_{50} model (Barth model) needs to be corrected for PSD.

3. The cut-point correction factors (K) for 1D3D and 2D2D cyclone were developed through regression fits from theoretically traced cut-points and experimental cut-points.
4. The corrected d_{50} is more sensitive to GSD than to MMD.
5. The theoretical overall efficiency model developed in this research can be used for cyclone total efficiency calculation with the corrected d_{50} and PSD. No fractional efficiency curves are needed for calculating total efficiency.

CHAPTER VI

AIR DENSITY EFFECT ON CYCLONE PERFORMANCE*

INTRODUCTION

The cyclone, because of its simplicity and low operating cost, is probably the most widely used dust collector in industry. With the growing concern for the environmental effects of particulate pollution, it becomes increasingly important to be able to optimize the design of pollution control systems. As a result, many studies have been made to characterize cyclone performance as affected by design and operational parameters. Unfortunately, there is no information available on the effect of air density on the cyclone inlet design velocity, and consequently on its performance.

The cyclone design procedure outlined in Cooper and Alley (1994) is perceived as a standard method and has been considered by some engineers to be acceptable. However, this design process, hereafter referred to as the classical cyclone design (CCD) process, does not consider the cyclone inlet velocity in developing cyclone dimensions. Previous research at Texas A&M University (TAMU) (Parnell, 1990) indicated that the efficiency of a cyclone increased, and emission concentration decreased, with increasing inlet velocity. But at relatively high inlet velocities, the cyclone efficiency actually began to decrease. A dramatic increase in emission concentration has been observed at velocities higher than a certain threshold level (Parnell, 1996). The level at which the

---

* Reprinted with permission from Air Density Effect on Cyclone Performance by L. Wang , M.D. Buser, C.B. Parnell and B.W. Shaw, 2003. *Transactions of the American Society of Agricultural Engineers*. 46(4): 1193-1201. ©2003 American Society of Agricultural Engineers.

inlet velocities were too high and caused increased emissions was different for each cyclone design. The Texas A&M cyclone design (TCD) process specifies the "ideal" cyclone inlet velocities (design velocities) for different cyclone designs for optimum cyclone performance. The design inlet velocities for 1D3D, 2D2D, and 1D2D cyclones are 16 m/s ±2 m/s (3200 ft/min ±400 ft/min), 15 m/s ±2 m/s (3000 ft/min ±400 ft/min), and 12 m/s ±2 m/s (2400 ft/min ±400 ft/min), respectively. The TCD process allows an engineer to design the cyclone using a cyclone inlet velocity specific for the type of cyclone being considered. However, there is one problem with the CCD and TCD cyclone design processes. None of these cyclone design methods specify whether the cyclone design velocity should be based on the standard air density or actual air density.

Air density is primarily determined by barometric pressure. Barometric pressure is a function of height above sea level and weather patterns. Typically, at 1219 m (4000 ft) above sea level, the air density will be 1.04 kg per dry standard cubic meter, kg/dscm (0.065 lb per dry standard cubic foot, lb/dscf), compared to 1.20 kg/dscm (0.075 lb/dscf) at sea level - the standard air density at 21°C (70°F), 1 atm of barometric pressure, and zero relative humidity. The actual air density can be determined by:

$$\rho_a = \frac{(P_b - RH * P_s) * MW_{da}}{R * T} + \frac{RH * P_s * MW_{wv}}{R * T} \tag{74}$$

The relationships of cyclone airflow rate, inlet velocity, and air densities can be described by equations 75 and 76:

$$Q_a = \left(\frac{\rho_s}{\rho_a}\right) * Q_s \tag{75}$$

$$V_a = \left(\frac{\rho_s}{\rho_a}\right) * V_s \tag{76}$$

A design velocity of 16 m/s (3200 ft/min) based on standard air density (1.20 kg/dscm or 0.075 lb/dscf) would be 19 m/s (3700 ft/min) based on actual air density (1.04 kg/dscm or 0.065 lb/dscf). If the TAMU design process were to be used, then the 19 m/s (3700 ft/min) design velocity would be outside the acceptable range of inlet velocities for 1D3D cyclones (16 m/s ±2 m/s). Which is correct? Should cyclones be designed based on standard air density or actual air density?

It was hypothesized that cyclone performance and pressure drop would be affected by varying air density. The goal of this research was to quantify the air density effects on cyclone performance, and ultimately, to recommend a cyclone design philosophy based on either actual or standard air density.

EXPERIMENTAL METHOD

Cyclone airflow rate and inlet velocity change with air density. In this research, tests were conducted to evaluate 1D3D and 2D2D cyclone emission concentrations and pressure drops with two sets of inlet design velocities: one set based on actual airflow rate, and the other set based on dry standard airflow rate. All the tests were conducted at Amarillo, Texas, where the altitude is 1128 m (3700 ft) and consequently the air density is relatively low (1.04 kg per dry standard cubic meter). During the tests, barometric pressure, air temperature, and relative humidity were monitored by a digital weather station (Davis Perception II) to determine the air density by equation 74.

Cyclones

In the agricultural processing industry, 2D2D and 1D3D cyclones have been used for particulate matter control for many years. In this research, only fine dust and 1D3D and 2D2D cyclones were used to conduct experiments. Both 1D3D and 2D2D cyclones used in this research were 15 cm (6 in.) in diameter.

Testing Material

Fly ash, cornstarch, screened manure dust, and regular manure dust were used as test materials in this research ("screened manure dust" refers to cattle feedyard dust that has been passed through a screen with 100 μm openings, and "regular manure dust" refers to manure dust from the same source as the screened manure dust with the larger than 100 μm PM included). The particle densities of fly ash, cornstarch, and manure dust were 2.7 g/cm^3, 1.5 g/cm^3, and 1.8 g/cm^3, respectively. Emission concentrations for specific cyclone designs were directly related to the fine dust inlet loadings and the particle size distributions of inlet particulate matter. Tests were conducted with inlet concentrations of the dust at 1 and 2 g/m^3. A Coulter Counter Multisizer 3 (CCM) (Coulter Electronics, 2002) was used to analyze PSD's of inlet dust and emitted dust on the filters. The CCM is an electronic particle sizer that operates on a resistance principle to measure PSD in electrolyte liquid suspensions (Hinds, 1999). Figures 16 to 19 show the CCM PSD's of the four inlet PM. Mass median diameter and geometric standard deviation are two parameters that characterize PSD's. The MMD is the aerodynamic equivalent diameter such that 50% of PM mass is larger or smaller than this diameter. The GSD is defined by the following equation (Cooper and Alley, 1994):

$$GSD = \frac{d_{84.1}}{d_{50}} = \frac{d_{50}}{d_{15.9}} = \left(\frac{d_{84.1}}{d_{15.9}}\right)^{1/2} \tag{77}$$

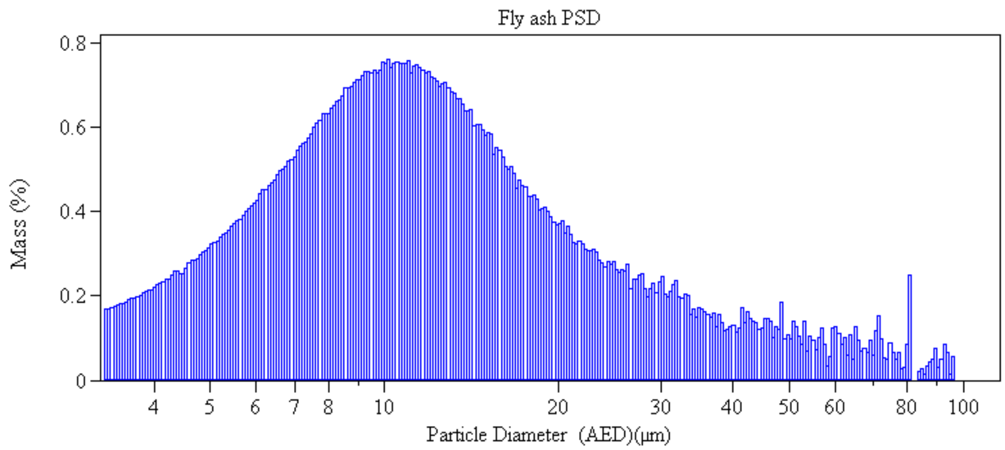

Figure16. PSD for fly ash (MMD = 11.34 μm, GSD = 1.82)

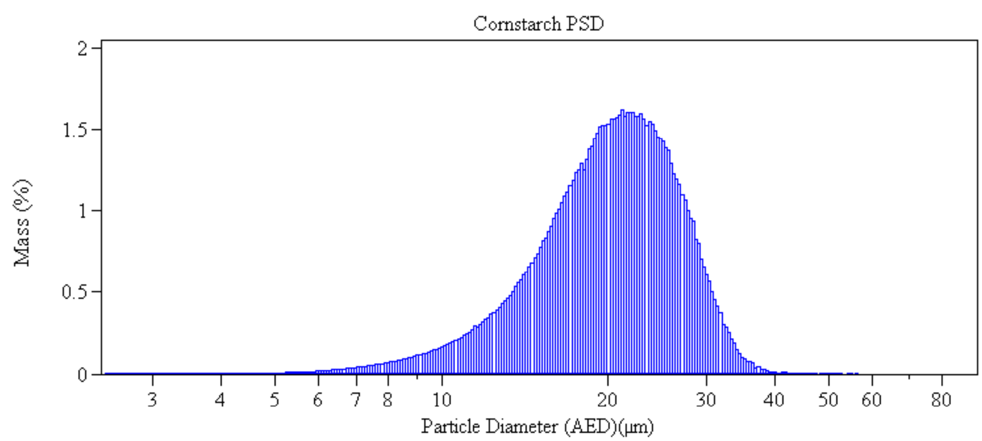

Figure 17. PSD for cornstarch (MMD = 20.38 μm, GSD = 1.39)

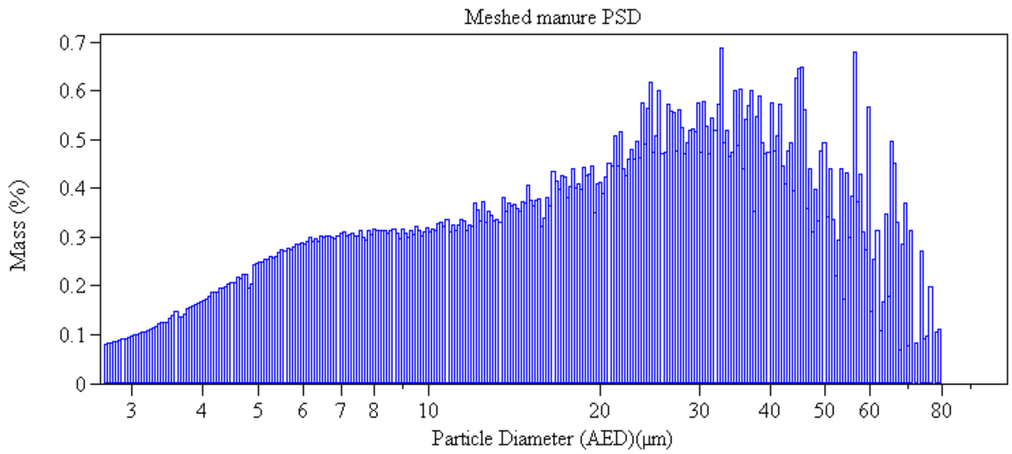

Figure 18. PSD for screened manure dust (MMD = 20.81 µm, GSD = 3.04)

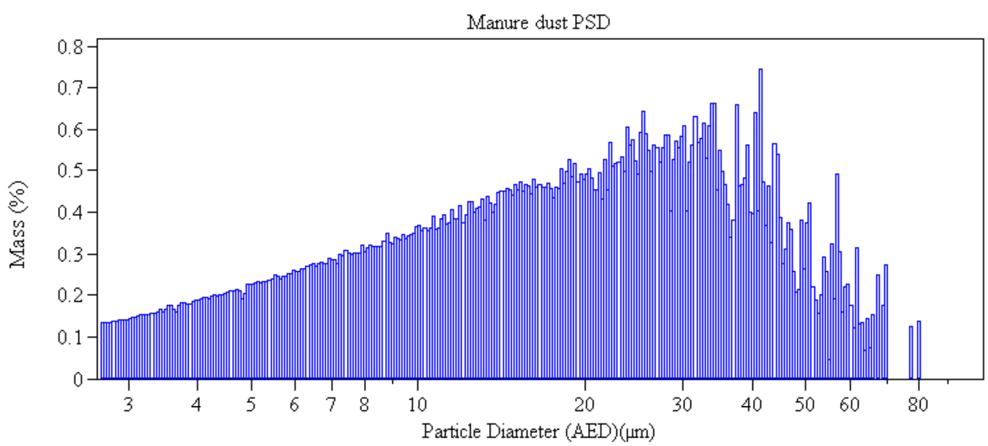

Figure 19. PSD for regular manure dust (MMD = 18.43 µm, GSD = 2.76)

Testing System

The testing system was a pull system, as shown in figure 20. The blowers pull the air from the feeding mechanism directly into a pipe and then to the cyclone. A collection hopper was connected to the bottom of the cyclone dust outlet to store the dust collected by the cyclone. Cleaned air flowed out of the cyclone through the outlet-conveying duct to a filter holder. The filter captured all the dust emitted from the cyclone, and clean air flowed through an orifice meter and the blowers and was discharged into the testing room. The designed airflow rate was maintained by monitoring the pressure drop across the orifice meter during the test. The equipment used in the testing system is listed in table 19, and the relationship between flow rate and pressure drop across the orifice meter is shown in equation 53.

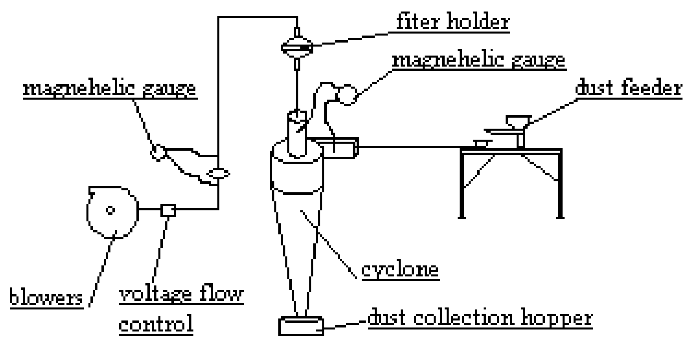

Figure 20. Cyclone testing system

Table 19. Equipment used for the testing system

Equipment	Model and Make	Parameter
Hand-held blowers	Cadillac HP-33, Clements National Co., Chicago, Ill.	1.42 m^3/min, 2989 Pa (50 cfm, 12 in. w.g.)
Orifice meter	Made in house	Range: 0 to 3.11 m^3/min; accuracy: ±0.7% reading. Calibrated with laminar flow element (Meriam Process Technologies, Cleveland, Ohio).
Magnahelic differential pressure gauges	Dwyer Instruments, Michigan City, Ind.	Range: 0 to 1245 Pa (0 to 5 in. w.g.); accuracy: ±24.9 Pa (±0.1 in. w.g.)
Magnetic dust feeder	Syntron F-TO, FMC Technologies, Homer City, Pa.	--
Filter holder	Made in house	20.3 × 25.4 cm (8 × 10 in.)

Testing time was 3 min for each test, and the system was cleaned between tests. The filters were conditioned in an environmental chamber for 24 h at 25°C and 46% relative humidity, as specified by EPA, and weighed with a microbalance (range: 0 to 101 mg, accuracy: ±0.1 mg) that was located in the environmental chamber before and after testing to determine total penetrating weights. The feeding rates and emission concentrations were determined with equations 78 and 79:

$$F = L * Q \tag{78}$$

$$EC = \frac{FW_2 - FW_1}{Q * T} * 1000 \tag{79}$$

The airflow rates of the testing system were determined by using the TCD design velocity. Table 20 shows the airflow rate and cyclone inlet velocity. Equations 75 and 76 were used to calculate cyclone airflow rates and inlet velocities based on actual or standard conditions.

Table 20. Airflow rate of the testing system

	Diameter of cyclone	Design velocity	Airflow rate of system
1D3D	15 cm (6 in.)	16 m/s (3200 ft/min)	0.05 m^3/s (100 ft^3/min)
2D2D	15 cm (6 in.)	15 m/s (3000 ft/min)	0.04 m^3/s (94 ft^3/min)

The same testing system was used to measure cyclone pressure drops at two inlet velocity treatments. In order to accurately measure the static pressure drop across the cyclones, the static pressure taps were inserted into the air stream such that the static pressure sensing position was in the direction of airflow (figure 11). The pressure drop measurement was conducted without any dust feeding.

Experimental Design and Data Analysis

The tests were conducted as a 4-factorial experiment. The four factors were (1) inlet velocity (optimum design velocity at actual air condition, optimum design velocity at standard air condition), (2) cyclone design (1D3D, 2D2D), (3) inlet PSD's (fly ash, cornstarch, and manure dust), (4) inlet loading rates (1 and 2 g/m^3). Each treatment was based on three repeating observations, for a total of 60 observations. ANOVA tests, using Tukey's Studentized range (HSD) test at 95% confidence interval, were performed on the results.

Equation 79 was used to convert the actual air emission concentration to standard air emission concentration for the comparison:

$$EC_a = \left(\frac{\rho_a}{\rho_s}\right) * EC_s \tag{80}$$

Besides the emission concentration, another important parameter to characterize cyclone performance is cyclone fractional efficiency. Cyclone fractional efficiency curves were developed based on the cyclone inlet concentration (feeding rate), inlet PSD (measured by CCM), emission concentration, and the PSD of PM emitted (on the filter, measured by CCM). The inlet and outlet concentrations for various size ranges were calculated using inlet and outlet PM concentrations and the fraction of particulate in those size ranges obtained from the Coulter Counter PSD analysis. The outlet concentration was divided by the corresponding inlet concentration for each particle size range and subtracted from one, with the resulting values being the fractional efficiency for each particle size range:

$$\eta_j = 1 - \frac{Con._{outj}}{Con._{inj}} \tag{81}$$

As was described in the chapter I, a cyclone fractional efficiency curve (FEC) can be represented by a cumulative lognormal distribution. This FEC distribution is defined by the cut-point (d_{50}) and sharpness-of-cut (the slope of the FEC).

TEST RESULTS AND DISCUSSION

Emission Concentration Measurements

Tables 21 and 22 contain the average emission concentrations for the tests conducted on the 1D3D and 2D2D cyclones. The null hypothesis for the 1D3D cyclone design was that there was no difference in emission concentrations for inlet velocities of 16 actual m/s (3200 afpm) versus 16 standard m/s (3200 sfpm or 3800 afpm); at an air density of 1.02 kg/m^3 (0.0635 lb/ft^3), the 16 standard m/s (3200 sfpm) velocity corresponds to 19 actual m/s (3800 afpm). For comparison purposes, all the emission concentrations were converted from mg per actual cubic meter (mg/acm) into mg per dry standard cubic meter (mg/dscm).

Table 21. Average emission concentrations from 1D3D and 2D2D cyclones with fly ash and cornstarch

Inlet Velocity (V_{in}, m/s)	Actual Air Density (kg/m^3)	Inlet Loading			
		Fly Ash		Corn Starch	
		1 g/m^3	2 g/m^3	1 g/m^3	2 g/m^3
1D3D					
16 actual air	1.02	50	93	7a	18b
16 standard air	1.02	42	73	6a	17b
2D2D					
15 actual air	1.02	57a	109	9b	20c
15 standard air	1.01	51a	96	8b	18c

- Emission concentration = mg/dscm (dscm=cubic meter of dry standard air)
- Three tests were performed for each condition. Means followed by the same letter are not significantly different at 0.05 level.

Table 22. Average emission concentrations from 1D3D cyclone with manure dust

Inlet Velocity (V_{in}, m/s)	Actual Air Density (kg/m^3)	Inlet Loading: Screened Manure 2 g/m^3	Inlet Loading: Regular Manure 2 g/m^3
16 actual air	1.01	75c	50
16 standard air	1.01	74c	43

- Emission concentration = mg/dscm (dscm=cubic meter of dry standard air)
- Three tests were performed for each condition. Means followed by the same letter are not significantly different at 0.05 level.

The statistical analyses indicated that the cyclone emission concentrations were highly dependent on cyclone design, inlet loading rates, PSDs of inlet PM, as well as air density. The following observations were noted:

1. For the fly ash tests, the average emission concentrations were significantly higher for both 1D3D and 2D2D cyclones for inlet velocities of 16 and 15 actual m/s (3200 and 3000 afpm) compared to 16 and 15 standard m/s (3200 and 3000 sfpm). For an air density of 1.02 kg/m^3 (0.0635 lb/ft^3), 16 standard m/s (3200 sfpm) is equivalent to 19 actual m/s (3800 afpm), and 19 m/s (3800 afpm) is outside of the TCD ideal design velocity range of 16 ±2 m/s (3200 ±400 fpm) for the 1D3D cyclones. One would assume that higher emissions would occur at 19 m/s (3800 afpm). However, the measured data did not support this assumption. Experimental results indicate that the optimum design velocity for the 1D3D cyclone is 16 standard m/s (3200 sfpm), not 16 actual m/s (3200 afpm). The same observations were made for the 2D2D cyclone. With an air density of 1.01

kg/m^3 (0.063 lb/ft^3), 15 standard m/s (3000 sfpm) inlet velocity is equivalent to 18 actual m/s (3600 afpm), and 18 actual m/s (3600 afpm) is also outside of the TCD ideal design velocity range of 15 ±2 m/s (3000 ±400 fpm) for the 2D2D cyclones. Again, the experimental data indicate that the optimum design velocity for the 2D2D cyclone should be 15 standard m/s (3000 sfpm), not 15 actual m/s (3000 afpm).

2. For agricultural dust with larger MMD, such as cornstarch and manure dust, the trend of decreasing emission concentration for 1D3D and 2D2D cyclones was observed when the inlet design velocity was based on standard air density. However, the differences in the emission concentrations for inlet velocities based on actual versus standard air densities were not statistically significant.
3. Among the four test dusts, the rankings from the smallest to the largest MMD's are as follows: (1) fly ash, (2) regular manure, (3) cornstarch, and (4) screened manure (figures 16 to 19). The test results suggest that as the MMD of the PM decreases, the differences in emission concentrations resulting from inlet velocities based on standard versus actual air densities will increase (tables 21 and 22).
4. The results from both 1D3D and 2D2D cyclones also indicate that higher inlet loading rates increased the differences in the emission concentration with different inlet velocity treatments. This implies that the effect of air density is increased as cyclone inlet loadings increase.

The emission concentrations associated with inlet and outlet PSD's were also used to calculate cyclone fractional efficiencies and to develop cyclone fractional efficiency curves. The methodology used to develop fractional efficiency curves is similar to the one developed by Wang et al. (2002). It includes the following three steps:

- Obtain PSDs of inlet (original dust) and outlet PM (dust on the filter) using the CCM.
- Calculate the fractional efficiency curves using inlet and outlet concentrations and the PSDs.
- Obtain the "best-fit" lognormal distribution for the fractional efficiency curves obtained above.

Statistical analyses were also conducted on the cyclone cut-points and slopes. Table 23 lists the average cut-points and slopes for the 1D3D and 2D2D cyclones with fly ash. For the 1D3D cyclone, the cut-points are significantly different with different inlet velocity treatments and two inlet loading rates. However, for the 2D2D cyclone, the cut-points are not significantly different with different inlet velocity treatments. Air density effect on the 1D3D cyclone cut-point is greater than on the 2D2D cyclone cut-point.

Table 23. 1D3D and 2D2D cyclones cut-points and slopes with fly ash

Inlet Velocity (V_{in}, m/s)	Actual Air Density (kg/m^3)	Inlet Loading: 1 g/m^3 Cut-point (μm)	1 g/m^3 Slope	2 g/m^3 Cut-point (μm)	2 g/m^3 Slope
1D3D					
16 actual air	1.02	3.9	1.29a	4.1	1.24
16 standard air	1.02	3.4	1.43a	3.6	1.35
2D2D					
15 actual air	1.02	4.2a	1.23b	4.2a	1.26b
15 standard air	1.01	4.0a	1.30b	4.0a	1.28b

- Three tests were performed for each condition. Means followed by the same letter are not significantly different at 0.05 level.

Pressure Drop Measurement

Table 24 lists the pressure drop test results. Parnell (1990) reported that pressure drops for 1D3D and 2D2D cyclones operating at design velocities were 1145 and 921 Pa (4.6 and 3.7 in. w.g.). However, the experimental data (table 6) indicate that cyclone pressure drop is highly dependent on air density. Only when 1D3D and 2D2D cyclones operate at their respective design velocities of standard air will their pressure drops be near the previously reported value, i.e., 1145 Pa (4.6 in. w.g.) for 1D3D, and 921 Pa (3.7 in. w.g.) for 2D2D. It is important that air density be considered in the design of cyclone systems.

Table 24. Cyclone pressure drop measurement

Inlet Velocity (V_{in}, m/s)	Actual Air Density (kg/m^3)	Cyclone Pressure Drop
1D3D		ΔP_{1D3D} (Pa)
16 actual air	1.02	755
16 standard air	1.02	1238
2D2D		ΔP_{2D2D} (Pa)
15 actual air	1.02	580
15 standard air	1.01	827

- Five tests were performed for each condition.

CYCLONE SYSTEM DESIGN – SIZING CYCLONES

The first step in designing a cyclone abatement system is to size the cyclone. Cyclone size and configuration depend on the cyclone design velocity and the volume of air to be handled. Equation 9 (Parnell, 1996) can be used to size 1D3D, 2D2D and 1D2D cyclones. Based upon the research reported in this chapter, cyclone inlet design velocity is standard air velocity. Equations 75 and 76 can be used to calculate the standard airflow rate (Q) and standard air inlet velocity (V_{in}). Tables 25, 26 and 27 list the recommended sizes for 1D3D, 2D2D and 1D2D cyclones. They are similar to the tables reported by Parnell (1990). This research supports the practice of sizing cyclones based on the standard air volume flow rate.

Table 25. Recommended sizes for 1D3D cyclones

Air Volume, dscm/s (dscf/min)	Using 1 Cyclone		Using 2 Cyclones		Using 3 Cyclones		Using 4 Cyclones	
	D_c, m (in.)	Approx. Height, m (ft)	D_c, m (in.)	Approx. Height, m (ft)	D_c, m (in.)	Approx. Height, m (ft)	D_c, m (in.)	Approx. Height, m (ft)
0.7 (1,500)	0.6 (24)	0.2 (8)	--	--	--	--	--	--
1.0 (2,000)	0.7 (28)	0.3 (9)	0.5 (20)	0.2 (7)	--	--	--	--
1.2 (2,500)	0.8 (30)	0.3 (10)	0.6 (22)	0.2 (8)	--	--	--	--
1.4 (3,000)	0.8 (32)	0.3 (11)	0.6 (24)	0.2 (8)	0.5 (20)	0.2 (7)	--	--
1.9 (4,000)	1.0 (38)	0.3 (13)	0.7 (26)	0.2 (9)	0.6 (22)	0.2 (8)	0.5 (20)	0.2 (7)
2.4 (5,000)	1.1 (42)	0.4 (14)	0.8 (30)	0.3 (10)	0.6 (24)	0.2 (8)	0.6 (22)	0.2 (8)
2.8 (6,000)	1.2 (46)	0.4 (16)	0.8 (32)	0.3 (11)	0.7 (28)	0.3 (10)	0.6 (24)	0.2 (8)
3.3 (7,000)	--	--	0.9 (36)	0.3 (12)	0.8 (30)	0.3 (10)	0.7 (26)	0.2 (9)
3.8 (8,000)	--	--	1.0 (38)	0.3 (13)	0.8 (32)	0.3 (11)	0.7 (28)	0.3 (10)
4.3 (9,000)	--	--	1.0 (40)	0.4 (14)	0.8 (32)	0.3 (11)	0.7 (28)	0.3 (10)
4.7 (10,000)	--	--	1.1 (42)	0.4 (14)	0.9 (34)	0.3 (12)	0.8 (30)	0.3 (10)
5.2 (11,000)	--	--	1.1 (44)	0.4 (15)	0.9 (36)	0.3 (12)	0.8 (32)	0.3 (11)
5.7 (12,000)	--	--	1.2 (46)	0.4 (16)	1.0 (38)	0.3 (13)	0.8 (32)	0.3 (11)
6.6 (14,000)	--	--	--	--	1.1 (42)	0.4 (14)	0.9 (36)	0.3 (12)
7.6 (16,000)	--	--	--	--	1.1 (44)	0.4 (15)	1.0 (38)	0.3 (13)
8.5 (18,000)	--	--	--	--	1.2 (46)	0.4 (16)	1.0 (40)	0.4 (14)
9.4 (20,000)	--	--	--	--	--	--	1.1 (42)	0.4 (14)
10.4 (22,000)	--	--	--	--	--	--	1.1 (44)	0.4 (15)
11.3 (24,000)	--	--	--	--	--	--	1.2 (46)	0.4 (16)

- dscm = cubic meter of dry standard air
- dscf = cubic foot of dry standard air

Table 26. Recommended sizes for 2D2D cyclones

Air Volume, dscm/s (dscf/min)	Using 1 Cyclone		Using 2 Cyclones		Using 3 Cyclones		Using 4 Cyclones	
	D_c, m (in.)	Approx. Height, m (ft)	D_c, m (in.)	Approx. Height, m (ft)	D_c, m (in.)	Approx. Height, m(ft)	D_c, m (in.)	Approx. Height, m (ft)
0.7 (1,500)	0.6 (24)	0.2 (8)	--	--	--	--	--	--
1.0 (2,000)	0.7 (28)	0.3 (10)	0.5 (20)	0.2 (7)	--	--	--	--
1.2 (2,500)	0.8 (30)	0.3 (10)	0.6 (22)	0.2 (8)	--	--	--	--
1.4 (3,000)	09 (34)	0.3 (12)	0.6 (24)	0.2 (8)	0.5 (20)	0.2 (7)	--	--
1.9 (4,000)	1.0 (40)	0.4 (14)	0.7 (28)	0.3 (10)	0.6 (22)	0.2 (8)	0.5 (20)	0.2 (7)
2.4 (5,000)	1.1 (44)	0.4 (15)	0.8 (30)	0.3 (10)	0.7 (26)	0.2 (9)	0.6 (22)	0.2 (8)
2.8 (6,000)	1.2 (48)	0.4(16)	0.9 (34)	0.3 (12)	0.7 (28)	0.3 (10)	0.6 (24)	0.2 (8)
3.3 (7,000)	--	--	0.9 (36)	0.3 (12)	0.8 (30)	0.3 (10)	0.7 (26)	0.2 (9)
3.8 (8,000)	--	--	1.0 (40)	0.4 (14)	0.8 (32)	0.3 (11)	0.7 (28)	0.3 (10)
4.3 (9,000)	--	--	1.1 (42)	0.4 (14)	0.9 (34)	0.3 (12)	0.8 (30)	0.3 (10)
4.7 (10,000)	--	--	1.1 (44)	0.4 (15)	0.9 (36)	0.3 (12)	0.8 (30)	0.3 (10)
5.2 (11,000)	--	--	1.2 (46)	0.4 (16)	1.0 (38)	0.3 (13)	0.8 (32)	0.3 (11)
5.7 (12,000)	--	--	1.2 (48)	0.4 (16)	1.0 (40)	0.4 (14)	0.9 (34)	0.3 (12)
6.6 (14,000)	--	--	--	--	1.1 (42)	0.4 (14)	0.9 (36)	0.3 (12)
7.6 (16,000)	--	--	--	--	1.2 (46)	0.4 (16)	1.0 (40)	0.4 (14)
8.5 (18,000)	--	--	--	--	1.2 (48)	0.4 (16)	1.1 (42)	0.4 (14)
9.4 (20,000)	--	--	--	--	--	--	1.1 (44)	0.4 (15)
10.4 (22,000)	--	--	--	--	--	--	1.2 (46)	0.4 (16)
11.3 (24,000)	--	--	--	--	--	--	1.2 (48)	0.4 (16)

- dscm = cubic meter of dry standard air
- dscf = cubic foot of dry standard air

Table 27. Recommended sizes for 1D2D cyclones

Air Volume, dscm/s] (dscf/min)	Using 1 Cyclone		Using 2 Cyclones		Using 3 Cyclones		Using 4 Cyclones	
	D_c, m (in.)	Approx. Height, m (ft)	D_c, m (in.)	Approx. Height, m (ft)	D_c, m (in.)	Approx. Height, m (ft)	D_c, m (in.)	Approx. Height, m (ft)
0.7 (1,500)	0.7 (26)	0.2 (7)	--	--	--	--	--	--
1.0 (2,000)	0.8 (30)	0.2 (8)	0.6 (22)	0.2 (6)	--	--	--	--
1.2 (2,500)	0.9 (34)	0.2 (9)	0.6 (24)	0.2 (6)	--	--	--	--
1.4 (3,000)	1.0 (38)	0.3 (10)	0.7 (26)	0.2 (7)	0.6 (22)	0.2 (6)	--	--
1.9 (4,000)	1.1 (44)	0.3 (11)	0.8 (30)	0.2 (8)	0.7 (26)	0.2 (7)	0.6 (22)	0.2 (6)
2.4 (5,000)	1.2 (48)	0.3 (12)	0.9 (34)	0.2 (9)	0.7 (28)	0.2 (7)	0.6 (24)	0.2 (6)
2.8 (6,000)	1.4 (54)	0.4 (14)	1.0 (38)	0.3 (10)	0.8 (30)	0.2 (8)	0.7 (26)	0.2 (7)
3.3 (7,000)	--	--	1.0 (40)	0.3 (10)	0.9 (34)	0.2 (9)	0.7 (28)	0.2 (7)
3.8 (8,000)	--	--	1.1 (44)	0.3 (11)	0.9 (36)	0.2 (9)	0.8 (30)	0.2 (8)
4.3 (9,000)	--	--	1.2 (46)	0.3 (12)	1.0 (38)	0.3 (10)	0.8 (32)	0.2 (8)
4.7 (10,000)	--	--	1.2 (48)	0.3 (12)	1.0 (40)	0.3 (10)	0.9 (34)	0.2 (9)
5.2 (11,000)	--	--	1.3 (52)	0.3 (13)	1.1 (42)	0.3 (11)	0.9 (36)	0.2 (9)
5.7 (12,000)	--	--	1.4 (54)	0.4(14)	1.1 (44)	0.3 (11)	1.0 (38)	0.3 (10)
6.6 (14,000)	--	--	--	--	1.2 (48)	0.3 (12)	1.0 (40)	0.3 (10)
7.6 (16,000)	--	--	--	--	1.3 (50)	0.3 (13)	1.1 (44)	0.3 (11)
8.5 (18,000)	--	--	-	--	1.4 (54)	0.4 (14)	1.2 (46)	0.3 (12)
9.4 (20,000)	--	--	-	--	--	--	1.2 (48)	0.3 (12)
10.4 (22,000)	--	--	--	--	--	--	1.3 (52)	0.3 (13)
11.3 (24,000)	--	--	--	--	--	--	1.4 (54)	0.4 (14)

- dscm = cubic meter of dry standard air
- dscf = cubic foot of dry standard air

SUMMARY

The performance of 1D3D and 2D2D cyclones is highly dependent on the inlet air velocity and air density. Proposed cyclone design inlet velocities are:

- 16 m/s ± 2 m/s (3200 ft/min ± 400 ft/min) with air density at standard condition for 1D3D cyclones.
- 15 m/s ± 2 m/s (3000 ft/min ± 400 ft/min) with air density at standard condition for 2D2D cyclones.
- 12 m/s ± 2 m/s (2400 ft/min ± 400 ft/min) with air density at standard condition for 1D2D cyclones.

It is important to consider the air density effect on the cyclone performance in the design of cyclone abatement systems. TCD ideal design velocity for 1D3D, 2D2D, and 1D2D cyclones should be the ideal inlet velocity of standard air, not the ideal inlet velocity of actual air. In designing cyclone abatement systems, the proposed design velocity should be the basis for sizing the cyclone and determining the cyclone pressure drop. The recommended sizes for 1D3D, 2D2D, and 1D2D cyclones are reported in this chapter.

CHAPTER VII

SUMMARY AND CONCLUSIONS

SUMMARY – TCD PROCESS

The detailed new theoretical models for cyclone design developed in this research are summarized in appendix C. The results of this research extend the Texas A&M cyclone design method to be a comprehensive whole design process in terms of energy consumption and efficiency. Basically, following steps are involved in the Texas A&M cyclone design process:

1. Cyclone design velocity:

   1D3D: 16 m/s ± 2 m/s (3200 ft/min ± 400 ft/min) of standard air

   2D2D: 15 m/s ± 2 m/s (3000 ft/min ± 400 ft/min) of standard air

   1D2D: 12 m/s ± 2 m/s (2400 ft/min ± 400 ft/min) of standard air

2. Sizing cyclone:

   System flow rate and cyclone design velocity are the bases to size a cyclone. Equation 74 can be used to convert the actual airflow rate to standard airflow rate. Then, equation 9 can be used to determine cyclone diameter by using standard airflow rate and inlet velocity.

3. Determining cyclone collection efficiency:

   The following sub-steps are involved to determine collection efficiency:

   a. Determining particle size distribution to obtain MMD and GSD

   b. Determining cut-point correction factor by equations 71 and 72

c. Determining cut-points by equation 73

d. Determining cyclone overall efficiency by equation 68

4. Determining cyclone pressure drops by equation 10 or equations 40, 41, 46, 48, 50 and 51.

CONCLUSIONS

A new theoretical method for computing air stream travel distance and number of turns has been developed in this research. The flow pattern and cyclone dimensions determine the air stream travel distance in the outer vortex of a cyclone. The number of effective turns for different cyclone sizes was calculated based upon the air stream travel distance and the cyclone dimension. The theoretical calculations indicate that the number of effective turns is determined by the cyclone design, and is independent of cyclone diameter (size) and inlet velocity. There are 6.13 turns in both 1D3D and 2D2D cyclones and 2.67 turns in the 1D2D cyclone.

Cyclone pressure drop consists of five individual pressure drop components. The frictional loss in the outer vortex and the rotational energy loss in the cyclone are the major pressure loss components. A theoretical analyses of the pressure drop for five different size cyclones (0.1 m / 4 inch, 0.2 m / 6 inch, 0.3 m / 12 inch, 0.6 m / 24 inch and 0.9 m / 36 inch) show that cyclone pressure is independent of its diameter. However, cyclone pressure drop is a function of cyclone body height. Experiments were conducted to verify the theoretical analysis and gave excellent agreement. The new theoretical method can be used to predict the air stream travel distance, number of turns and cyclone pressure drop. For the 1D3D, 2D2D and 1D2D cyclone designs, the predictions of pressure drop are 1071 Pa (4.3 inch H_2O), 854 Pa (3.43 inch H_2O) and 390 Pa (1.57 inch H_2O) respectively at their own design inlet velocity (16 m/s / 3200 fpm, 15 m/s / 3000 fpm and 12 m/s / 2400 fpm, respectively).

Particle motion in the cyclone outer vortex was analyzed to establish the force balance differential equation. Barth's "static particle" theory combined with the force balance equation was applied in the theoretical analyses for the models of cyclone cut-point and collection probability distribution in the cyclone outer vortex. Cyclone cut-points for different dusts were traced from measured cyclone overall collection efficiencies and the theoretical model for the cyclone overall efficiency calculation. The theoretical predictions of cut-points for 1D3D and 2D2D cyclones with fly ash are 4.85 μm and 5.25 μm. Based upon the theoretical study of collection efficiency in this research the following conclusions are obtained:

- The traced cut-points indicate that cyclone cut-point is the function of dust PSD (MMD and GSD).
- Theoretical d_{50} model (Barth model) needs to be corrected for PSD.
- The cut-point correction factors (K) for 1D3D and 2D2D cyclone were developed through regression fits from theoretically traced cut-points and experimental cut-points.
- The corrected d_{50} is more sensitive to GSD than to MMD.

The theoretical overall efficiency model developed in this research can be used for cyclone total efficiency calculation with the corrected d_{50} and PSD. No fractional efficiency curves are need for calculating total efficiency.

The performance of 1D3D and 2D2D cyclones is highly dependent on the inlet air velocity and air density. Based on the experimental study in this research, proposed cyclone design inlet velocities are:

- 16 m/s ± 2 m/s (3200 ft/min ± 400 ft/min) with air density at standard condition for 1D3D cyclones.
- 15 m/s ± 2 m/s (3000 ft/min ± 400 ft/min) with air density at standard condition for 2D2D cyclones.
- 12 m/s ± 2 m/s (2400 ft/min ± 400 ft/min) with air density at standard condition for 1D2D cyclones.

It is important to consider the air density effect on the cyclone performance in the design of cyclone abatement systems. TCD ideal design velocity for 1D3D, 2D2D, and 1D2D cyclones should be the ideal inlet velocity of standard air, not the ideal inlet velocity of actual air. In designing cyclone abatement systems, the proposed design velocity should be the basis for sizing the cyclone and determining the cyclone pressure drop. The recommended sizes for 1D3D, 2D2D, and 1D2D cyclones are reported in this research.

REFERENCES

Barth W. 1956. Design and layout of the cyclone separator on the basis of new investigations. *Brennstoff-Warme-Kraft* 8: 1-9.

Cooper, C.C. and G.C Alley. 1994. *Air Pollution Control; A Design Approach.* Prospect Heights, Ill.: Waveland Press, Inc.

Coulter Electronics, 2002. Multisizer 3 Coulter Counter Software V3.51 and Operator's Manual. Hialeah, Fla.: Beckman Coulter Inc.

First, M.W., 1950. Fundamental Factors in the Design of Cyclone Dust Collectors. Ph.D. dissertation. Cambridge, Mass.: Harvard University.

Hinds, William C., 1999. *Aerosol Technology*. New York: John Wiley & Sons

Kaspar, P., K.D. Mihalski and C.B. Parnell, Jr. 1993. Evaluation and development of cyclone design theory. In *Proc. 1993 Beltwide Cotton Production Conferences*. New Orleans, La. National Cotton Council.

Lapple, C. E. 1951. Processes use many collector types. *Chemical Engineering* 58 (5):144-151

Leith, D. and W. Licht, 1972. The collection efficiency of cyclone type particle collectors – A new theoretical approach. *AIChE Symposium Series* 126, 68: 196-206

Leith, D. and D. Mehta, 1973. Cyclone performance and design *Atmospheric Environ.* 7: 527-549

Mathcad 11, 2002. Cambridge, Mass.: Mathsoft Engineering & Education, Inc.

Mihalski, K., P. Kaspar and C. B. Parnell, Jr. 1993. Design of pre-separators for cyclone collectors. In *Proc. 1993 Beltwide Cotton Production Conferences*, 1561-1568. Memphis, Tenn.: National Cotton Council.

Parnell, C. B. Jr. 1990. Cyclone design for cotton gins. ASAE Paper No. 905102. Presented at the 1990 ASAE International Winter Meeting. St. Joseph, Mich.: ASAE.

Parnell, C. B. Jr. 1996. Cyclone design for air pollution abatement associated with agricultural operations. In *Proc. 1996 Beltwide Cotton Production Conferences*. Nashville, Tenn.: National Cotton Council.

Parnell, C.B. Jr. and D.D. Davis, 1979. Predicted effects of the use of new cyclone designs on agricultural processing particle emissions. ASAE Paper No. SWR-79-040, Presented at 1979 Southwest Region Meeting of the ASAE, Hot Springs, Ark.

Shepherd, C. B. and C. E. Lapple, 1939. Flow pattern and pressure drop in cyclone dust collectors. *Industrial and Engineering Chemistry* 31(8): 972-984.

Simpson, S. and C.B. Parnell, Jr., 1995. New low-pressure cyclone design for cotton gins. In *Proc. 1995 Beltwide Cotton Production Conferences*, Memphis, Tenn.: National Cotton Council.

Stairmand, C.J. 1949. Pressure drop in cyclone separators. *Industrial and Engineering Chemistry* 16 (B): 409-411.

Stairmand, C.J. 1951. The design and performance of cyclone separators. *Transactions of Chemical Engineers* 29(1): 356-373

Ter Linden, A.J. 1949. Investigation into cyclone dust collectors. *Inst. Mech. Engrs.* 160: 233-240

Wang, L., 2000. A new engineering approach to cyclone design for cotton gins. M.S. Thesis. Department of Agricultural Engineering, Texas A&M University.

Wang, L., C. B. Parnell and B. W. Shaw, 1999. Performance characteristics for the 1D2D, 2D2D, 1D3D and barrel cyclones. ASAE Paper No. 99-4195. Presented at the 1999 ASAE Annual Meeting. Toronto, Canada.

Wang, L., C. B. Parnell and B. W. Shaw, 2000. 1D2D, 1D3D, 2D2D cyclone fractional efficiency curves for fine dust. In *Proc. 2000 Beltwide Cotton Production Conferences*. San Antonio, Tex.: National Cotton Council.

Wang, L., C. B. Parnell and B. W. Shaw, 2001. A new theoretical approach for predicting number of turns and cyclone pressure drop. ASAE Paper No. 01-4009. Presented at the 2001 ASAE Annual Meeting. Sacramento, Calif.

Wang, L., M. D. Buser, C. B. Parnell and B. W. Shaw, 2003. Effect of air density on cyclone performance and system design. *Transactions of the ASAE* 46 (4): 1193-1201

APPENDIX A

DEFINITIONS OF VARIABLES

$\bar{a}$: particle acceleration (m/s^2)

$\bar{a}_r$: particle radial acceleration (m/s^2)

$\bar{a}_t$: particle tangential acceleration (m/s^2)

A_p: surface area of control volume I (equation 15)

A_z: outer vortex cross-section area at Z location along axial direction (annular area, m^2)

C_1: constant 1

C_2: constant 2

C_3: constant 3

C_4: constant 4

C_5: constant 5 = 1

C_6: constant 6 = 1.8

$Con._{inj}$: inlet concentration of j^{th} size range (mg/m^3)

$Con._{outj}$: outlet concentration of j^{th} size range (mg/m^3)

D: Pipe diameter (equation 45)

$d_{15.9}$: (1) diameter of particles collected with 15.9% efficiency (equation 11)

(2) diameter such that particles constituting 15.9% of the total mass of particles are smaller than this size (equation 77)

d_{50}: (1) diameter of particles collected with 50% efficiency (equations 11, 66, 70, 73)

(2) diameter such that particles constituting 50% of the total mass of particles are smaller than this size (equation 77)

$d_{84.1}$: (1) diameter of particles collected with 84.1% efficiency (equation 11)

(2) diameter such that particles constituting 84.1% of the total mass of particles are smaller than this size (equation 77)

D_c: cyclone body diameter (m)

D_e: diameter of outlet tube (m)

D_o: (1) diameter of interface (m)
(2) orifice diameter (equation 53 only, m)

d_p: particle diameter (μm)

d_{pc}: diameter of particle collected with 50% efficiency (m)

$\bar{d}_{pj}$: characteristic diameter of the j^{th} particle size range (m)

D_s: equivalent stream diameter in the outer vortex (m)

D_{s1}: equivalent stream diameter in the barrel (m)

D_{s2}: equivalent stream diameter in the cone (m)

$d\phi$: angle that the control volume I covered (equations 14, 15, 16, and 17)

EC: emission concentration (mg/m^3)

EC_a: actual air emission concentration (mg/m^3)

EC_s: standard air emission concentration (mg/dry standard cubic meter)

f: friction factor for frictional pressure loss

F: feeding rate (g/s)

F_c: centrifugal force (N)

F_C: centrifugal force acting on the particle (N)

F_D: drag force against particle radial motion (N)

F_{DG}: drag force to against gravity settling (N)

F_G: gravity force (N)

F_p: pressure force on the surface of control volume (equations 15 and 16)

F(d): cumulative particle size distribution (%)

$\sum \vec{F}$: all the external forces (N)

FW_1: pre-weight of filter (g)

FW_2: post-weight of filter (g)

h: height of control volume I (equations 14, 15, 16, and 17)

H: height of cyclone inlet duct (m)

H_c: height of cyclone inlet duct (m)

H_v: pressure drop expressed in number of inlet velocity heads

K: (1) cyclone pressure drop constant (equations 7 and 10)

(2) orifice meter coefficient (equation 53)

(3) cut-point correction factor (equation 73)

K_{1D3D}: cut-point correction factor for 1D3D cyclone

K_{2D2D}: cut-point correction factor for 2D2D cyclone

L: (1) air stream travel distance in the outer vortex (m)

(2) total inlet loading rate (equation 78 only g/m^3)

L_1: air stream travel distance in the barrel part (m)

L_2: air stream travel distance in the cone part (m)

L_c: length of cyclone body (m)

m_j: mass fraction of particles in the jth size range (%)

m_p: particle mass (kg)

MW_{da}: molecular weights of dry air (28.96 g/g-mole)

MW_{wv}: molecular weights of water vapor (18 g/g-mole)

n: flow pattern factor

N_e: number of effective turns

N_{e1}: number of effective turns in the barrel part

N_{e2}: number of effective turns in the cone part

P: (1) pressure acting on the control volume surface (equations 15 – 17)

(2) pressure distribution in the outer vortex (equations 18 and 19)

P(d): particle collection probability distribution (%)

P_b: barometric pressure (atm)

P_s: saturated water vapor pressure at dry bulb temperature (Pa)

ΔP: (1) cyclone pressure drop (N/m^2 or Pa)

(2) pressure drop across orifice equation 52 only, Pa)

ΔP_f: frictional pressure loss in the outer vortex (Pa)

ΔP_{f1}: frictional pressure loss in the barrel part of outer vortex (Pa)

ΔP_{f2}: frictional pressure loss in the cone part of outer vortex (Pa)

ΔP_e: cyclone entry pressure loss (Pa)

ΔP_k: kinetic pressure loss (Pa)

ΔP_o: pressure loss in the inner vortex and outlet tube

ΔP_r: rotational pressure loss (Pa)

Q: system air volume flow rate (m^3/s)

Q_a: actual airflow rate (m^3/s)

Q_{in}: inlet airflow rate (m^3/s)

Q_z: downward air flow rate in the outer vortex (m^3/s)

Q_s: standard airflow rate (m^3/s)

r: radial position in the outer vortex space (m)

R: (1) cyclone body radius (m)

(2) ideal gas constant (82.06 atm-cm^3/g-mole-K, equation 74 only)

$\vec{R}$: radial unit vector

R_e: Reynolds number

r_o: interface radius (m) (figure 6)

$r\frac{d\theta}{dt}$: particle tangential velocity (m/s)

$r_p(z)$: particle radial trajectory

RH: relative humidity (%)

T: (1) temperature (equation 74, K)

(2) testing time for each sample (equation 79, s)

$\vec{T}$: tangential unit vector

t_1: air stream traveling time in the barrel (s)

t_2: air stream traveling time in the cone (s)

V: fluid velocity in the pipe (equation 45)

V_1: total average gas velocity in the barrel part (m/s)

V_2: total average gas velocity in the cone part (m/s)

V_a: actual air inlet velocity (m/s)

V_s: standard air inlet velocity (m/s)

V_i: gas inlet velocity (m/s)

V_{gr}: gas radial velocity (m/s)

V_{in}: cyclone inlet velocity (m/s)

$\bar{V}_p$: particle velocity vector (m/s)

V_{pr}: particle radial velocity (m/s)

V_{pz}: particle axial velocity (m/s)

V_{r2}: gas radial velocity in the cone part (m/s)

V_{r21}: gas radial velocity in the zone 1 of a 1D2D cone part (m/s)

V_{r22}: gas radial velocity in the zone 2 of a 1D2D cone part (m/s)

V_{s1}: air stream velocity in the barrel part (m/s)

V_{s2}: air stream velocity in the cone part (m/s)

V_t: gas tangential velocity (m/s)

V_{t1}: gas tangential velocity in the barrel part (m/s)

V_{t2}: gas tangential velocity in the cone part (m/s)

V_{TS}: particle terminal settling velocity (m/s)

V_{z1}: gas axial velocity in the barrel (m/s)

V_{z2}: gas axial velocity in the cone (m/s)

V_{z21}: gas axial velocity in the zone 1 of a 1D2D cone part (m/s)

V_{z22}: gas axial velocity in the zone 2 of a 1D2D cone part (m/s)

VP_i: inlet velocity pressure (N/m^2 or Pa)

VP_{in}: cyclone inlet velocity pressure (N/m^2 or Pa)

VP_o: outlet velocity pressure (N/m^2 or Pa)

VP_{out}: cyclone outlet velocity pressure (N/m^2 or Pa)

VP_s: air stream velocity pressure at time t in the outer vortex (Pa)

VP_{s1}: air stream velocity pressure at time t in the barrel part of outer vortex (Pa)

VP_{s2}: air stream velocity pressure at time t in the cone part of outer vortex (Pa)

W: width of cyclone inlet duct (m)

Z: axial position in the outer vortex (m)

Z_1: height of barrel part (m)

Z_c: length of cyclone cone (m)

Z_o: effective length (figure 6, m)

Z_{o2}: cyclone effective length in the cone part figure 8)

Z_p: particle axial location (m)

η_o: overall collection efficiency (%)

η_j: collection efficiency for j^{th} particle size range (%)

θ: cyclone cone angle

μ: gas viscosity (kg/m-s)

ρ: fluid density (kg/m^3)

ρ_a: air density (kg/m^3)

ρ_g: gas density (kg/m^3)

ρ_p: particle density (kg/m^3)

ρ_s: standard air density (kg/m^3)

τ: particle relaxation time (s)

ω: angular velocity

APPENDIX B

LIST OF ACRONYMS

AED: aerodynamic equivalent diameter

CCD: classical cyclone design

CCM: Coulter Counter Multisizer

ESD: equivalent spherical diameter

FEC: fractional efficiency curve

GSD: geometric standard deviation

MMD: mass median diameter

PM: particulate matter

PSD: particle size distribution

TCD: Texas A&M cyclone design

APPENDIX C

SUMMARY OF THE NEW THEORETICAL MODELS DEVELOPED IN THIS RESEARCH

TRAVEL DISTANCE IN THE BARREL PART

- $L_1 = 1.53\ \pi D_c = 4.8\ D_c$ (For 1D3D)
- $L_1 = 3.06\ \pi D_c = 9.6\ D_c$ (For 2D2D)
- $L_1 = 1.66\ \pi D_c = 5.2\ D_c$ (For 1D2D) (***Equation 34***)

TRAVEL DISTANCE IN THE BARREL PART

- **1D3D:**

$$L_2 = \int_0^{2D_c} \sqrt{\left(\frac{1}{Z+2D_c}\right)^2 + \left(\frac{1}{Z\pi+4\pi D_c}\right)^2 + \left(\frac{1}{8\pi Z+32\pi D_c}\right)} * (Z+4D_c)\pi * dz$$

(Equation 36)

$L_2 = 10.83\ D_c$ ***(Equation 37)***

- **2D2D:**

$$L_2 = \int_0^{4D_c/3} \sqrt{\left(\frac{1}{3Z+4D_c}\right)^2 + \left(\frac{1}{3Z\pi+8\pi D_c}\right)^2 + \left(\frac{1}{48\pi Z+128\pi D_c}\right)} * (3Z+8D_c)\pi * dz$$

(Equation 36)

$L_2 = 7.22\ D_c$ ***(Equation 37)***

- **1D2D:**

$$L_2 = \int_{11D_c/8}^{3D_c/2} \sqrt{\left(\frac{D_c}{2Z+5D_c}\right)^2 + \left(\frac{1}{13\pi}\right)^2 + \left(\frac{1}{104\pi}\right)^2} * 13\pi * dz$$

$$+ \int_0^{11D_c/8} \sqrt{\left(\frac{1}{4Z+10D_c}\right)^2 + \left(\frac{1}{3Z\pi+15D_c\pi}\right)^2 + \left(\frac{1}{24Z\pi+120D_c\pi}\right)^2} * (3Z+15D_c) * dz$$

(Equation 36)

$L_2 = 2.57\ D_c$ ***(Equation 36)***

NUMBER OF EFFECTIVE TURNS

- **In The Barrel Part**

$$N_{e1} = \frac{L_1}{\pi * D_c}$$ ***(Equation 38)***

- **In The Cone Part**

$$N_{e2} = \frac{L_2}{\pi * \left(\frac{D_c + D_o}{2}\right)}$$ ***(Equation 39)***

CYCLONE TOTAL PRESSURE DROP

$$\Delta P_{total} = \Delta P_e + \Delta P_k + \Delta P_f + \Delta P_r + \Delta P_o$$ ***(Equation 52)***

- **Friction Loss In The Barrel Part**

$$\Delta P_{f1} = \int_0^{L_1} f * \frac{VP_{s1}}{D_{s1}} dL = \int_0^{Z_1} f * \frac{VP_{s1}}{D_{s1}} * V_1 * \frac{dZ}{V_{z1}}$$ ***(Equation 44)***

$\Delta P_{f1} = 0.13 * VP_{s1} = 0.14 * VP_{in}$ (For 1D3D)

$\Delta P_{f1} = 0.27 * VP_{s1} = 0.28 * VP_{in}$ (For 2D2D)

$\Delta P_{f1} = 0.14 * VP_{s1} = 0.15 * VP_{in}$ (For 1D2D) ***(Equation 46)***

- **Friction Loss In The Cone Part**

$$\Delta P_{f2} = \int_0^{L_2} f * \frac{VP_{s2}}{D_{s2}} dL = \int_{Z_{o2}}^{0} f * \frac{VP_{s2}}{D_{s2}} * V_2 * \frac{dZ}{V_{z2}}$$ ***(Equation 48)***

- **1D3D:**

$$\Delta P_{f2} = \int_0^{2D_c} \frac{f}{2} * VP_{in} * \left(\frac{\pi}{D_c}\right)^{\frac{3}{2}} * \left(\frac{Z + 4D_c}{\sqrt{Z}}\right) *$$

$$\left[\left(\frac{4D_c}{Z + 2D_c}\right)^2 + \left(\frac{4D_c}{Z\pi + 4D_c\pi}\right)^2 + \left(\frac{D_c}{2Z\pi + 8D_c\pi}\right)^2\right]^{\frac{7}{4}} dZ$$

- **2D2D:**

$$\Delta P_{f2} = \int_0^{4D_c/3} \frac{f}{\sqrt{24}} * VP_{in} * \left(\frac{\pi}{D_c}\right)^{\frac{3}{2}} * \left(\frac{3Z + 8D_c}{\sqrt{Z}}\right) *$$

$$\left[\left(\frac{8D_c}{3Z + 4D_c}\right)^2 + \left(\frac{8D_c}{3Z\pi + 8D_c\pi}\right)^2 + \left(\frac{3D_c}{6Z\pi + 16D_c\pi}\right)^2\right]^{\frac{7}{4}} dZ$$

- **1D2D:**

$$\Delta P_{f2} = \int_0^{3D_c/2} \frac{f\sqrt{3}}{16} * VP_{in} * \left(\frac{\pi}{D_c}\right)^{\frac{3}{2}} * \left(\frac{3Z + 15D_c}{\sqrt{Z}}\right) *$$

$$\left[\left(\frac{8D_c}{2Z + 5D_c}\right)^2 + \left(\frac{16D_c}{3Z\pi + 15D_c\pi}\right)^2 + \left(\frac{2D_c}{3Z\pi + 15D_c\pi}\right)^2\right]^{\frac{7}{4}} dZ$$

- **Rotational Pressure loss**

$$\Delta P_r = \rho * V_{in}^2 * \left(\frac{R}{r_o} - 1\right) \qquad \textbf{\textit{(Equation 50)}}$$

$\Delta P_r = 2\ VP_{in}$ (1D3D and 2D2D)

$\Delta P_r = 1.22\ VP_{in}$ (1D2D)

CYCLONE COLLECETION EFFICIENCY

- **Cut-point Model**

$$d_{50} = K * \sqrt{\frac{9\mu Q}{\rho_p * \pi * V_{in}^2 * Z_o}}$$ ***(Equation 73)***

$$K_{1D3D} = 5.3 + 0.02 * MMD - 2.4 * GSD$$ ***(Equation 71)***

$$K_{2D2D} = 5.5 + 0.02 * MMD - 2.5 * GSD$$ ***(Equation 72)***

- **Overall Efficiency Model**

$$P(d) = \int_{d_{50}}^{\infty} \frac{1}{\sqrt{2\pi} d_p \ln(GSD)} \exp\left[-\frac{\left(\ln(d_p) - \ln(MMD)\right)^2}{2\left(\ln(GSD)\right)^2} \right] dd_p$$

(Equation 68)

APPENDIX D

CALCULATIONS OF TRAVEL DISTANCE IN THE CONE PART OF A CYCLONE

Travel Distance In The Cone (L) – 1D3D

D_1 = 0.1 m (4 inch) D_3 = 0.3 m (12 inch) D_5 = 0.9 m (36 inch)

D_2 = 0.2 m (6 inch) D_4 = 0.6 m (24 inch)

- $$L_1 = \int_0^{2D_1} \sqrt{\left(\frac{1}{Z+2D_1}\right)^2 + \left[\frac{1}{\pi*(Z+4D_1)}\right]^2 + \left[\frac{1}{\pi*(8Z+32D_1)}\right]^2} * (Z+4D_1) * \pi * dZ$$

  = 43.315 = 10.83 D

- $$L_2 = \int_0^{2D_2} \sqrt{\left(\frac{1}{Z+2D_2}\right)^2 + \left[\frac{1}{\pi*(Z+4D_2)}\right]^2 + \left[\frac{1}{\pi*(8Z+32D_2)}\right]^2} * (Z+4D_2) * \pi * dZ$$

  = 64.973 = 10.83 D

- $$L_3 = \int_0^{2D_3} \sqrt{\left(\frac{1}{Z+2D_3}\right)^2 + \left[\frac{1}{\pi*(Z+4D_3)}\right]^2 + \left[\frac{1}{\pi*(8Z+32D_3)}\right]^2} * (Z+4D_3) * \pi * dZ$$

  = 129.946 = 10.83 D

- $$L_4 = \int_0^{2D_4} \sqrt{\left(\frac{1}{Z+2D_4}\right)^2 + \left[\frac{1}{\pi*(Z+4D_4)}\right]^2 + \left[\frac{1}{\pi*(8Z+32D_4)}\right]^2} * (Z+4D_4) * \pi * dZ$$

  = 259.892 = 10.83 D

- $$L_5 = \int_0^{2D_5} \sqrt{\left(\frac{1}{Z+2D_5}\right)^2 + \left[\frac{1}{\pi*(Z+4D_5)}\right]^2 + \left[\frac{1}{\pi*(8Z+32D_5)}\right]^2} * (Z+4D_5) * \pi * dZ$$

  = 389.837 = 10.83 D

Travel Distance In The Cone (L) – 2D2D

D_1 = 0.1 m (4 inch) D_3 = 0.3 m (12 inch) D_5 = 0.9 m (36 inch)

D_2 = 0.2 m (6 inch) D_4 = 0.6 m (24 inch)

- $$L_1 = \int_0^{\frac{4}{3}D_1} \sqrt{\left(\frac{1}{3Z+4D_1}\right)^2 + \left[\frac{1}{\pi * (3Z+8D_1)}\right]^2 + \left[\frac{1}{\pi * (48Z+128D_1)}\right]^2} * (3Z+8D_1) * \pi * dZ$$

  = 28.887 = 7.22 D

- $$L_2 = \int_0^{\frac{4}{3}D_2} \sqrt{\left(\frac{1}{3Z+4D_2}\right)^2 + \left[\frac{1}{\pi * (3Z+8D_2)}\right]^2 + \left[\frac{1}{\pi * (48Z+128D_2)}\right]^2} * (3Z+8D_2) * \pi * dZ$$

  = 43.33 = 7.22 D

- $$L_3 = \int_0^{\frac{4}{3}D_3} \sqrt{\left(\frac{1}{3Z+4D_3}\right)^2 + \left[\frac{1}{\pi * (3Z+8D_3)}\right]^2 + \left[\frac{1}{\pi * (48Z+128D_3)}\right]^2} * (3Z+8D_3) * \pi * dZ$$

  = 86.613 = 7.22 D

- $$L_4 = \int_0^{\frac{4}{3}D_4} \sqrt{\left(\frac{1}{3Z+4D_4}\right)^2 + \left[\frac{1}{\pi * (3Z+8D_4)}\right]^2 + \left[\frac{1}{\pi * (48Z+128D_4)}\right]^2} * (3Z+8D_4) * \pi * dZ$$

  = 173.226 = 7.22 D

- $$L_5 = \int_0^{\frac{4}{3}D_5} \sqrt{\left(\frac{1}{3Z+4D_5}\right)^2 + \left[\frac{1}{\pi * (3Z+8D_5)}\right]^2 + \left[\frac{1}{\pi * (48Z+128D_5)}\right]^2} * (3Z+8D_5) * \pi * dZ$$

  = 259.839 = 7.22 D

Travel Distance In The Cone (L) – 1D2D

D_1 = 0.1 m (4 inch) D_3 = 0.3 m (12 inch) D_5 = 0.9 m (36 inch)

D_2 = 0.2 m (6 inch) D_4 = 0.6 m (24 inch)

- $$L_1 = \int_{1.375D_1}^{1.5D_1} 13\pi\sqrt{\left(\frac{D_1}{2Z+5D_1}\right)^2+\left[\frac{1}{13\pi}\right]^2+\left[\frac{1}{104\pi}\right]^2}\,dZ +$$

$$\int_0^{1.375D_1}\sqrt{\left(\frac{1}{4Z+10D_1}\right)^2+\left[\frac{1}{\pi*(3Z+15D_1)}\right]^2+\left[\frac{1}{\pi*(24Z+120D_1)}\right]^2}*(3Z+15D_1)*dZ$$

$= 10.261 = 2.565$ D

- $$L_2 = \int_{1.375D_2}^{1.5D_2} 13\pi\sqrt{\left(\frac{D_2}{2Z+5D_2}\right)^2+\left[\frac{1}{13\pi}\right]^2+\left[\frac{1}{104\pi}\right]^2}\,dZ +$$

$$\int_0^{1.375D_2}\sqrt{\left(\frac{1}{4Z+10D_2}\right)^2+\left[\frac{1}{\pi*(3Z+15D_2)}\right]^2+\left[\frac{1}{\pi*(24Z+120D_2)}\right]^2}*(3Z+15D_2)*dZ$$

$= 15.392 = 2.565$ D

- $$L_3 = \int_{1.375D_3}^{1.5D_3} 13\pi\sqrt{\left(\frac{D_3}{2Z+5D_3}\right)^2+\left[\frac{1}{13\pi}\right]^2+\left[\frac{1}{104\pi}\right]^2}\,dZ +$$

$$\int_0^{1.375D_3}\sqrt{\left(\frac{1}{4Z+10D_3}\right)^2+\left[\frac{1}{\pi*(3Z+15D_3)}\right]^2+\left[\frac{1}{\pi*(24Z+120D_3)}\right]^2}*(3Z+15D_3)*dZ$$

$= 30.784 = 2.565$ D

- $$L_4 = \int_{1.375D_4}^{1.5D_4} 13\pi\sqrt{\left(\frac{D_4}{2Z+5D_4}\right)^2 + \left[\frac{1}{13\pi}\right]^2 + \left[\frac{1}{104\pi}\right]^2}\, dZ +$$

$$\int_{0}^{1.375D_4} \sqrt{\left(\frac{1}{4Z+10D_4}\right)^2 + \left[\frac{1}{\pi*(3Z+15D_4)}\right]^2 + \left[\frac{1}{\pi*(24Z+120D_4)}\right]^2} * (3Z+15D_4) * dZ$$

$$= 61.568 = 2.565\ D$$

- $$L_5 = \int_{1.375D_5}^{1.5D_5} 13\pi\sqrt{\left(\frac{D_5}{2Z+5D_5}\right)^2 + \left[\frac{1}{13\pi}\right]^2 + \left[\frac{1}{104\pi}\right]^2}\, dZ +$$

$$\int_{0}^{1.375D_5} \sqrt{\left(\frac{1}{4Z+10D_5}\right)^2 + \left[\frac{1}{\pi*(3Z+15D_5)}\right]^2 + \left[\frac{1}{\pi*(24Z+120D_5)}\right]^2} * (3Z+15D_5) * dZ$$

$$= 92.353 = 2.565\ D$$

APPENDIX E

CALCULATIONS OF FRICTIONAL LOSS IN THE CONE PART OF A CYCLONE

Frictional Loss In The Cone (ΔP_f) @ V_{in} = 5 m/s (1000 fpm) – 1D3D

D_1 = 0.1 m (4 inch) D_3 = 0.3 m (12 inch) D_5 = 0.9 m (36 inch)

D_2 = 0.2 m (6 inch) D_4 = 0.6 m (24 inch)

- $$\Delta P_1 = \int_0^{2D_1} \frac{0.0076*\left[\frac{(Z+4D_1)}{\sqrt{Z}}\right]*\left\{\left(\frac{4D_1}{Z+2D_1}\right)^2+\left[\frac{4D_1}{\pi*(Z+4D_1)}\right]^2+\left[\frac{D_1}{\pi*(2Z+8D_1)}\right]^2\right\}^{\frac{7}{4}}}{4(D_1)^{\frac{3}{2}}}*dZ$$

  = 35 Pa (0.14 in H_2O)

- $$\Delta P_2 = \int_0^{2D_2} \frac{0.0076*\left[\frac{(Z+4D_2)}{\sqrt{Z}}\right]*\left\{\left(\frac{4D_2}{Z+2D_2}\right)^2+\left[\frac{4D_2}{\pi*(Z+4D_2)}\right]^2+\left[\frac{D_2}{\pi*(2Z+8D_2)}\right]^2\right\}^{\frac{7}{4}}}{4(D_2)^{\frac{3}{2}}}*dZ$$

  = 35 Pa (0.14 in H_2O)

- $$\Delta P_3 = \int_0^{2D_3} \frac{0.0076*\left[\frac{(Z+4D_3)}{\sqrt{Z}}\right]*\left\{\left(\frac{4D_3}{Z+2D_3}\right)^2+\left[\frac{4D_3}{\pi*(Z+4D_3)}\right]^2+\left[\frac{D_3}{\pi*(2Z+8D_3)}\right]^2\right\}^{\frac{7}{4}}}{4(D_3)^{\frac{3}{2}}}*dZ$$

  = 35 Pa (0.14 in H_2O)

- $$\Delta P_4 = \int_0^{2D_4} \frac{0.0076*\left[\frac{(Z+4D_4)}{\sqrt{Z}}\right]*\left\{\left(\frac{4D_4}{Z+2D_4}\right)^2+\left[\frac{4D_4}{\pi*(Z+4D_4)}\right]^2+\left[\frac{D_4}{\pi*(2Z+8D_4)}\right]^2\right\}^{\frac{7}{4}}}{4(D_4)^{\frac{3}{2}}}*dZ$$

  = 35 Pa (0.14 in H_2O)

- $$\Delta P_5 = \int_0^{2D_5} \frac{0.0076*\left[\frac{(Z+4D_5)}{\sqrt{Z}}\right]*\left\{\left(\frac{4D_5}{Z+2D_5}\right)^2+\left[\frac{4D_5}{\pi*(Z+4D_5)}\right]^2+\left[\frac{D_5}{\pi*(2Z+8D_5)}\right]^2\right\}^{\frac{7}{4}}}{4(D_5)^{\frac{3}{2}}}*dZ$$

  = 35 Pa (0.14 in H_2O)

Frictional Loss In The Cone (ΔP_f) @ V_{in} = 8 m/s (1500 fpm) – 1D3D

D_1 = 0.1 m (4 inch) D_3 = 0.3 m (12 inch) D_5 = 0.9 m (36 inch)

D_2 = 0.2 m (6 inch) D_4 = 0.6 m (24 inch)

- $$\Delta P_1 = \int_0^{2D_1} \frac{0.0171*\left[\frac{(Z+4D_1)}{\sqrt{Z}}\right]*\left\{\left(\frac{4D_1}{Z+2D_1}\right)^2+\left[\frac{4D_1}{\pi*(Z+4D_1)}\right]^2+\left[\frac{D_1}{\pi*(2Z+8D_1)}\right]^2\right\}^{\frac{7}{4}}}{4(D_1)^{\frac{3}{2}}}*dZ$$

= 78.7 Pa (0.316 in H_2O)

- $$\Delta P_2 = \int_0^{2D_2} \frac{0.0171*\left[\frac{(Z+4D_2)}{\sqrt{Z}}\right]*\left\{\left(\frac{4D_2}{Z+2D_2}\right)^2+\left[\frac{4D_2}{\pi*(Z+4D_2)}\right]^2+\left[\frac{D_2}{\pi*(2Z+8D_2)}\right]^2\right\}^{\frac{7}{4}}}{4(D_2)^{\frac{3}{2}}}*dZ$$

= 78.7 Pa (0.316 in H_2O)

- $$\Delta P_3 = \int_0^{2D_3} \frac{0.0171*\left[\frac{(Z+4D_3)}{\sqrt{Z}}\right]*\left\{\left(\frac{4D_3}{Z+2D_3}\right)^2+\left[\frac{4D_3}{\pi*(Z+4D_3)}\right]^2+\left[\frac{D_3}{\pi*(2Z+8D_3)}\right]^2\right\}^{\frac{7}{4}}}{4(D_3)^{\frac{3}{2}}}*dZ$$

= 78.7 Pa (0.316 in H_2O)

- $$\Delta P_4 = \int_0^{2D_4} \frac{0.0171*\left[\frac{(Z+4D_4)}{\sqrt{Z}}\right]*\left\{\left(\frac{4D_4}{Z+2D_4}\right)^2+\left[\frac{4D_4}{\pi*(Z+4D_4)}\right]^2+\left[\frac{D_4}{\pi*(2Z+8D_4)}\right]^2\right\}^{\frac{7}{4}}}{4(D_4)^{\frac{3}{2}}}*dZ$$

= 78.7 Pa (0.316 in H_2O)

- $$\Delta P_5 = \int_0^{2D_5} \frac{0.0171*\left[\frac{(Z+4D_5)}{\sqrt{Z}}\right]*\left\{\left(\frac{4D_5}{Z+2D_5}\right)^2+\left[\frac{4D_5}{\pi*(Z+4D_5)}\right]^2+\left[\frac{D_5}{\pi*(2Z+8D_5)}\right]^2\right\}^{\frac{7}{4}}}{4(D_5)^{\frac{3}{2}}}*dZ$$

= 78.7 Pa (0.316 in H_2O)

Frictional Loss In The Cone (ΔP_f) @ V_{in} = 10 m/s (2000 fpm) – 1D3D

D_1 = 0.1 m (4 inch) D_3 = 0.3 m (12 inch) D_5 = 0.9 m (36 inch)

D_2 = 0.2 m (6 inch) D_4 = 0.6 m (24 inch)

- $$\Delta P_1 = \int_0^{2D_1} \frac{0.0305*\left[\frac{(Z+4D_1)}{\sqrt{Z}}\right]*\left\{\left(\frac{4D_1}{Z+2D_1}\right)^2+\left[\frac{4D_1}{\pi*(Z+4D_1)}\right]^2+\left[\frac{D_1}{\pi*(2Z+8D_1)}\right]^2\right\}^{\frac{7}{4}}}{4(D_1)^{\frac{3}{2}}}*dZ$$

= 140 Pa (0.563 in H_2O)

- $$\Delta P_2 = \int_0^{2D_2} \frac{0.0305*\left[\frac{(Z+4D_2)}{\sqrt{Z}}\right]*\left\{\left(\frac{4D_2}{Z+2D_2}\right)^2+\left[\frac{4D_2}{\pi*(Z+4D_2)}\right]^2+\left[\frac{D_2}{\pi*(2Z+8D_2)}\right]^2\right\}^{\frac{7}{4}}}{4(D_2)^{\frac{3}{2}}}*dZ$$

= 140 Pa (0.563 in H_2O)

- $$\Delta P_3 = \int_0^{2D_3} \frac{0.0305*\left[\frac{(Z+4D_3)}{\sqrt{Z}}\right]*\left\{\left(\frac{4D_3}{Z+2D_3}\right)^2+\left[\frac{4D_3}{\pi*(Z+4D_3)}\right]^2+\left[\frac{D_3}{\pi*(2Z+8D_3)}\right]^2\right\}^{\frac{7}{4}}}{4(D_3)^{\frac{3}{2}}}*dZ$$

= 140 Pa (0.563 in H_2O)

- $$\Delta P_4 = \int_0^{2D_4} \frac{0.0305*\left[\frac{(Z+4D_4)}{\sqrt{Z}}\right]*\left\{\left(\frac{4D_4}{Z+2D_4}\right)^2+\left[\frac{4D_4}{\pi*(Z+4D_4)}\right]^2+\left[\frac{D_4}{\pi*(2Z+8D_4)}\right]^2\right\}^{\frac{7}{4}}}{4(D_4)^{\frac{3}{2}}}*dZ$$

= 140 Pa (0.563 in H_2O)

- $$\Delta P_5 = \int_0^{2D_5} \frac{0.0305*\left[\frac{(Z+4D_5)}{\sqrt{Z}}\right]*\left\{\left(\frac{4D_5}{Z+2D_5}\right)^2+\left[\frac{4D_5}{\pi*(Z+4D_5)}\right]^2+\left[\frac{D_5}{\pi*(2Z+8D_5)}\right]^2\right\}^{\frac{7}{4}}}{4(D_5)^{\frac{3}{2}}}*dZ$$

= 140 Pa (0.563 in H_2O)

Frictional Loss In The Cone (ΔP_f) @ V_{in} = 13 m/s (2500 fpm) – 1D3D

D_1 = 0.1 m (4 inch) D_3 = 0.3 m (12 inch) D_5 = 0.9 m (36 inch)

D_2 = 0.2 m (6 inch) D_4 = 0.6 m (24 inch)

- $$\Delta P_1 = \int_0^{2D_1} \frac{0.0476*\left[\frac{(Z+4D_1)}{\sqrt{Z}}\right]*\left\{\left(\frac{4D_1}{Z+2D_1}\right)^2+\left[\frac{4D_1}{\pi*(Z+4D_1)}\right]^2+\left[\frac{D_1}{\pi*(2Z+8D_1)}\right]^2\right\}^{\frac{7}{4}}}{4(D_1)^{\frac{3}{2}}}*dZ$$

  = 219 Pa (0.879 in H_2O)

- $$\Delta P_2 = \int_0^{2D_2} \frac{0.0476*\left[\frac{(Z+4D_2)}{\sqrt{Z}}\right]*\left\{\left(\frac{4D_2}{Z+2D_2}\right)^2+\left[\frac{4D_2}{\pi*(Z+4D_2)}\right]^2+\left[\frac{D_2}{\pi*(2Z+8D_2)}\right]^2\right\}^{\frac{7}{4}}}{4(D_2)^{\frac{3}{2}}}*dZ$$

  = 219 Pa (0.879 in H_2O)

- $$\Delta P_3 = \int_0^{2D_3} \frac{0.0476*\left[\frac{(Z+4D_3)}{\sqrt{Z}}\right]*\left\{\left(\frac{4D_3}{Z+2D_3}\right)^2+\left[\frac{4D_3}{\pi*(Z+4D_3)}\right]^2+\left[\frac{D_3}{\pi*(2Z+8D_3)}\right]^2\right\}^{\frac{7}{4}}}{4(D_3)^{\frac{3}{2}}}*dZ$$

  = 219 Pa (0.879 in H_2O)

- $$\Delta P_4 = \int_0^{2D_4} \frac{0.0476*\left[\frac{(Z+4D_4)}{\sqrt{Z}}\right]*\left\{\left(\frac{4D_4}{Z+2D_4}\right)^2+\left[\frac{4D_4}{\pi*(Z+4D_4)}\right]^2+\left[\frac{D_4}{\pi*(2Z+8D_4)}\right]^2\right\}^{\frac{7}{4}}}{4(D_4)^{\frac{3}{2}}}*dZ$$

  = 219 Pa (0.879 in H_2O)

- $$\Delta P_5 = \int_0^{2D_5} \frac{0.0476*\left[\frac{(Z+4D_5)}{\sqrt{Z}}\right]*\left\{\left(\frac{4D_5}{Z+2D_5}\right)^2+\left[\frac{4D_5}{\pi*(Z+4D_5)}\right]^2+\left[\frac{D_5}{\pi*(2Z+8D_5)}\right]^2\right\}^{\frac{7}{4}}}{4(D_5)^{\frac{3}{2}}}*dZ$$

  = 219 Pa (0.879 in H_2O)

Frictional Loss In The Cone (ΔP_f) @ V_{in} = 15 m/s (3000 fpm) – 1D3D

D_1 = 0.1 m (4 inch) D_3 = 0.3 m (12 inch) D_5 = 0.9 m (36 inch)

D_2 = 0.2 m (6 inch) D_4 = 0.6 m (24 inch)

- $$\Delta P_1 = \int_0^{2D_1} \frac{0.0686*\left[\frac{(Z+4D_1)}{\sqrt{Z}}\right]*\left\{\left(\frac{4D_1}{Z+2D_1}\right)^2+\left[\frac{4D_1}{\pi*(Z+4D_1)}\right]^2+\left[\frac{D_1}{\pi*(2Z+8D_1)}\right]^2\right\}^{\frac{7}{4}}}{4(D_1)^{\frac{3}{2}}}*dZ$$

  = 315 Pa (1.267 in H_2O)

- $$\Delta P_2 = \int_0^{2D_2} \frac{0.0686*\left[\frac{(Z+4D_2)}{\sqrt{Z}}\right]*\left\{\left(\frac{4D_2}{Z+2D_2}\right)^2+\left[\frac{4D_2}{\pi*(Z+4D_2)}\right]^2+\left[\frac{D_2}{\pi*(2Z+8D_2)}\right]^2\right\}^{\frac{7}{4}}}{4(D_2)^{\frac{3}{2}}}*dZ$$

  = 315 Pa (1.267 in H_2O)

- $$\Delta P_3 = \int_0^{2D_3} \frac{0.0686*\left[\frac{(Z+4D_3)}{\sqrt{Z}}\right]*\left\{\left(\frac{4D_3}{Z+2D_3}\right)^2+\left[\frac{4D_3}{\pi*(Z+4D_3)}\right]^2+\left[\frac{D_3}{\pi*(2Z+8D_3)}\right]^2\right\}^{\frac{7}{4}}}{4(D_3)^{\frac{3}{2}}}*dZ$$

  = 315 Pa (1.267 in H_2O)

- $$\Delta P_4 = \int_0^{2D_4} \frac{0.0686*\left[\frac{(Z+4D_4)}{\sqrt{Z}}\right]*\left\{\left(\frac{4D_4}{Z+2D_4}\right)^2+\left[\frac{4D_4}{\pi*(Z+4D_4)}\right]^2+\left[\frac{D_4}{\pi*(2Z+8D_4)}\right]^2\right\}^{\frac{7}{4}}}{4(D_4)^{\frac{3}{2}}}*dZ$$

  = 315 Pa (1.267 in H_2O)

- $$\Delta P_5 = \int_0^{2D_5} \frac{0.0686*\left[\frac{(Z+4D_5)}{\sqrt{Z}}\right]*\left\{\left(\frac{4D_5}{Z+2D_5}\right)^2+\left[\frac{4D_5}{\pi*(Z+4D_5)}\right]^2+\left[\frac{D_5}{\pi*(2Z+8D_5)}\right]^2\right\}^{\frac{7}{4}}}{4(D_5)^{\frac{3}{2}}}*dZ$$

  = 315 Pa (1.267 in H_2O)

Frictional Loss In The Cone (ΔP_f) @ V_{in} = 16 m/s (3200 fpm) – 1D3D

D_1 = 0.1 m (4 inch) D_3 = 0.3 m (12 inch) D_5 = 0.9 m (36 inch)

D_2 = 0.2 m (6 inch) D_4 = 0.6 m (24 inch)

- $$\Delta P_1 = \int_0^{2D_1} \frac{0.078*\left[\frac{(Z+4D_1)}{\sqrt{Z}}\right]*\left\{\left(\frac{4D_1}{Z+2D_1}\right)^2+\left[\frac{4D_1}{\pi*(Z+4D_1)}\right]^2+\left[\frac{D_1}{\pi*(2Z+8D_1)}\right]^2\right\}^{\frac{7}{4}}}{4(D_1)^{\frac{3}{2}}}*dZ$$

  = 358 Pa (1.44 in H_2O)

- $$\Delta P_2 = \int_0^{2D_2} \frac{0.078*\left[\frac{(Z+4D_2)}{\sqrt{Z}}\right]*\left\{\left(\frac{4D_2}{Z+2D_2}\right)^2+\left[\frac{4D_2}{\pi*(Z+4D_2)}\right]^2+\left[\frac{D_2}{\pi*(2Z+8D_2)}\right]^2\right\}^{\frac{7}{4}}}{4(D_2)^{\frac{3}{2}}}*dZ$$

  = 358 Pa (1.44 in H_2O)

- $$\Delta P_3 = \int_0^{2D_3} \frac{0.078*\left[\frac{(Z+4D_3)}{\sqrt{Z}}\right]*\left\{\left(\frac{4D_3}{Z+2D_3}\right)^2+\left[\frac{4D_3}{\pi*(Z+4D_3)}\right]^2+\left[\frac{D_3}{\pi*(2Z+8D_3)}\right]^2\right\}^{\frac{7}{4}}}{4(D_3)^{\frac{3}{2}}}*dZ$$

  = 358 Pa (1.44 in H_2O)

- $$\Delta P_4 = \int_0^{2D_4} \frac{0.078*\left[\frac{(Z+4D_4)}{\sqrt{Z}}\right]*\left\{\left(\frac{4D_4}{Z+2D_4}\right)^2+\left[\frac{4D_4}{\pi*(Z+4D_4)}\right]^2+\left[\frac{D_4}{\pi*(2Z+8D_4)}\right]^2\right\}^{\frac{7}{4}}}{4(D_4)^{\frac{3}{2}}}*dZ$$

  = 358 Pa (1.44 in H_2O)

- $$\Delta P_5 = \int_0^{2D_5} \frac{0.078*\left[\frac{(Z+4D_5)}{\sqrt{Z}}\right]*\left\{\left(\frac{4D_5}{Z+2D_5}\right)^2+\left[\frac{4D_5}{\pi*(Z+4D_5)}\right]^2+\left[\frac{D_5}{\pi*(2Z+8D_5)}\right]^2\right\}^{\frac{7}{4}}}{4(D_5)^{\frac{3}{2}}}*dZ$$

  = 358 Pa (1.44 in H_2O)

Frictional Loss In The Cone (ΔP_f) @ V_{in} = 18 m/s (3500 fpm) – 1D3D

D_1 = 0.1 m (4 inch) D_3 = 0.3 m (12 inch) D_5 = 0.9 m (36 inch)

D_2 = 0.2 m (6 inch) D_4 = 0.6 m (24 inch)

- $$\Delta P_1 = \int_0^{2D_1} \frac{0.0934*\left[\frac{(Z+4D_1)}{\sqrt{Z}}\right]*\left\{\left(\frac{4D_1}{Z+2D_1}\right)^2+\left[\frac{4D_1}{\pi*(Z+4D_1)}\right]^2+\left[\frac{D_1}{\pi*(2Z+8D_1)}\right]^2\right\}^{\frac{7}{4}}}{4(D_1)^{\frac{3}{2}}}*dZ$$

  = 430 Pa (1.725 in H_2O)

- $$\Delta P_2 = \int_0^{2D_2} \frac{0.0934*\left[\frac{(Z+4D_2)}{\sqrt{Z}}\right]*\left\{\left(\frac{4D_2}{Z+2D_2}\right)^2+\left[\frac{4D_2}{\pi*(Z+4D_2)}\right]^2+\left[\frac{D_2}{\pi*(2Z+8D_2)}\right]^2\right\}^{\frac{7}{4}}}{4(D_2)^{\frac{3}{2}}}*dZ$$

  = 430 Pa (1.725 in H_2O)

- $$\Delta P_3 = \int_0^{2D_3} \frac{0.0934*\left[\frac{(Z+4D_3)}{\sqrt{Z}}\right]*\left\{\left(\frac{4D_3}{Z+2D_3}\right)^2+\left[\frac{4D_3}{\pi*(Z+4D_3)}\right]^2+\left[\frac{D_3}{\pi*(2Z+8D_3)}\right]^2\right\}^{\frac{7}{4}}}{4(D_3)^{\frac{3}{2}}}*dZ$$

  = 430 Pa (1.725 in H_2O)

- $$\Delta P_4 = \int_0^{2D_4} \frac{0.0934*\left[\frac{(Z+4D_4)}{\sqrt{Z}}\right]*\left\{\left(\frac{4D_4}{Z+2D_4}\right)^2+\left[\frac{4D_4}{\pi*(Z+4D_4)}\right]^2+\left[\frac{D_4}{\pi*(2Z+8D_4)}\right]^2\right\}^{\frac{7}{4}}}{4(D_4)^{\frac{3}{2}}}*dZ$$

  = 430 Pa (1.725 in H_2O)

- $$\Delta P_5 = \int_0^{2D_5} \frac{0.0934*\left[\frac{(Z+4D_5)}{\sqrt{Z}}\right]*\left\{\left(\frac{4D_5}{Z+2D_5}\right)^2+\left[\frac{4D_5}{\pi*(Z+4D_5)}\right]^2+\left[\frac{D_5}{\pi*(2Z+8D_5)}\right]^2\right\}^{\frac{7}{4}}}{4(D_5)^{\frac{3}{2}}}*dZ$$

  = 430 Pa (1.725 in H_2O)

Frictional Loss In The Cone (ΔP_f) @ V_{in} = 20 m/s (4000 fpm) – 1D3D

D_1 = 0.1 m (4 inch) D_3 = 0.3 m (12 inch) D_5 = 0.9 m (36 inch)

D_2 = 0.2 m (6 inch) D_4 = 0.6 m (24 inch)

- $$\Delta P_1 = \int_0^{2D_1} \frac{0.122*\left[\frac{(Z+4D_1)}{\sqrt{Z}}\right]*\left\{\left(\frac{4D_1}{Z+2D_1}\right)^2+\left[\frac{4D_1}{\pi*(Z+4D_1)}\right]^2+\left[\frac{D_1}{\pi*(2Z+8D_1)}\right]^2\right\}^{\frac{7}{4}}}{4(D_1)^{\frac{3}{2}}}*dZ$$

  = 561 Pa (2.253 in H_2O)

- $$\Delta P_2 = \int_0^{2D_2} \frac{0.122*\left[\frac{(Z+4D_2)}{\sqrt{Z}}\right]*\left\{\left(\frac{4D_2}{Z+2D_2}\right)^2+\left[\frac{4D_2}{\pi*(Z+4D_2)}\right]^2+\left[\frac{D_2}{\pi*(2Z+8D_2)}\right]^2\right\}^{\frac{7}{4}}}{4(D_2)^{\frac{3}{2}}}*dZ$$

  = 561 Pa (2.253 in H_2O)

- $$\Delta P_3 = \int_0^{2D_3} \frac{0.122*\left[\frac{(Z+4D_3)}{\sqrt{Z}}\right]*\left\{\left(\frac{4D_3}{Z+2D_3}\right)^2+\left[\frac{4D_3}{\pi*(Z+4D_3)}\right]^2+\left[\frac{D_3}{\pi*(2Z+8D_3)}\right]^2\right\}^{\frac{7}{4}}}{4(D_3)^{\frac{3}{2}}}*dZ$$

  = 561 Pa (2.253 in H_2O)

- $$\Delta P_4 = \int_0^{2D_4} \frac{0.122*\left[\frac{(Z+4D_4)}{\sqrt{Z}}\right]*\left\{\left(\frac{4D_4}{Z+2D_4}\right)^2+\left[\frac{4D_4}{\pi*(Z+4D_4)}\right]^2+\left[\frac{D_4}{\pi*(2Z+8D_4)}\right]^2\right\}^{\frac{7}{4}}}{4(D_4)^{\frac{3}{2}}}*dZ$$

  = 561 Pa (2.253 in H_2O)

- $$\Delta P_5 = \int_0^{2D_5} \frac{0.122*\left[\frac{(Z+4D_5)}{\sqrt{Z}}\right]*\left\{\left(\frac{4D_5}{Z+2D_5}\right)^2+\left[\frac{4D_5}{\pi*(Z+4D_5)}\right]^2+\left[\frac{D_5}{\pi*(2Z+8D_5)}\right]^2\right\}^{\frac{7}{4}}}{4(D_5)^{\frac{3}{2}}}*dZ$$

  = 561 Pa (2.253 in H_2O)

Frictional Loss In The Cone (ΔP_f) @ V_{in} = 5 m/s (1000 fpm) – 2D2D

D_1 = 0.1 m (4 inch) D_3 = 0.3 m (12 inch) D_5 = 0.9 m (36 inch)

D_2 = 0.2 m (6 inch) D_4 = 0.6 m (24 inch)

- $$\Delta P_1 = \int_0^{\frac{4}{3}D_1} \frac{0.006*\left[\frac{(3Z+8D_1)}{\sqrt{Z}}\right]*\left\{\left(\frac{8D_1}{3Z+4D_1}\right)^2+\left[\frac{8D_1}{\pi*(3Z+8D_1)}\right]^2+\left[\frac{3D_1}{\pi*(6Z+16D_1)}\right]^2\right\}^{\frac{7}{4}}}{8(D_1)^{\frac{3}{2}}}*dZ$$

= 22.7 Pa (0.091 in H_2O)

- $$\Delta P_2 = \int_0^{\frac{4}{3}D_2} \frac{0.006*\left[\frac{(3Z+8D_2)}{\sqrt{Z}}\right]*\left\{\left(\frac{8D_2}{3Z+4D_2}\right)^2+\left[\frac{8D_2}{\pi*(3Z+8D_2)}\right]^2+\left[\frac{3D_2}{\pi*(6Z+16D_2)}\right]^2\right\}^{\frac{7}{4}}}{8(D_2)^{\frac{3}{2}}}*dZ$$

= 22.7 Pa (0.091 in H_2O)

- $$\Delta P_3 = \int_0^{\frac{4}{3}D_3} \frac{0.006*\left[\frac{(3Z+8D_3)}{\sqrt{Z}}\right]*\left\{\left(\frac{8D_3}{3Z+4D_3}\right)^2+\left[\frac{8D_3}{\pi*(3Z+8D_3)}\right]^2+\left[\frac{3D_3}{\pi*(6Z+16D_3)}\right]^2\right\}^{\frac{7}{4}}}{8(D_3)^{\frac{3}{2}}}*dZ$$

= 22.7 Pa (0.091 in H_2O)

- $$\Delta P_4 = \int_0^{\frac{4}{3}D_4} \frac{0.006*\left[\frac{(3Z+8D_4)}{\sqrt{Z}}\right]*\left\{\left(\frac{8D_4}{3Z+4D_4}\right)^2+\left[\frac{8D_4}{\pi*(3Z+8D_4)}\right]^2+\left[\frac{3D_4}{\pi*(6Z+16D_4)}\right]^2\right\}^{\frac{7}{4}}}{8(D_4)^{\frac{3}{2}}}*dZ$$

= 22.7 Pa (0.091 in H_2O)

- $$\Delta P_5 = \int_0^{\frac{4}{3}D_5} \frac{0.006*\left[\frac{(3Z+8D_5)}{\sqrt{Z}}\right]*\left\{\left(\frac{8D_5}{3Z+4D_5}\right)^2+\left[\frac{8D_5}{\pi*(3Z+8D_5)}\right]^2+\left[\frac{3D_5}{\pi*(6Z+16D_5)}\right]^2\right\}^{\frac{7}{4}}}{8(D_5)^{\frac{3}{2}}}*dZ$$

= 22.7 Pa (0.091 in H_2O)

Frictional Loss In The Cone (ΔP_f) @ V_{in} = 8 m/s (1500 fpm) – 2D2D

D_1 = 0.1 m (4 inch) D_3 = 0.3 m (12 inch) D_5 = 0.9 m (36 inch)

D_2 = 0.2 m (6 inch) D_4 = 0.6 m (24 inch)

- $$\Delta P_1 = \int_0^{\frac{4}{3}D_1} \frac{0.014*\left[\frac{(3Z+8D_1)}{\sqrt{Z}}\right]*\left\{\left(\frac{8D_1}{3Z+4D_1}\right)^2+\left[\frac{8D_1}{\pi*(3Z+8D_1)}\right]^2+\left[\frac{3D_1}{\pi*(6Z+16D_1)}\right]^2\right\}^{\frac{7}{4}}}{8(D_1)^{\frac{3}{2}}}*dZ$$

  = 52.5 Pa (0.211 in H_2O)

- $$\Delta P_2 = \int_0^{\frac{4}{3}D_2} \frac{0.014*\left[\frac{(3Z+8D_2)}{\sqrt{Z}}\right]*\left\{\left(\frac{8D_2}{3Z+4D_2}\right)^2+\left[\frac{8D_2}{\pi*(3Z+8D_2)}\right]^2+\left[\frac{3D_2}{\pi*(6Z+16D_2)}\right]^2\right\}^{\frac{7}{4}}}{8(D_2)^{\frac{3}{2}}}*dZ$$

  = 52.5 Pa (0.211 in H_2O)

- $$\Delta P_3 = \int_0^{\frac{4}{3}D_3} \frac{0.014*\left[\frac{(3Z+8D_3)}{\sqrt{Z}}\right]*\left\{\left(\frac{8D_3}{3Z+4D_3}\right)^2+\left[\frac{8D_3}{\pi*(3Z+8D_3)}\right]^2+\left[\frac{3D_3}{\pi*(6Z+16D_3)}\right]^2\right\}^{\frac{7}{4}}}{8(D_3)^{\frac{3}{2}}}*dZ$$

  = 52.5 Pa (0.211 in H_2O)

- $$\Delta P_4 = \int_0^{\frac{4}{3}D_4} \frac{0.014*\left[\frac{(3Z+8D_4)}{\sqrt{Z}}\right]*\left\{\left(\frac{8D_4}{3Z+4D_4}\right)^2+\left[\frac{8D_4}{\pi*(3Z+8D_4)}\right]^2+\left[\frac{3D_4}{\pi*(6Z+16D_4)}\right]^2\right\}^{\frac{7}{4}}}{8(D_4)^{\frac{3}{2}}}*dZ$$

  = 52.5 Pa (0.211 in H_2O)

- $$\Delta P_5 = \int_0^{\frac{4}{3}D_5} \frac{0.014*\left[\frac{(3Z+8D_5)}{\sqrt{Z}}\right]*\left\{\left(\frac{8D_5}{3Z+4D_5}\right)^2+\left[\frac{8D_5}{\pi*(3Z+8D_5)}\right]^2+\left[\frac{3D_5}{\pi*(6Z+16D_5)}\right]^2\right\}^{\frac{7}{4}}}{8(D_5)^{\frac{3}{2}}}*dZ$$

  = 52.5 Pa (0.211 in H_2O)

Frictional Loss In The Cone (ΔP_f) @ V_{in} = 10 m/s (2000 fpm) – 2D2D

D_1 = 0.1 m (4 inch) D_3 = 0.3 m (12 inch) D_5 = 0.9 m (36 inch)

D_2 = 0.2 m (6 inch) D_4 = 0.6 m (24 inch)

- $$\Delta P_1 = \int_0^{\frac{4}{3}D_1} \frac{0.025*\left[\frac{(3Z+8D_1)}{\sqrt{Z}}\right]*\left\{\left(\frac{8D_1}{3Z+4D_1}\right)^2+\left[\frac{8D_1}{\pi*(3Z+8D_1)}\right]^2+\left[\frac{3D_1}{\pi*(6Z+16D_1)}\right]^2\right\}^{\frac{7}{4}}}{8(D_1)^{\frac{3}{2}}}*dZ$$

  = 93.9 Pa (0.377 in H_2O)

- $$\Delta P_2 = \int_0^{\frac{4}{3}D_2} \frac{0.025*\left[\frac{(3Z+8D_2)}{\sqrt{Z}}\right]*\left\{\left(\frac{8D_2}{3Z+4D_2}\right)^2+\left[\frac{8D_2}{\pi*(3Z+8D_2)}\right]^2+\left[\frac{3D_2}{\pi*(6Z+16D_2)}\right]^2\right\}^{\frac{7}{4}}}{8(D_2)^{\frac{3}{2}}}*dZ$$

  = 93.9 Pa (0.377 in H_2O)

- $$\Delta P_3 = \int_0^{\frac{4}{3}D_3} \frac{0.025*\left[\frac{(3Z+8D_3)}{\sqrt{Z}}\right]*\left\{\left(\frac{8D_3}{3Z+4D_3}\right)^2+\left[\frac{8D_3}{\pi*(3Z+8D_3)}\right]^2+\left[\frac{3D_3}{\pi*(6Z+16D_3)}\right]^2\right\}^{\frac{7}{4}}}{8(D_3)^{\frac{3}{2}}}*dZ$$

  = 93.9 Pa (0.377 in H_2O)

- $$\Delta P_4 = \int_0^{\frac{4}{3}D_4} \frac{0.025*\left[\frac{(3Z+8D_4)}{\sqrt{Z}}\right]*\left\{\left(\frac{8D_4}{3Z+4D_4}\right)^2+\left[\frac{8D_4}{\pi*(3Z+8D_4)}\right]^2+\left[\frac{3D_4}{\pi*(6Z+16D_4)}\right]^2\right\}^{\frac{7}{4}}}{8(D_4)^{\frac{3}{2}}}*dZ$$

  = 93.9 Pa (0.377 in H_2O)

- $$\Delta P_5 = \int_0^{\frac{4}{3}D_5} \frac{0.025*\left[\frac{(3Z+8D_5)}{\sqrt{Z}}\right]*\left\{\left(\frac{8D_5}{3Z+4D_5}\right)^2+\left[\frac{8D_5}{\pi*(3Z+8D_5)}\right]^2+\left[\frac{3D_5}{\pi*(6Z+16D_5)}\right]^2\right\}^{\frac{7}{4}}}{8(D_5)^{\frac{3}{2}}}*dZ$$

  = 93.9 Pa (0.377 in H_2O)

Frictional Loss In The Cone (ΔP_f) @ V_{in} = 13 m/s (2500 fpm) – 2D2D

D_1 = 0.1 m (4 inch) D_3 = 0.3 m (12 inch) D_5 = 0.9 m (36 inch)

D_2 = 0.2 m (6 inch) D_4 = 0.6 m (24 inch)

- $$\Delta P_1 = \int_0^{\frac{4}{3}D_1} \frac{0.039*\left[\frac{(3Z+8D_1)}{\sqrt{Z}}\right]*\left\{\left(\frac{8D_1}{3Z+4D_1}\right)^2+\left[\frac{8D_1}{\pi*(3Z+8D_1)}\right]^2+\left[\frac{3D_1}{\pi*(6Z+16D_1)}\right]^2\right\}^{\frac{7}{4}}}{8(D_1)^{\frac{3}{2}}}*dZ$$

  = 146.7 Pa (0.589 in H_2O)

- $$\Delta P_2 = \int_0^{\frac{4}{3}D_2} \frac{0.039*\left[\frac{(3Z+8D_2)}{\sqrt{Z}}\right]*\left\{\left(\frac{8D_2}{3Z+4D_2}\right)^2+\left[\frac{8D_2}{\pi*(3Z+8D_2)}\right]^2+\left[\frac{3D_2}{\pi*(6Z+16D_2)}\right]^2\right\}^{\frac{7}{4}}}{8(D_2)^{\frac{3}{2}}}*dZ$$

  = 146.7 Pa (0.589 in H_2O)

- $$\Delta P_3 = \int_0^{\frac{4}{3}D_3} \frac{0.039*\left[\frac{(3Z+8D_3)}{\sqrt{Z}}\right]*\left\{\left(\frac{8D_3}{3Z+4D_3}\right)^2+\left[\frac{8D_3}{\pi*(3Z+8D_3)}\right]^2+\left[\frac{3D_3}{\pi*(6Z+16D_3)}\right]^2\right\}^{\frac{7}{4}}}{8(D_3)^{\frac{3}{2}}}*dZ$$

  = 146.7 Pa (0.589 in H_2O)

- $$\Delta P_4 = \int_0^{\frac{4}{3}D_4} \frac{0.039*\left[\frac{(3Z+8D_4)}{\sqrt{Z}}\right]*\left\{\left(\frac{8D_4}{3Z+4D_4}\right)^2+\left[\frac{8D_4}{\pi*(3Z+8D_4)}\right]^2+\left[\frac{3D_4}{\pi*(6Z+16D_4)}\right]^2\right\}^{\frac{7}{4}}}{8(D_4)^{\frac{3}{2}}}*dZ$$

  = 146.7 Pa (0.589 in H_2O)

- $$\Delta P_5 = \int_0^{\frac{4}{3}D_5} \frac{0.039*\left[\frac{(3Z+8D_5)}{\sqrt{Z}}\right]*\left\{\left(\frac{8D_5}{3Z+4D_5}\right)^2+\left[\frac{8D_5}{\pi*(3Z+8D_5)}\right]^2+\left[\frac{3D_5}{\pi*(6Z+16D_5)}\right]^2\right\}^{\frac{7}{4}}}{8(D_5)^{\frac{3}{2}}}*dZ$$

  = 146.7 Pa (0.589 in H_2O)

Frictional Loss In The Cone (ΔP_f) @ V_{in} = 15 m/s (3000 fpm) – 2D2D

D_1 = 0.1 m (4 inch) D_3 = 0.3 m (12 inch) D_5 = 0.9 m (36 inch)

D_2 = 0.2 m (6 inch) D_4 = 0.6 m (24 inch)

- $$\Delta P_1 = \int_0^{\frac{4}{3}D_1} \frac{0.056*\left[\frac{(3Z+8D_1)}{\sqrt{Z}}\right]*\left\{\left(\frac{8D_1}{3Z+4D_1}\right)^2+\left[\frac{8D_1}{\pi*(3Z+8D_1)}\right]^2+\left[\frac{3D_1}{\pi*(6Z+16D_1)}\right]^2\right\}^{\frac{7}{4}}}{8(D_1)^{\frac{3}{2}}}*dZ$$

  = 210.4 Pa (0.845 in H_2O)

- $$\Delta P_2 = \int_0^{\frac{4}{3}D_2} \frac{0.056*\left[\frac{(3Z+8D_2)}{\sqrt{Z}}\right]*\left\{\left(\frac{8D_2}{3Z+4D_2}\right)^2+\left[\frac{8D_2}{\pi*(3Z+8D_2)}\right]^2+\left[\frac{3D_2}{\pi*(6Z+16D_2)}\right]^2\right\}^{\frac{7}{4}}}{8(D_2)^{\frac{3}{2}}}*dZ$$

  = 210.4 Pa (0.845 in H_2O)

- $$\Delta P_3 = \int_0^{\frac{4}{3}D_3} \frac{0.056*\left[\frac{(3Z+8D_3)}{\sqrt{Z}}\right]*\left\{\left(\frac{8D_3}{3Z+4D_3}\right)^2+\left[\frac{8D_3}{\pi*(3Z+8D_3)}\right]^2+\left[\frac{3D_3}{\pi*(6Z+16D_3)}\right]^2\right\}^{\frac{7}{4}}}{8(D_3)^{\frac{3}{2}}}*dZ$$

  = 210.4 Pa (0.845 in H_2O)

- $$\Delta P_4 = \int_0^{\frac{4}{3}D_4} \frac{0.056*\left[\frac{(3Z+8D_4)}{\sqrt{Z}}\right]*\left\{\left(\frac{8D_4}{3Z+4D_4}\right)^2+\left[\frac{8D_4}{\pi*(3Z+8D_4)}\right]^2+\left[\frac{3D_4}{\pi*(6Z+16D_4)}\right]^2\right\}^{\frac{7}{4}}}{8(D_4)^{\frac{3}{2}}}*dZ$$

  = 210.4 Pa (0.845 in H_2O)

- $$\Delta P_5 = \int_0^{\frac{4}{3}D_5} \frac{0.056*\left[\frac{(3Z+8D_5)}{\sqrt{Z}}\right]*\left\{\left(\frac{8D_5}{3Z+4D_5}\right)^2+\left[\frac{8D_5}{\pi*(3Z+8D_5)}\right]^2+\left[\frac{3D_5}{\pi*(6Z+16D_5)}\right]^2\right\}^{\frac{7}{4}}}{8(D_5)^{\frac{3}{2}}}*dZ$$

  = 210.4 Pa (0.845 in H_2O)

Frictional Loss In The Cone (ΔP_f) @ V_{in} = 16 m/s (3200 fpm) – 2D2D

D_1 = 0.1 m (4 inch) D_3 = 0.3 m (12 inch) D_5 = 0.9 m (36 inch)

D_2 = 0.2 m (6 inch) D_4 = 0.6 m (24 inch)

- $$\Delta P_1 = \int_0^{\frac{4}{3}D_1} \frac{0.064*\left[\frac{(3Z+8D_1)}{\sqrt{Z}}\right]*\left\{\left(\frac{8D_1}{3Z+4D_1}\right)^2+\left[\frac{8D_1}{\pi*(3Z+8D_1)}\right]^2+\left[\frac{3D_1}{\pi*(6Z+16D_1)}\right]^2\right\}^{\frac{7}{4}}}{8(D_1)^{\frac{3}{2}}}*dZ$$

= 240.5 Pa (0.966 in H_2O)

- $$\Delta P_2 = \int_0^{\frac{4}{3}D_2} \frac{0.064*\left[\frac{(3Z+8D_2)}{\sqrt{Z}}\right]*\left\{\left(\frac{8D_2}{3Z+4D_2}\right)^2+\left[\frac{8D_2}{\pi*(3Z+8D_2)}\right]^2+\left[\frac{3D_2}{\pi*(6Z+16D_2)}\right]^2\right\}^{\frac{7}{4}}}{8(D_2)^{\frac{3}{2}}}*dZ$$

= 240.5 Pa (0.966 in H_2O)

- $$\Delta P_3 = \int_0^{\frac{4}{3}D_3} \frac{0.064*\left[\frac{(3Z+8D_3)}{\sqrt{Z}}\right]*\left\{\left(\frac{8D_3}{3Z+4D_3}\right)^2+\left[\frac{8D_3}{\pi*(3Z+8D_3)}\right]^2+\left[\frac{3D_3}{\pi*(6Z+16D_3)}\right]^2\right\}^{\frac{7}{4}}}{8(D_3)^{\frac{3}{2}}}*dZ$$

= 240.5 Pa (0.966 in H_2O)

- $$\Delta P_4 = \int_0^{\frac{4}{3}D_4} \frac{0.064*\left[\frac{(3Z+8D_4)}{\sqrt{Z}}\right]*\left\{\left(\frac{8D_4}{3Z+4D_4}\right)^2+\left[\frac{8D_4}{\pi*(3Z+8D_4)}\right]^2+\left[\frac{3D_4}{\pi*(6Z+16D_4)}\right]^2\right\}^{\frac{7}{4}}}{8(D_4)^{\frac{3}{2}}}*dZ$$

= 240.5 Pa (0.966 in H_2O)

- $$\Delta P_5 = \int_0^{\frac{4}{3}D_5} \frac{0.064*\left[\frac{(3Z+8D_5)}{\sqrt{Z}}\right]*\left\{\left(\frac{8D_5}{3Z+4D_5}\right)^2+\left[\frac{8D_5}{\pi*(3Z+8D_5)}\right]^2+\left[\frac{3D_5}{\pi*(6Z+16D_5)}\right]^2\right\}^{\frac{7}{4}}}{8(D_5)^{\frac{3}{2}}}*dZ$$

= 240.5 Pa (0.966 in H_2O)

Frictional Loss In The Cone (ΔP_f) @ V_{in} = 18 m/s (3500 fpm) – 2D2D

D_1 = 0.1 m (4 inch) D_3 = 0.3 m (12 inch) D_5 = 0.9 m (36 inch)

D_2 = 0.2 m (6 inch) D_4 = 0.6 m (24 inch)

- $$\Delta P_1 = \int_0^{\frac{4}{3}D_1} \frac{0.076*\left[\frac{(3Z+8D_1)}{\sqrt{Z}}\right]*\left\{\left(\frac{8D_1}{3Z+4D_1}\right)^2+\left[\frac{8D_1}{\pi*(3Z+8D_1)}\right]^2+\left[\frac{3D_1}{\pi*(6Z+16D_1)}\right]^2\right\}^{\frac{7}{4}}}{8(D_1)^{\frac{3}{2}}}*dZ$$

  = 285.6 Pa (1.147 in H_2O)

- $$\Delta P_2 = \int_0^{\frac{4}{3}D_2} \frac{0.076*\left[\frac{(3Z+8D_2)}{\sqrt{Z}}\right]*\left\{\left(\frac{8D_2}{3Z+4D_2}\right)^2+\left[\frac{8D_2}{\pi*(3Z+8D_2)}\right]^2+\left[\frac{3D_2}{\pi*(6Z+16D_2)}\right]^2\right\}^{\frac{7}{4}}}{8(D_2)^{\frac{3}{2}}}*dZ$$

  = 285.6 Pa (1.147 in H_2O)

- $$\Delta P_3 = \int_0^{\frac{4}{3}D_3} \frac{0.076*\left[\frac{(3Z+8D_3)}{\sqrt{Z}}\right]*\left\{\left(\frac{8D_3}{3Z+4D_3}\right)^2+\left[\frac{8D_3}{\pi*(3Z+8D_3)}\right]^2+\left[\frac{3D_3}{\pi*(6Z+16D_3)}\right]^2\right\}^{\frac{7}{4}}}{8(D_3)^{\frac{3}{2}}}*dZ$$

  = 285.6 Pa (1.147 in H_2O)

- $$\Delta P_4 = \int_0^{\frac{4}{3}D_4} \frac{0.076*\left[\frac{(3Z+8D_4)}{\sqrt{Z}}\right]*\left\{\left(\frac{8D_4}{3Z+4D_4}\right)^2+\left[\frac{8D_4}{\pi*(3Z+8D_4)}\right]^2+\left[\frac{3D_4}{\pi*(6Z+16D_4)}\right]^2\right\}^{\frac{7}{4}}}{8(D_4)^{\frac{3}{2}}}*dZ$$

  = 285.6 Pa (1.147 in H_2O)

- $$\Delta P_5 = \int_0^{\frac{4}{3}D_5} \frac{0.076*\left[\frac{(3Z+8D_5)}{\sqrt{Z}}\right]*\left\{\left(\frac{8D_5}{3Z+4D_5}\right)^2+\left[\frac{8D_5}{\pi*(3Z+8D_5)}\right]^2+\left[\frac{3D_5}{\pi*(6Z+16D_5)}\right]^2\right\}^{\frac{7}{4}}}{8(D_5)^{\frac{3}{2}}}*dZ$$

  = 285.6 Pa (1.147 in H_2O)

Frictional Loss In The Cone (ΔP_f) @ V_{in} = 20 m/s (4000 fpm) – 2D2D

D_1 = 0.1 m (4 inch) D_3 = 0.3 m (12 inch) D_5 = 0.9 m (36 inch)

D_2 = 0.2 m (6 inch) D_4 = 0.6 m (24 inch)

- $$\Delta P_1 = \int_0^{\frac{4}{3}D_1} \frac{0.1*\left[\frac{(3Z+8D_1)}{\sqrt{Z}}\right]*\left\{\left(\frac{8D_1}{3Z+4D_1}\right)^2+\left[\frac{8D_1}{\pi*(3Z+8D_1)}\right]^2+\left[\frac{3D_1}{\pi*(6Z+16D_1)}\right]^2\right\}^{\frac{7}{4}}}{8(D_1)^{\frac{3}{2}}}*dZ$$

  = 375.7 Pa (1.509 in H_2O)

- $$\Delta P_2 = \int_0^{\frac{4}{3}D_2} \frac{0.1*\left[\frac{(3Z+8D_2)}{\sqrt{Z}}\right]*\left\{\left(\frac{8D_2}{3Z+4D_2}\right)^2+\left[\frac{8D_2}{\pi*(3Z+8D_2)}\right]^2+\left[\frac{3D_2}{\pi*(6Z+16D_2)}\right]^2\right\}^{\frac{7}{4}}}{8(D_2)^{\frac{3}{2}}}*dZ$$

  = 375.7 Pa (1.509 in H_2O)

- $$\Delta P_3 = \int_0^{\frac{4}{3}D_3} \frac{0.1*\left[\frac{(3Z+8D_3)}{\sqrt{Z}}\right]*\left\{\left(\frac{8D_3}{3Z+4D_3}\right)^2+\left[\frac{8D_3}{\pi*(3Z+8D_3)}\right]^2+\left[\frac{3D_3}{\pi*(6Z+16D_3)}\right]^2\right\}^{\frac{7}{4}}}{8(D_3)^{\frac{3}{2}}}*dZ$$

  = 375.7 Pa (1.509 in H_2O)

- $$\Delta P_4 = \int_0^{\frac{4}{3}D_4} \frac{0.1*\left[\frac{(3Z+8D_4)}{\sqrt{Z}}\right]*\left\{\left(\frac{8D_4}{3Z+4D_4}\right)^2+\left[\frac{8D_4}{\pi*(3Z+8D_4)}\right]^2+\left[\frac{3D_4}{\pi*(6Z+16D_4)}\right]^2\right\}^{\frac{7}{4}}}{8(D_4)^{\frac{3}{2}}}*dZ$$

  = 375.7 Pa (1.509 in H_2O)

- $$\Delta P_5 = \int_0^{\frac{4}{3}D_5} \frac{0.1*\left[\frac{(3Z+8D_5)}{\sqrt{Z}}\right]*\left\{\left(\frac{8D_5}{3Z+4D_5}\right)^2+\left[\frac{8D_5}{\pi*(3Z+8D_5)}\right]^2+\left[\frac{3D_5}{\pi*(6Z+16D_5)}\right]^2\right\}^{\frac{7}{4}}}{8(D_5)^{\frac{3}{2}}}*dZ$$

  = 375.7 Pa (1.509 in H_2O)

Frictional Loss In The Cone (ΔP_f) @ V_{in} = 5 m/s (1000 fpm) – 1D2D

D_1 = 0.1 m (4 inch) D_3 = 0.3 m (12 inch) D_5 = 0.9 m (36 inch)

D_2 = 0.2 m (6 inch) D_4 = 0.6 m (24 inch)

- $$\Delta P_1 = \int_0^{1.5D_1} \frac{0.007*\left[\frac{(3Z+15D_1)}{\sqrt{Z}}\right]*\left\{\left(\frac{8D_1}{2Z+5D_1}\right)^2+\left[\frac{2D_1}{\pi*(3Z+15D_1)}\right]^2+\left[\frac{16D_1}{\pi*(3Z+15D_1)}\right]^2\right\}^{\frac{7}{4}}}{16(D_1)^{\frac{3}{2}}}*dZ$$

  = 14.7 Pa (0.059 in H_2O)

- $$\Delta P_2 = \int_0^{1.5D_2} \frac{0.007*\left[\frac{(3Z+15D_2)}{\sqrt{Z}}\right]*\left\{\left(\frac{8D_2}{2Z+5D_2}\right)^2+\left[\frac{2D_2}{\pi*(3Z+15D_2)}\right]^2+\left[\frac{16D_2}{\pi*(3Z+15D_2)}\right]^2\right\}^{\frac{7}{4}}}{16(D_2)^{\frac{3}{2}}}*dZ$$

  = 14.7 Pa (0.059 in H_2O)

- $$\Delta P_3 = \int_0^{1.5D_3} \frac{0.007*\left[\frac{(3Z+15D_3)}{\sqrt{Z}}\right]*\left\{\left(\frac{8D_3}{2Z+5D_3}\right)^2+\left[\frac{2D_3}{\pi*(3Z+15D_3)}\right]^2+\left[\frac{16D_3}{\pi*(3Z+15D_3)}\right]^2\right\}^{\frac{7}{4}}}{16(D_3)^{\frac{3}{2}}}*dZ$$

  = 14.7 Pa (0.059 in H_2O)

- $$\Delta P_4 = \int_0^{1.5D_4} \frac{0.007*\left[\frac{(3Z+15D_4)}{\sqrt{Z}}\right]*\left\{\left(\frac{8D_4}{2Z+5D_4}\right)^2+\left[\frac{2D_4}{\pi*(3Z+15D_4)}\right]^2+\left[\frac{16D_4}{\pi*(3Z+15D_4)}\right]^2\right\}^{\frac{7}{4}}}{16(D_4)^{\frac{3}{2}}}*dZ$$

  = 14.7 Pa (0.059 in H_2O)

- $$\Delta P_5 = \int_0^{1.5D_5} \frac{0.007*\left[\frac{(3Z+15D_5)}{\sqrt{Z}}\right]*\left\{\left(\frac{8D_5}{2Z+5D_5}\right)^2+\left[\frac{2D_5}{\pi*(3Z+15D_5)}\right]^2+\left[\frac{16D_5}{\pi*(3Z+15D_5)}\right]^2\right\}^{\frac{7}{4}}}{16(D_5)^{\frac{3}{2}}}*dZ$$

  = 14.7 Pa (0.059 in H_2O)

Frictional Loss In The Cone (ΔP_f) @ V_{in} = 8 m/s (1500 fpm) – 1D2D

D_1 = 0.1 m (4 inch) D_3 = 0.3 m (12 inch) D_5 = 0.9 m (36 inch)

D_2 = 0.2 m (6 inch) D_4 = 0.6 m (24 inch)

- $$\Delta P_1 = \int_0^{1.5D_1} \frac{0.015*\left[\frac{(3Z+15D_1)}{\sqrt{Z}}\right]*\left\{\left(\frac{8D_1}{2Z+5D_1}\right)^2+\left[\frac{2D_1}{\pi*(3Z+15D_1)}\right]^2+\left[\frac{16D_1}{\pi*(3Z+15D_1)}\right]^2\right\}^{\frac{7}{4}}}{16(D_1)^{\frac{3}{2}}}*dZ$$

$= 31.6$ Pa (0.127 in H_2O)

- $$\Delta P_2 = \int_0^{1.5D_2} \frac{0.015*\left[\frac{(3Z+15D_2)}{\sqrt{Z}}\right]*\left\{\left(\frac{8D_2}{2Z+5D_2}\right)^2+\left[\frac{2D_2}{\pi*(3Z+15D_2)}\right]^2+\left[\frac{16D_2}{\pi*(3Z+15D_2)}\right]^2\right\}^{\frac{7}{4}}}{16(D_2)^{\frac{3}{2}}}*dZ$$

$= 31.6$ Pa (0.127 in H_2O)

- $$\Delta P_3 = \int_0^{1.5D_3} \frac{0.015*\left[\frac{(3Z+15D_3)}{\sqrt{Z}}\right]*\left\{\left(\frac{8D_3}{2Z+5D_3}\right)^2+\left[\frac{2D_3}{\pi*(3Z+15D_3)}\right]^2+\left[\frac{16D_3}{\pi*(3Z+15D_3)}\right]^2\right\}^{\frac{7}{4}}}{16(D_3)^{\frac{3}{2}}}*dZ$$

$= 31.6$ Pa (0.127 in H_2O)

- $$\Delta P_4 = \int_0^{1.5D_4} \frac{0.015*\left[\frac{(3Z+15D_4)}{\sqrt{Z}}\right]*\left\{\left(\frac{8D_4}{2Z+5D_4}\right)^2+\left[\frac{2D_4}{\pi*(3Z+15D_4)}\right]^2+\left[\frac{16D_4}{\pi*(3Z+15D_4)}\right]^2\right\}^{\frac{7}{4}}}{16(D_4)^{\frac{3}{2}}}*dZ$$

$= 31.6$Pa (0.127 in H_2O)

- $$\Delta P_5 = \int_0^{1.5D_5} \frac{0.015*\left[\frac{(3Z+15D_5)}{\sqrt{Z}}\right]*\left\{\left(\frac{8D_5}{2Z+5D_5}\right)^2+\left[\frac{2D_5}{\pi*(3Z+15D_5)}\right]^2+\left[\frac{16D_5}{\pi*(3Z+15D_5)}\right]^2\right\}^{\frac{7}{4}}}{16(D_5)^{\frac{3}{2}}}*dZ$$

$= 31.6$ Pa (0.127 in H_2O)

Frictional Loss In The Cone (ΔP_f) @ V_{in} = 10 m/s (2000 fpm) – 1D2D

D_1 = 0.1 m (4 inch) D_3 = 0.3 m (12 inch) D_5 = 0.9 m (36 inch)

D_2 = 0.2 m (6 inch) D_4 = 0.6 m (24 inch)

- $$\Delta P_1 = \int_0^{1.5D_1} \frac{0.026*\left[\frac{(3Z+15D_1)}{\sqrt{Z}}\right]*\left\{\left(\frac{8D_1}{2Z+5D_1}\right)^2+\left[\frac{2D_1}{\pi*(3Z+15D_1)}\right]^2+\left[\frac{16D_1}{\pi*(3Z+15D_1)}\right]^2\right\}^{\frac{7}{4}}}{16(D_1)^{\frac{3}{2}}}*dZ$$

  = 55 Pa (0.221 in H_2O)

- $$\Delta P_2 = \int_0^{1.5D_2} \frac{0.026*\left[\frac{(3Z+15D_2)}{\sqrt{Z}}\right]*\left\{\left(\frac{8D_2}{2Z+5D_2}\right)^2+\left[\frac{2D_2}{\pi*(3Z+15D_2)}\right]^2+\left[\frac{16D_2}{\pi*(3Z+15D_2)}\right]^2\right\}^{\frac{7}{4}}}{16(D_2)^{\frac{3}{2}}}*dZ$$

  = 55 Pa (0.221 in H_2O)

- $$\Delta P_3 = \int_0^{1.5D_3} \frac{0.026*\left[\frac{(3Z+15D_3)}{\sqrt{Z}}\right]*\left\{\left(\frac{8D_3}{2Z+5D_3}\right)^2+\left[\frac{2D_3}{\pi*(3Z+15D_3)}\right]^2+\left[\frac{16D_3}{\pi*(3Z+15D_3)}\right]^2\right\}^{\frac{7}{4}}}{16(D_3)^{\frac{3}{2}}}*dZ$$

  = 55 Pa (0.221 in H_2O)

- $$\Delta P_4 = \int_0^{1.5D_4} \frac{0.026*\left[\frac{(3Z+15D_4)}{\sqrt{Z}}\right]*\left\{\left(\frac{8D_4}{2Z+5D_4}\right)^2+\left[\frac{2D_4}{\pi*(3Z+15D_4)}\right]^2+\left[\frac{16D_4}{\pi*(3Z+15D_4)}\right]^2\right\}^{\frac{7}{4}}}{16(D_4)^{\frac{3}{2}}}*dZ$$

  = 55 Pa (0.221 in H_2O)

- $$\Delta P_5 = \int_0^{1.5D_5} \frac{0.026*\left[\frac{(3Z+15D_5)}{\sqrt{Z}}\right]*\left\{\left(\frac{8D_5}{2Z+5D_5}\right)^2+\left[\frac{2D_5}{\pi*(3Z+15D_5)}\right]^2+\left[\frac{16D_5}{\pi*(3Z+15D_5)}\right]^2\right\}^{\frac{7}{4}}}{16(D_5)^{\frac{3}{2}}}*dZ$$

  = 55 Pa (0.221 in H_2O)

Frictional Loss In The Cone (ΔP_f) @ V_{in} = 12 m/s (2400 fpm) – 1D2D

D_1 = 0.1 m (4 inch) | D_3 = 0.3 m (12 inch) | D_5 = 0.9 m (36 inch)

D_2 = 0.2 m (6 inch) | D_4 = 0.6 m (24 inch)

- $$\Delta P_1 = \int_0^{1.5D_1} \frac{0.038*\left[\frac{(3Z+15D_1)}{\sqrt{Z}}\right]*\left\{\left(\frac{8D_1}{2Z+5D_1}\right)^2+\left[\frac{2D_1}{\pi*(3Z+15D_1)}\right]^2+\left[\frac{16D_1}{\pi*(3Z+15D_1)}\right]^2\right\}^{\frac{7}{4}}}{16(D_1)^{\frac{3}{2}}}*dZ$$

  = 80.4 Pa (0.323 in H_2O)

- $$\Delta P_2 = \int_0^{1.5D_2} \frac{0.038*\left[\frac{(3Z+15D_2)}{\sqrt{Z}}\right]*\left\{\left(\frac{8D_2}{2Z+5D_2}\right)^2+\left[\frac{2D_2}{\pi*(3Z+15D_2)}\right]^2+\left[\frac{16D_2}{\pi*(3Z+15D_2)}\right]^2\right\}^{\frac{7}{4}}}{16(D_2)^{\frac{3}{2}}}*dZ$$

  = 80.4 Pa (0.323 in H_2O)

- $$\Delta P_3 = \int_0^{1.5D_3} \frac{0.038*\left[\frac{(3Z+15D_3)}{\sqrt{Z}}\right]*\left\{\left(\frac{8D_3}{2Z+5D_3}\right)^2+\left[\frac{2D_3}{\pi*(3Z+15D_3)}\right]^2+\left[\frac{16D_3}{\pi*(3Z+15D_3)}\right]^2\right\}^{\frac{7}{4}}}{16(D_3)^{\frac{3}{2}}}*dZ$$

  = 80.4 Pa (0.323 in H_2O)

- $$\Delta P_4 = \int_0^{1.5D_4} \frac{0.038*\left[\frac{(3Z+15D_4)}{\sqrt{Z}}\right]*\left\{\left(\frac{8D_4}{2Z+5D_4}\right)^2+\left[\frac{2D_4}{\pi*(3Z+15D_4)}\right]^2+\left[\frac{16D_4}{\pi*(3Z+15D_4)}\right]^2\right\}^{\frac{7}{4}}}{16(D_4)^{\frac{3}{2}}}*dZ$$

  = 80.4 Pa (0.323 in H_2O)

- $$\Delta P_5 = \int_0^{1.5D_5} \frac{0.038*\left[\frac{(3Z+15D_5)}{\sqrt{Z}}\right]*\left\{\left(\frac{8D_5}{2Z+5D_5}\right)^2+\left[\frac{2D_5}{\pi*(3Z+15D_5)}\right]^2+\left[\frac{16D_5}{\pi*(3Z+15D_5)}\right]^2\right\}^{\frac{7}{4}}}{16(D_5)^{\frac{3}{2}}}*dZ$$

  = 80.4 Pa (0.323 in H_2O)

Frictional Loss In The Cone (ΔP_f) @ V_{in} = 15 m/s (3000 fpm) – 1D2D

D_1 = 0.1 m (4 inch) D_3 = 0.3 m (12 inch) D_5 = 0.9 m (36 inch)

D_2 = 0.2 m (6 inch) D_4 = 0.6 m (24 inch)

- $$\Delta P_1 = \int_0^{1.5D_1} \frac{0.059*\left[\frac{(3Z+15D_1)}{\sqrt{Z}}\right]*\left\{\left(\frac{8D_1}{2Z+5D_1}\right)^2+\left[\frac{2D_1}{\pi*(3Z+15D_1)}\right]^2+\left[\frac{16D_1}{\pi*(3Z+15D_1)}\right]^2\right\}^{\frac{7}{4}}}{16(D_1)^{\frac{3}{2}}}*dZ$$

  = 124.7 Pa (0.501 in H_2O)

- $$\Delta P_2 = \int_0^{1.5D_2} \frac{0.059*\left[\frac{(3Z+15D_2)}{\sqrt{Z}}\right]*\left\{\left(\frac{8D_2}{2Z+5D_2}\right)^2+\left[\frac{2D_2}{\pi*(3Z+15D_2)}\right]^2+\left[\frac{16D_2}{\pi*(3Z+15D_2)}\right]^2\right\}^{\frac{7}{4}}}{16(D_2)^{\frac{3}{2}}}*dZ$$

  = 124.7 Pa (0.501 in H_2O)

- $$\Delta P_3 = \int_0^{1.5D_3} \frac{0.059*\left[\frac{(3Z+15D_3)}{\sqrt{Z}}\right]*\left\{\left(\frac{8D_3}{2Z+5D_3}\right)^2+\left[\frac{2D_3}{\pi*(3Z+15D_3)}\right]^2+\left[\frac{16D_3}{\pi*(3Z+15D_3)}\right]^2\right\}^{\frac{7}{4}}}{16(D_3)^{\frac{3}{2}}}*dZ$$

  = 124.7 Pa (0.501 in H_2O)

- $$\Delta P_4 = \int_0^{1.5D_4} \frac{0.059*\left[\frac{(3Z+15D_4)}{\sqrt{Z}}\right]*\left\{\left(\frac{8D_4}{2Z+5D_4}\right)^2+\left[\frac{2D_4}{\pi*(3Z+15D_4)}\right]^2+\left[\frac{16D_4}{\pi*(3Z+15D_4)}\right]^2\right\}^{\frac{7}{4}}}{16(D_4)^{\frac{3}{2}}}*dZ$$

  = 124.7 Pa (0.501 in H_2O)

- $$\Delta P_5 = \int_0^{1.5D_5} \frac{0.059*\left[\frac{(3Z+15D_5)}{\sqrt{Z}}\right]*\left\{\left(\frac{8D_5}{2Z+5D_5}\right)^2+\left[\frac{2D_5}{\pi*(3Z+15D_5)}\right]^2+\left[\frac{16D_5}{\pi*(3Z+15D_5)}\right]^2\right\}^{\frac{7}{4}}}{16(D_5)^{\frac{3}{2}}}*dZ$$

  = 124.7 Pa (0.501 in H_2O)

Frictional Loss In The Cone (ΔP_f) @ V_{in} = 16 m/s (3200 fpm) – 1D2D

D_1 = 0.1 m (4 inch) D_3 = 0.3 m (12 inch) D_5 = 0.9 m (36 inch)

D_2 = 0.2 m (6 inch) D_4 = 0.6 m (24 inch)

- $$\Delta P_1 = \int_0^{1.5D_1} \frac{0.068*\left[\frac{(3Z+15D_1)}{\sqrt{Z}}\right]*\left\{\left(\frac{8D_1}{2Z+5D_1}\right)^2+\left[\frac{2D_1}{\pi*(3Z+15D_1)}\right]^2+\left[\frac{16D_1}{\pi*(3Z+15D_1)}\right]^2\right\}^{\frac{7}{4}}}{16(D_1)^{\frac{3}{2}}}*dZ$$

  = 143.7 Pa (0.577 in H_2O)

- $$\Delta P_2 = \int_0^{1.5D_2} \frac{0.068*\left[\frac{(3Z+15D_2)}{\sqrt{Z}}\right]*\left\{\left(\frac{8D_2}{2Z+5D_2}\right)^2+\left[\frac{2D_2}{\pi*(3Z+15D_2)}\right]^2+\left[\frac{16D_2}{\pi*(3Z+15D_2)}\right]^2\right\}^{\frac{7}{4}}}{16(D_2)^{\frac{3}{2}}}*dZ$$

  = 143.7 Pa (0.577 in H_2O)

- $$\Delta P_3 = \int_0^{1.5D_3} \frac{0.068*\left[\frac{(3Z+15D_3)}{\sqrt{Z}}\right]*\left\{\left(\frac{8D_3}{2Z+5D_3}\right)^2+\left[\frac{2D_3}{\pi*(3Z+15D_3)}\right]^2+\left[\frac{16D_3}{\pi*(3Z+15D_3)}\right]^2\right\}^{\frac{7}{4}}}{16(D_3)^{\frac{3}{2}}}*dZ$$

  = 143.7 Pa (0.577 in H_2O)

- $$\Delta P_4 = \int_0^{1.5D_4} \frac{0.068*\left[\frac{(3Z+15D_4)}{\sqrt{Z}}\right]*\left\{\left(\frac{8D_4}{2Z+5D_4}\right)^2+\left[\frac{2D_4}{\pi*(3Z+15D_4)}\right]^2+\left[\frac{16D_4}{\pi*(3Z+15D_4)}\right]^2\right\}^{\frac{7}{4}}}{16(D_4)^{\frac{3}{2}}}*dZ$$

  = 143.7 Pa (0.577 in H_2O)

- $$\Delta P_5 = \int_0^{1.5D_5} \frac{0.068*\left[\frac{(3Z+15D_5)}{\sqrt{Z}}\right]*\left\{\left(\frac{8D_5}{2Z+5D_5}\right)^2+\left[\frac{2D_5}{\pi*(3Z+15D_5)}\right]^2+\left[\frac{16D_5}{\pi*(3Z+15D_5)}\right]^2\right\}^{\frac{7}{4}}}{16(D_5)^{\frac{3}{2}}}*dZ$$

  = 143.7 Pa (0.577 in H_2O)

Frictional Loss In The Cone (ΔP_f) @ V_{in} = 18 m/s (3500 fpm) – 1D2D

D_1 = 0.1 m (4 inch) D_3 = 0.3 m (12 inch) D_5 = 0.9 m (36 inch)

D_2 = 0.2 m (6 inch) D_4 = 0.6 m (24 inch)

- $$\Delta P_1 = \int_0^{1.5D_1} \frac{0.081*\left[\frac{(3Z+15D_1)}{\sqrt{Z}}\right]*\left\{\left(\frac{8D_1}{2Z+5D_1}\right)^2+\left[\frac{2D_1}{\pi*(3Z+15D_1)}\right]^2+\left[\frac{16D_1}{\pi*(3Z+15D_1)}\right]^2\right\}^{\frac{7}{4}}}{16(D_1)^{\frac{3}{2}}}*dZ$$

  = 171.3 Pa (0.688 in H_2O)

- $$\Delta P_2 = \int_0^{1.5D_2} \frac{0.081*\left[\frac{(3Z+15D_2)}{\sqrt{Z}}\right]*\left\{\left(\frac{8D_2}{2Z+5D_2}\right)^2+\left[\frac{2D_2}{\pi*(3Z+15D_2)}\right]^2+\left[\frac{16D_2}{\pi*(3Z+15D_2)}\right]^2\right\}^{\frac{7}{4}}}{16(D_2)^{\frac{3}{2}}}*dZ$$

  = 171.3 Pa (0.688 in H_2O)

- $$\Delta P_3 = \int_0^{1.5D_3} \frac{0.081*\left[\frac{(3Z+15D_3)}{\sqrt{Z}}\right]*\left\{\left(\frac{8D_3}{2Z+5D_3}\right)^2+\left[\frac{2D_3}{\pi*(3Z+15D_3)}\right]^2+\left[\frac{16D_3}{\pi*(3Z+15D_3)}\right]^2\right\}^{\frac{7}{4}}}{16(D_3)^{\frac{3}{2}}}*dZ$$

  = 171.3 Pa (0.688 in H_2O)

- $$\Delta P_4 = \int_0^{1.5D_4} \frac{0.081*\left[\frac{(3Z+15D_4)}{\sqrt{Z}}\right]*\left\{\left(\frac{8D_4}{2Z+5D_4}\right)^2+\left[\frac{2D_4}{\pi*(3Z+15D_4)}\right]^2+\left[\frac{16D_4}{\pi*(3Z+15D_4)}\right]^2\right\}^{\frac{7}{4}}}{16(D_4)^{\frac{3}{2}}}*dZ$$

  = 171.3Pa (0.688 in H_2O)

- $$\Delta P_5 = \int_0^{1.5D_5} \frac{0.081*\left[\frac{(3Z+15D_5)}{\sqrt{Z}}\right]*\left\{\left(\frac{8D_5}{2Z+5D_5}\right)^2+\left[\frac{2D_5}{\pi*(3Z+15D_5)}\right]^2+\left[\frac{16D_5}{\pi*(3Z+15D_5)}\right]^2\right\}^{\frac{7}{4}}}{16(D_5)^{\frac{3}{2}}}*dZ$$

  = 171.3 Pa (0.688 in H_2O)

Frictional Loss In The Cone (ΔP_f) @ V_{in} = 20 m/s (4000 fpm) – 1D2D

D_1 = 0.1 m (4 inch) D_3 = 0.3 m (12 inch) D_5 = 0.9 m (36 inch)

D_2 = 0.2 m (6 inch) D_4 = 0.6 m (24 inch)

- $$\Delta P_1 = \int_0^{1.5D_1} \frac{0.106*\left[\frac{(3Z+15D_1)}{\sqrt{Z}}\right]*\left\{\left(\frac{8D_1}{2Z+5D_1}\right)^2+\left[\frac{2D_1}{\pi*(3Z+15D_1)}\right]^2+\left[\frac{16D_1}{\pi*(3Z+15D_1)}\right]^2\right\}^{\frac{7}{4}}}{16(D_1)^{\frac{3}{2}}}*dZ$$

  = 224 Pa (0.9 in H_2O)

- $$\Delta P_2 = \int_0^{1.5D_2} \frac{0.106*\left[\frac{(3Z+15D_2)}{\sqrt{Z}}\right]*\left\{\left(\frac{8D_2}{2Z+5D_2}\right)^2+\left[\frac{2D_2}{\pi*(3Z+15D_2)}\right]^2+\left[\frac{16D_2}{\pi*(3Z+15D_2)}\right]^2\right\}^{\frac{7}{4}}}{16(D_2)^{\frac{3}{2}}}*dZ$$

  = 224 Pa (0.9 in H_2O)

- $$\Delta P_3 = \int_0^{1.5D_3} \frac{0.106*\left[\frac{(3Z+15D_3)}{\sqrt{Z}}\right]*\left\{\left(\frac{8D_3}{2Z+5D_3}\right)^2+\left[\frac{2D_3}{\pi*(3Z+15D_3)}\right]^2+\left[\frac{16D_3}{\pi*(3Z+15D_3)}\right]^2\right\}^{\frac{7}{4}}}{16(D_3)^{\frac{3}{2}}}*dZ$$

  = 224 Pa (0.9 in H_2O)

- $$\Delta P_4 = \int_0^{1.5D_4} \frac{0.106*\left[\frac{(3Z+15D_4)}{\sqrt{Z}}\right]*\left\{\left(\frac{8D_4}{2Z+5D_4}\right)^2+\left[\frac{2D_4}{\pi*(3Z+15D_4)}\right]^2+\left[\frac{16D_4}{\pi*(3Z+15D_4)}\right]^2\right\}^{\frac{7}{4}}}{16(D_4)^{\frac{3}{2}}}*dZ$$

  = 224 Pa (0.9 in H_2O)

- $$\Delta P_5 = \int_0^{1.5D_5} \frac{0.106*\left[\frac{(3Z+15D_5)}{\sqrt{Z}}\right]*\left\{\left(\frac{8D_5}{2Z+5D_5}\right)^2+\left[\frac{2D_5}{\pi*(3Z+15D_5)}\right]^2+\left[\frac{16D_5}{\pi*(3Z+15D_5)}\right]^2\right\}^{\frac{7}{4}}}{16(D_5)^{\frac{3}{2}}}*dZ$$

  = 224 Pa (0.9 in H_2O)

APPENDIX F

COPYRIGHT RELEASE

The Society for engineering in agricultural, food, and biological systems

February 16, 2004

Lingjuan Wang
Ph. D. Candidate, EIT
Graduate Research Assistant
Department of Biological & Agricultural Engineering
Texas A & M University
College Station, Texas 77843-2117

Dear Linqiuan,

As you are listed as an author on all three of the documents we can grant permission to this request. Please note that the permission extends only to inclusion in your dissertation. If you would like to use the full-text in later publications, please let us know the details at that time.

Good luck with your project. I'll mail a copy of this correspondence on ASAE letterhead and include my signature.

Sincerely,

Donna M. Hull
Director, Publications

American Society of Agricultural Engineers
2950 Niles Road, St. Joseph, MI 49085-9659, USA | 269.429.0300 | Fax 269.429.3852 | hq@asae.org | www.asae.org

The Society for engineering
in agricultural, food, and
biological systems

Sandy Rutter

Subject: RE: Copyright Release from ASAE

Dear Ms. Hull:

This is a respectful request for the copyright release to reproduce the following papers in my Ph.D dissertation.

1. "A New Theoretical Approach for Predicting Number of Turns and Cyclone Pressure Drop"
2001 ASAE meeting paper No. 01-4009

2. "Analysis of Cyclone Collection Efficiency" 2003 ASAE meeting paper No. 034114

3."Air Density Effect on Cyclone Performance" Transaction of ASAE Vol. 46(4):1193-1201

Would you please grant me a written permission with your official letter head? Your help will be greatly appreciated!

Best Regards,
Sincerely,
Lingjuan Wang,

****

Lingjuan Wang
Ph. D. Candidate, EIT
Graduate Research Assistant
Department of Biological & Agricultural Engineering
Texas A & M University
College Station, Texas 77843-2117
Phone: (979) 845-3693
Fax: (979) 845-3932
E-mail: Lwang@cora.tamu.edu
****

2/16/2004

VITA

LINGJUAN WANG

Permanent Address:

c/o Fengzheng Wang,

Room 204, Building 5, District D

Song Tao Yuan, Nanhu Garden, Wuchang

Wuhan City, Hubei Province, P.R. China 430064

Education:

Ph.D. May 2004: Biological & Agricultural Engineering, Texas A&M University

M.S. December 2000: Agricultural Engineering, Texas A&M University

B.Eng. July 1985: Cotton Engineering, Anhui Institute of Finance & Trade, China

Certification:

Engineer-In-Training (EIT): # 33178, Texas Board of Professional Engineers

Design Engineer: # ZZ-18 (1993) Professional Engineer Committee, Ministry of Commerce, P.R. China

Professional Experience:

1999 – 2004: Graduate Research / Teaching Assistant, Texas A&M University

1998 – 1999: Visiting Scholar, Texas A&M University

1985 –1998: Research and design engineer, All-China Federation of Supply and Marketing Cooperatives Zhengzhou Cotton & Jute Engineering Technology Design and Research Institute

Publication:

Wang, L., M. D. Buser, C. B. Parnell and B. W. Shaw, 2003. Effect of air density on cyclone performance and system design. *Transactions of the ASAE* 46 (4): 1193-1201

Wang, L., C. B. Parnell and B. W. Shaw, 2002. Performance characteristics of cyclones in cotton-gin dust removal. *Agricultural Engineering International: The CIGR Journal of Scientific Research and Development*. Manuscript BC02001. Vol. IV. August 2002. Available at http://cigr-ejournal.tamu.edu/volume4.html.

Wang, L., C. B. Parnell and B. W. Shaw, 2002. Study of the cyclone fractional efficiency curves. *Agricultural Engineering International: The CIGR Journal of Scientific Research and Development*. Manuscript BC02002. Vol. IV. June 2002. Available at http://cigr-ejournal.tamu.edu/volume4.html.